An Introduction to the NRAO Very Large Array

Edition 2.0
Last revised: August 1992

Written by the Staff of the National Radio Astronomy Observatory*

Edited by R.M. Hjellming

Last compiled: 29 July 1992

* The National Radio Astronomy Observatory is operated by Associated Universities, Inc. under a cooperative agreement with the U.S. National Science Foundation.

Place © message on this page

Preface

The purpose of an *Introduction to the NRAO VLA* is to provide astronomers who wish to observe with the VLA most of the basic information they need to use the instrument. It is an introduction rather than a complete user's manual because we wish to provide both an overall view of the instrument and a level of information appropriate to those who may not already be experienced with interferometry and aperture synthesis.

When the first edition of this Introduction was produced in 1978 as a "bound" volume, there were formidable barriers to up-dating. This resulted in a delay of almost four years before an up-dated version was produced. In 1982 a revised second edition was produced with some co-authors of individual chapters and a three-ring notebook format. The hope was that co-authors would aid in providing updating of separate chapters, and that replacement of out of date chapters would be easy. Except for updates of a few chapters in 1983, this did not work, and by late 1989, changes in the VLA and associated software made much of the "Green Book" out of date.

This 1992 version of the *Introduction* is a re-write of the general aspects of the previous versions. Material related to computer hardware and software is deleted and other material that will change rapidly has been omitted. In some sense this is an introductory "Green Booklet," with other booklets or documentation covering more dynamic aspects of use of the VLA. Some of these are:

1. The AIPS Cookbook describing AIPS calibration, editing, imaging, image display, and image processing.
2. In Introduction to ISIS
3. the Observer's Reference Manual (ORM)
4. the Calibrator manual
5. the Observational Status Report

   and
6. the Guides for Continuum and Spectral Line Observers for AIPS and ISIS

The user may obtain copies of most of these manual from the Socorro Array Operations Center. For many purposes the copies kept at appropriate places around the VLA site and the AOC should be sufficient.

Another general source of information about the VLA is the Proceeding of the NRAO-VLA Workshop on "Synthesis Mapping." These proceedings contain lectures on various topics prepared by NRAO staff, with many details about matters important to those who wish to obtain a deeper understanding of aperture synthesis instruments like the VLA.

Many individuals have contributed to producing the past and present versions of this *Introduction*. Also, many of the ideas and text used in various portions of this introduction are borrowed or paraphrased from the work of individuals on the VLA staff who are too numerous to mention here.

1 The Basic Instrument

Abstract

We present a general overview of the aperture synthesis radio telescope called the Very Large Array (VLA). This includes a brief history of the background of the instrument and a summary of the general characteristics of its major hardware components.

1.1 The History and Concept of the VLA

The basic concept behind the VLA is that of an aperture synthesis radio telescope capable of making radio pictures over the entire northern sky with a resolution comparable to that of optical telescopes. Before describing the basic instrument, let us briefly describe the evolution of the VLA concept and the early history of its implementation.

The ideas behind the VLA were developed at NRAO within a few years after the beginnings of NRAO itself. Because of the pioneering efforts of M. Ryle, B. Mills and W. Christiansen, radio astronomers during the period 1957 to 1962 were well aware that the way to obtain a high-resolution radio mapping instrument was to place radio telescopes in large arrays and use the resulting interferometric data in conjunction with the aperture synthesis technique originated by Ryle. Therefore, in the years following the ground breaking for NRAO in Green Bank on October 17, 1957, two weeks after Sputnik, the beginnings of the VLA concept arose as a natural result of NRAO's mandate to provide radio astronomy instrumentation for US radio astronomy. In 1960 the National Science Foundation (NSF) established a committee of radio astronomers, headed by John Pierce of Bell Telephone Laboratories, to consider the future of radio astronomy. During the following year it became clear that NRAO should provide a high-resolution radio picture-making instrument. In 1962 the Pierce committee report recommended to the NSF that NRAO should proceed with the design of a $1'$ resolution array. D. S. Heeschen, then acting director of NRAO, distributed a memo assigning specific array design responsibilities to NRAO staff members in September of 1962. Development of an $8''$ resolution array in Green Bank was begun the next spring as a first step in familiarizing NRAO personnel with interferometer arrays. This resulted in the linking of a second 85-foot telescope to the original 85-foot Howard E. Tatel telescope to form NRAO's first interferometer pair. A third 85-foot telescope and a radio link to a 42-foot (later 45-foot) telescope were added later to give spacings from 100 m to 35 km.

In the summer of 1964 detailed design studies for the VLA began at NRAO. In August of that year the Whitford report gave its highest recommendation in the area of astronomy instrumentation to a large array consisting, as an example, of 100 85-foot antennas capable of 10" resolution mapping. NSF funded the detailed design work for such an instrument in fiscal years 1965 through 1967, at which time there was a specific NRAO design group headed by G. W. Swenson, then on leave from the University of Illinois. In January 1966 the first progress report of this design group was released. It recommended that the design goal of the instrument be changed to 1" resolution so it would be a radio imaging device with resolution comparable to optical telescopes. Their report was followed in January 1967 by the publication of Volumes I and II of the VLA proposal. The specifications of the VLA at this time involved 36 25-meter antennas operating mainly at 11 cm and located on three arms of a Y, with each arm 21 km in length. It was part of this plan that 3-cm and (21-cm) spectral line capabilities would eventually be added. The Y-shaped array concept was suggested by Y. L. Chow, who served as a consultant to the VLA design group.

During the summer of 1967 it was announced that NSF had declined to ask for funding for the VLA, and shortly thereafter the design group was largely disbanded, though some members remained on the NRAO staff. A low-key design effort continued at NRAO and in January 1969 Volume III of the VLA proposal was released. This volume reduced the number of proposed VLA antennas to twenty-seven. The preparation of Volume III was, in part, a response to the first meeting of the Dicke committee which had recommended, as part of a proposed plan for instrumentation in radio astronomy, that the funding of VLA design be continued. At a later meeting the Dicke committee recommended the building of a number of instruments, including the VLA. Based upon the Volume III modifications of the VLA proposal, the arguments for the construction of the VLA continued during the years 1969 to 1971. This was the period in which the Greenstein committee was considering various proposals for astronomy instrumentation. The VLA proposal was also being discussed by the President's Science Advisory Committee and the Office of Science and Technology. In late spring 1971 the final report of the Greenstein committee was released, with the VLA described as first priority amongst four strongly recommended projects.

The VLA project was widely supported by the US astronomical community; therefore, in October 1971 the NSF requested three million dollars for FY1973 to begin construction of the VLA. In December 1971 Volume IV of the VLA proposal, dealing with possible sites for the array, was released. At that time the site on the Plains of San Augustin in New Mexico was favored, and during the next year it was chosen as the site for the VLA because it was large, flat, isolated, relatively inexpensive to acquire, and located at a high altitude. In January 1972 the VLA appeared as a line item in the Presidential budget and the following August Congress appropriated three million dollars for the first year of VLA construction. The project was budgeted at 76 million dollars and was to be completed in 1981, with a basic funding rate of ten million dollars a year. During the period 1972-1973 the basic design of the VLA electronics system was conceived by S. Weinreb. Also during this period the basic concepts of the on-line and off-line computer systems were formulated by B. G. Clark, R. M. Hjellming and W. R. Burns.

During 1972 NRAO began hiring VLA construction staff, J. H. Lancaster was named program manager, initial items were procured and contracts let. E-Systems was selected as contractor for the 28 antennas (27 in normal operation with one undergoing regular maintenance). By this time the design of the electronics system had evolved to the point in which operation at four wavelength ranges, 18-21 cm, 6 cm, 2 cm, and 1.3 cm, was planned. Both continuum and spectral line work was envisioned and four different configurations of the 27 antennas, designated A (35-km maximum dimension), B (11-km), C (3.5-km), and D (1-km), were chosen.

In April 1974 the initial site and wye construction began. Next July construction started on the first two antennas, with delivery in late 1975. The antenna assembly building was completed in January 1975 and the first antenna transporter finished in July. Single-dish tests started on antenna 1 in August 1975 and on antenna 2 in October. Computer control of these antennas, initially located on stations W10 and W18, with 1.1-km separation, was implemented in the last half of 1975. The on-line computer system, and all electronics not located on the antennas, were housed in a trailer near W10. A second trailer provided offices for the on-line computer group. The only other VLA working area was the technical services building.

On February 18, 1976 the first "fringes" (interferometer signals) were obtained from antennas 1 and 2. By June 1976 the control building and the cafeteria were finished and transfer of equipment and personnel to these buildings began. Antenna 3 was functioning in the array, located on the southwest arm, in September 1976. At this point the pace of events was accelerating rapidly, with a new antenna being delivered roughly every seven weeks. On November 12-15, 1976 the first astronomy program was scheduled and carried out with four antennas functioning at 6 cm, two antennas functioning at 21 cm, two antennas functioning at 2 cm, and three antennas functioning at 1.3 cm. By late spring 1977 a characteristic pattern of two antennas functioning in a test subarray, and four or more antennas operating at the same time in a subarray devoted to astronomical programs, was well-established. The first map of an extended source was made May 24, 1977 when the planetary nebula NGC 40 was mapped at 6 cm, using 6 to 7 antennas by B. Balick, R. M. Hjellming and R. C. Bignell.

By early 1978 the array was scheduled for astronomical observing roughly half of the time so that operations at the site were a mixture of scientific observing and construction of the remaining antennas, electronics, railroad, and computer systems.

The last antenna, Number 28, was accepted on November 19, 1979, and by the middle of 1980 all antennas had been made operational. Formal dedication of the array occurred October 10, 1980.

By that time astronomers were regularly observing with nearly all 27 antennas, and the normal cycle of always working on maintenance of one antenna out of 28 in the antenna assembly begun. Regular operation of the entire array as a continuum and spectral line instrument dominated the activities at the VLA site by early 1981. The final construction budget for the VLA was $78.3 million, only slightly above the $76 million planned in 1972.

1.2 The VLA Site Buildings

Figure 1-1 shows photographs which give a panoramic view of the major buildings located at the VLA site. Most of these pictures were taken from the middle of the entrance road in front of the VLA control building. In the top picture the tall building in the left background is the antenna assembly and maintenance building, the trailer to the far left is the "bunkhouse" trailer used for back-up rooms when the visiting scientist's quarters (VSQ) are full, the building in front of the antenna assembly building is the technical services building with labs and offices, and the warehouse buildings are beyond the buses used for transportation between Socorro and the VLA. In the background are antennas west of the buildings. The middle picture in Figure 5-1 shows part of the VLA control building to the right, the office and library building (which also contains the VAX post-processing computers) in the background, and the area in front of the VLA control building with flagpole, sculpture, etc. The bottom picture is again a view from the entrance road with, from left to right, a portion of the office and library building, the control building, the cafeteria, and portions of the visiting scientists quarters (VSQ).

1.3 The Basic Antenna

The antennas constructed for the VLA were specially designed for VLA use. The mounts for each antenna are altazimuth and fully steerable. The reflector surfaces are 25 meters in diameter and are shaped with high-surface accuracy to optimize antenna efficiencies when used in the Cassegrain mode for wavelengths ranging from 1.3 cm to 21 cm. As seen in Figure 1-2, the base of each antenna is triangular, with sides of length 9.75 meters, with each corner having built-in bolts that mount on concrete foundation pedestals when located at an antenna station and on plates on an antenna transporter while being moved. Figure 1-3 shows an antenna transporter in action, moving an antenna along the twin railroad tracks that constitute the antenna transportation system. Table 1-1 contains some of the major design and performance parameters for the basic VLA antennas.

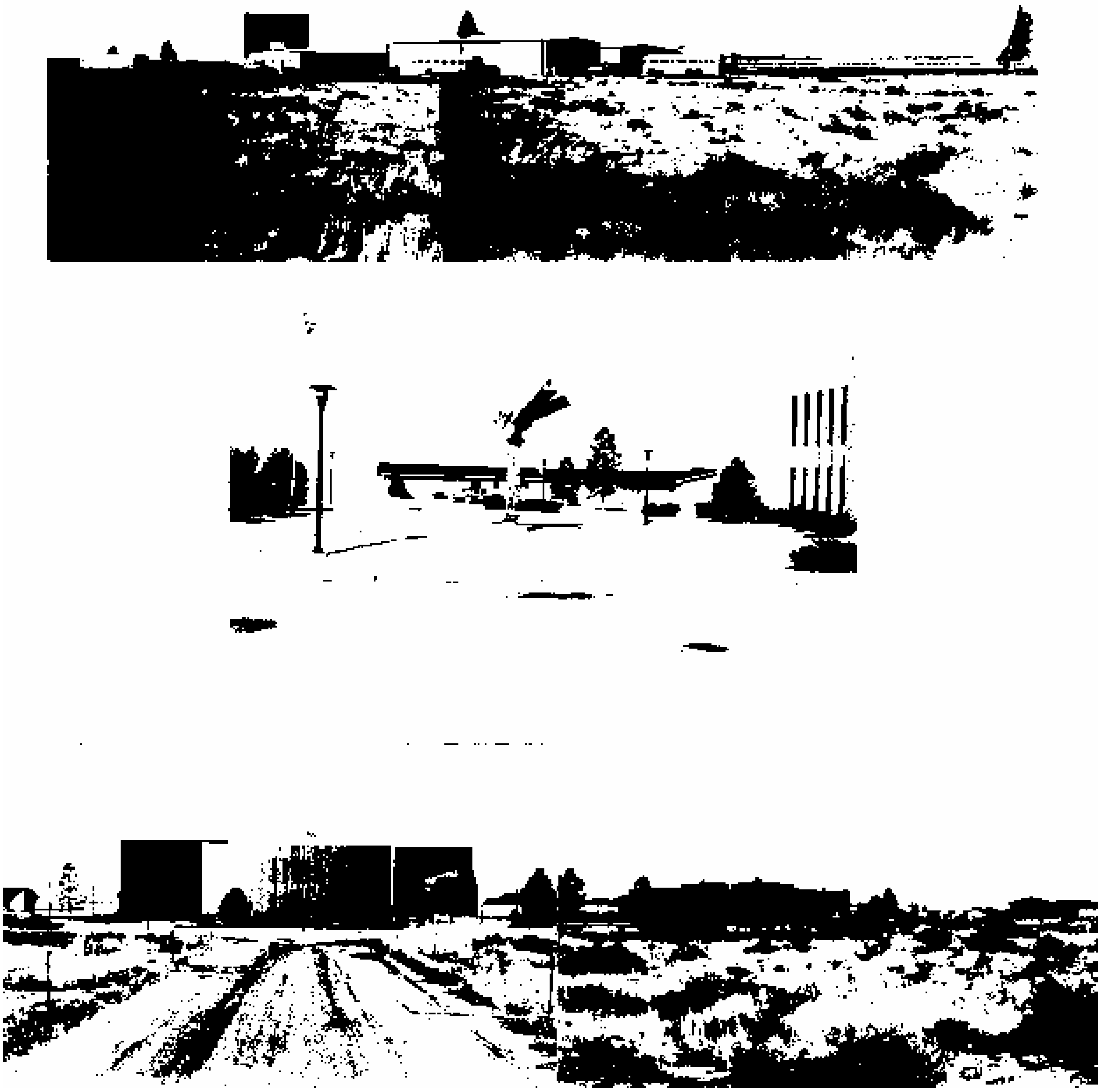

Figure 1 - 1. Photographs giving a panoramic view of the VLA buildings. The top picture, taken from the main entrance road, shows the bunkhouse trailer at the left, then the antenna assembly building, technical services building, and warehouse buildings. The center picture shows the sculpture in front of the control building, with the library/office building in the background. The bottom picture shows the control building, cafeteria, and visiting scientist quarters as viewed from the entrance road.

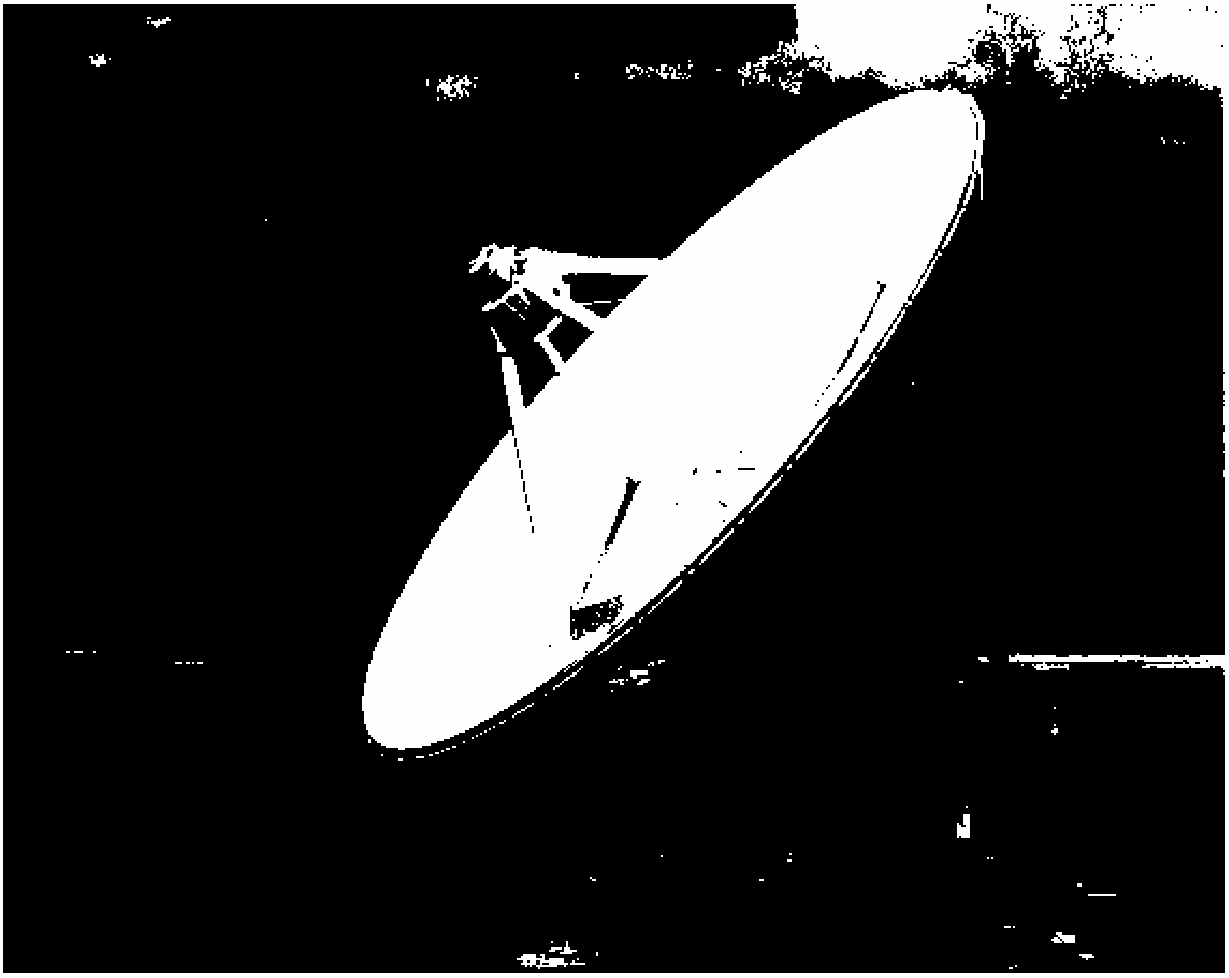

Figure 1 - 2. A photograph of a VLA antenna, showing the Cassegrain focus system, supporting structures, and the triangular antenna base mounted on three concrete pedestals. The tracks leading to other stations are seen beyond this antenna, and the twin railroad tracks of the southwest arm are seen at the lower left.

Figure 1 - 3. One of the VLA transporters moving a VLA antenna along the twin-railroad track that is the basis of the antenna transportation system.

1.4 The Antenna Feed System

The importance of allowing a number of different frequencies to be operational on the VLA antennas at any one time and the desirability of higher aperture efficiencies and lower spillover temperatures led to a Cassegrain feed system for the VLA antenna. An overall view of this system is shown in Figure 1-4 with a close-up of the feeds shown in Figure 1-5. The subreflector is located on a movable mount at the prime focus of the main reflector. The asymmetric subreflector has a hyperbolic surface which rotates under computer control so that, with the main beam aligned on the electrical axis of the antenna, incoming radiation is focused on a point on a circular ring of possible positions at the Cassegrain focus. In this geometry, the phase gradient across the aperture of the main reflector due to the feeds being off-axis is exactly canceled by a phase gradient introduced by the tilt of the subreflector. The feed ring has a radius of 98 cm with respect to the main reflector axis with the relative locations of the initial four feeds around the feed circle defined by the angles 6, 25, 135, and 335 degrees for the 1.3, 2, 18-21, and 6 cm feeds, respectively.

The choice of 1.3, 2, 6, and 18-21 cm as the main observing bands for the VLA was determined by a combination of technical and astronomical considerations. The prime consideration was the location of the radio astronomy protected bands and the various atomic and molecular lines associated with these bands as shown in Table 1-2.

Nominal antenna efficiencies for the six wavelength ranges are ??%, 50%, 65%, 60%, 54%, and 46% for 90, 18-21, 6, 3.6, 2, and 1.3 cm, respectively. The observing feed is changed by rotating the asymmetric subreflector about the main reflector axis so that the secondary focal point moves around the feed circle to the required feed. The time needed to rotate the subreflector between feeds is proportional to the angle between feeds measured around the feed circle. The longest travel time is the 25 seconds needed to rotate from the 6 cm feed to the 18-21 cm feed.

The 18-21 cm feed, which is the largest feed visible in Figure 1-5, (on the left), is a corrugated horn illuminating a hybrid lens of dielectric and in waveguide elements (short circular tubes). Because this feed is large and lies in the near field of the primary aperture, the lens and waveguide elements are necessary to focus the wave on the corrugated horn.

The 6-cm feed is also a corrugated horn. The 2- and 1.3-cm feeds are the more conventional pyramidal multimode horns. All feeds have changeable polarizers at their outputs so that either dual orthogonal linear polarization or right-hand and left-hand circular polarization can be provided. Changing polarizers takes roughly twenty minutes per feed per antenna. The normal observing mode for all feeds is circular polarization.

Measurements of the polarization properties of the antennas show that the right-hand and left-hand circularly-polarized beams are separated by 0.06 beamwidths. The direction of this beam separation or "squint" is perpendicular to the plane containing the feed and the main reflector axis. The squint effect occurs at these levels because of the combination of a shaped main reflector and off-axis feed. With a pure paraboloid the effect would be smaller, and with on-axis feeds the squint would not occur. The existence of the squint effect has a negligible effect on linear polarization measurement - linear polarization sidelobes have a four-lobed pattern, rather than the two-lobed "squint" pattern. Similarly, there are only small effects for circularly-polarized sources at the center of the antenna beam; however, the measurement of circularly-polarized structure is seriously compromised because the squint effect couples the antenna pointing errors into the polarization measurements. Various means of eliminating the squint effect are under study for future implementation.

1.5 Array Geometry

Four standard configurations of antennas along the array arms are available. These are called A, B, C, and D configurations, with A having the largest extent (but lacking the shortest baselines). The locations of the stations for these configurations are shown in Figure 1-6. Within a single configuration the distance of the antenna stations from the center of the wye is proportional to $m^{1.716}$, where m is an antenna location number, counting outwards along each arm. The power 1.716 is equal to the logarithm to the base 2 of the scale factor between adjacent configurations (3.285). With this choice of power, the m-th station on any configuration coincides with the 2 m-th station on the next smaller configuration (see Table 1-3), requiring only 72 stations to handle all four configurations. This concept, and the fact that such power-law arrangements give good coverage in the u,v plane for a three-armed array, was due to Y. L. Chow.

Tables 1-4, 1-5 and 1-6 give the locations, and radial distances from the center, for the antenna stations on the southwest, southeast and north arms. Stations affiliated with each configuration are labeled with an "x" in the appropriate columns in the tables. The stations are designated as Nn, En or Wn for the north, southeast and southwest arms. With this system of designation, stations Wn and En are approximately 13.65 $n^{1.716}$ meters from the center of the array, and stations Nn are approximately 12.31 $n^{1.716}$ of the array.

Table 1 - 1
VLA Antenna Parameters

main reflector diameter		25 m (82 feet)
antenna half-power beamwidth		1.5 λ (λ in cm)
total geometric aperture		491 square meters
focal length of main reflector		9 m
maximum asymmetric subreflector width		1.83 m
rms surface accuracy for panels		$<$ 0.38 mm
rms surface accuracy for panel setting		$<$ 0.46 mm
rms surface accuracy for gravity, wind, thermal		$<$ 0.36 mm
nonrepeatable pointing errors for wind $<$ 15 mph and $<$ 5 degrees temperature differences of structure		$<$ 15 arcsec
slew rate, azimuth		40 degrees per minute
slew rate, elevation		20 degrees per minute
drive, servo controlled 5 hp motors		2 per axis
minimum elevation		8 degrees
maximum elevation		125 degrees
minimum zenith angle for tracking		0.5 degrees
azimuth limits relative to track azimuth		$\pm$ 270 degrees
total weight of antenna		419,000 pounds
resonant freqency, torsional		2.2 Hz
resonant freqency, rocking		2.3 Hz
wind speed limit:	precision operation	$<$ 15 mph
	normal operation	$<$ 45 mph
	survival at stow (snow / ice load 20 lbs / sq. ft)	$<$ 110 mph

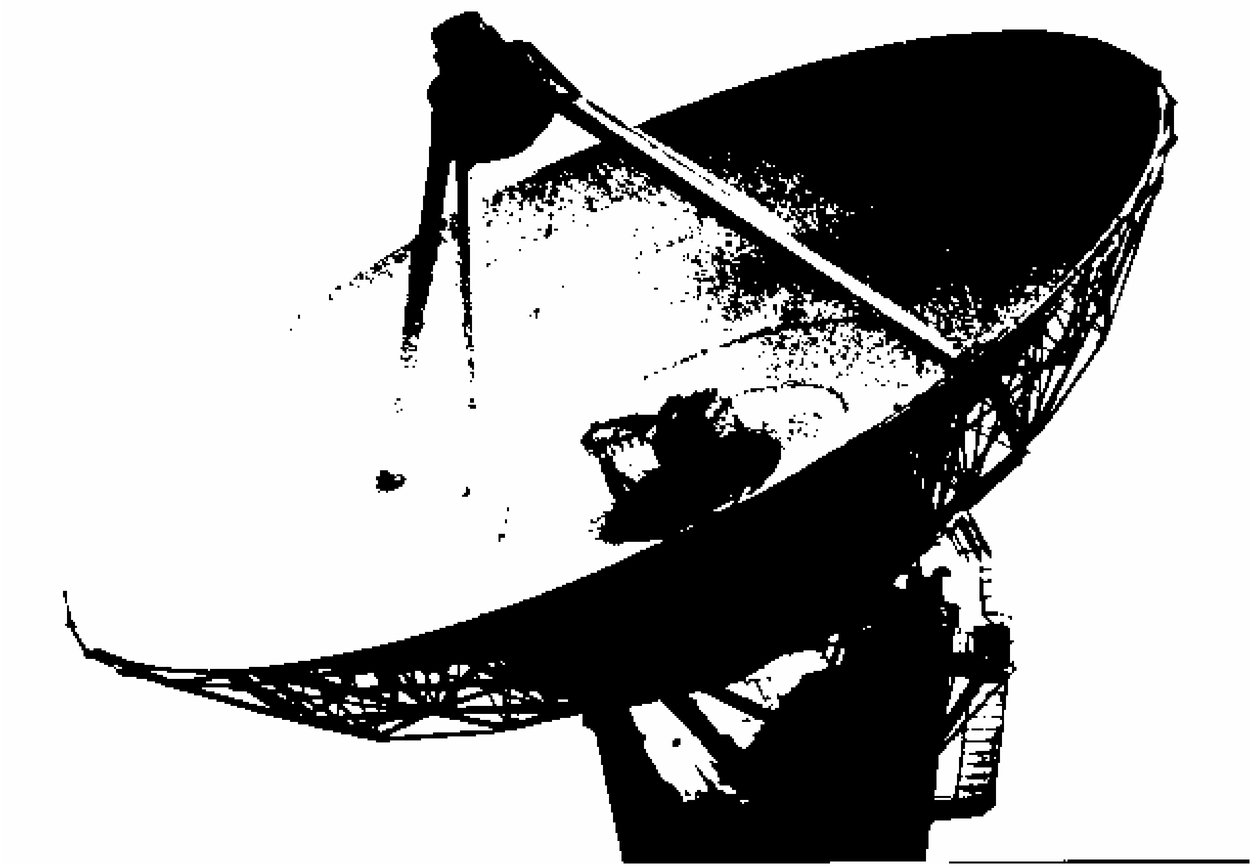

Figure 1 - 4. The Cassegrain system of a VLA antenna, showing the shaped parabolic reflector, a rotatable subreflector on a movable mount supported by four feed legs, and the four feeds on the feed ring at the Cassegrain focus.

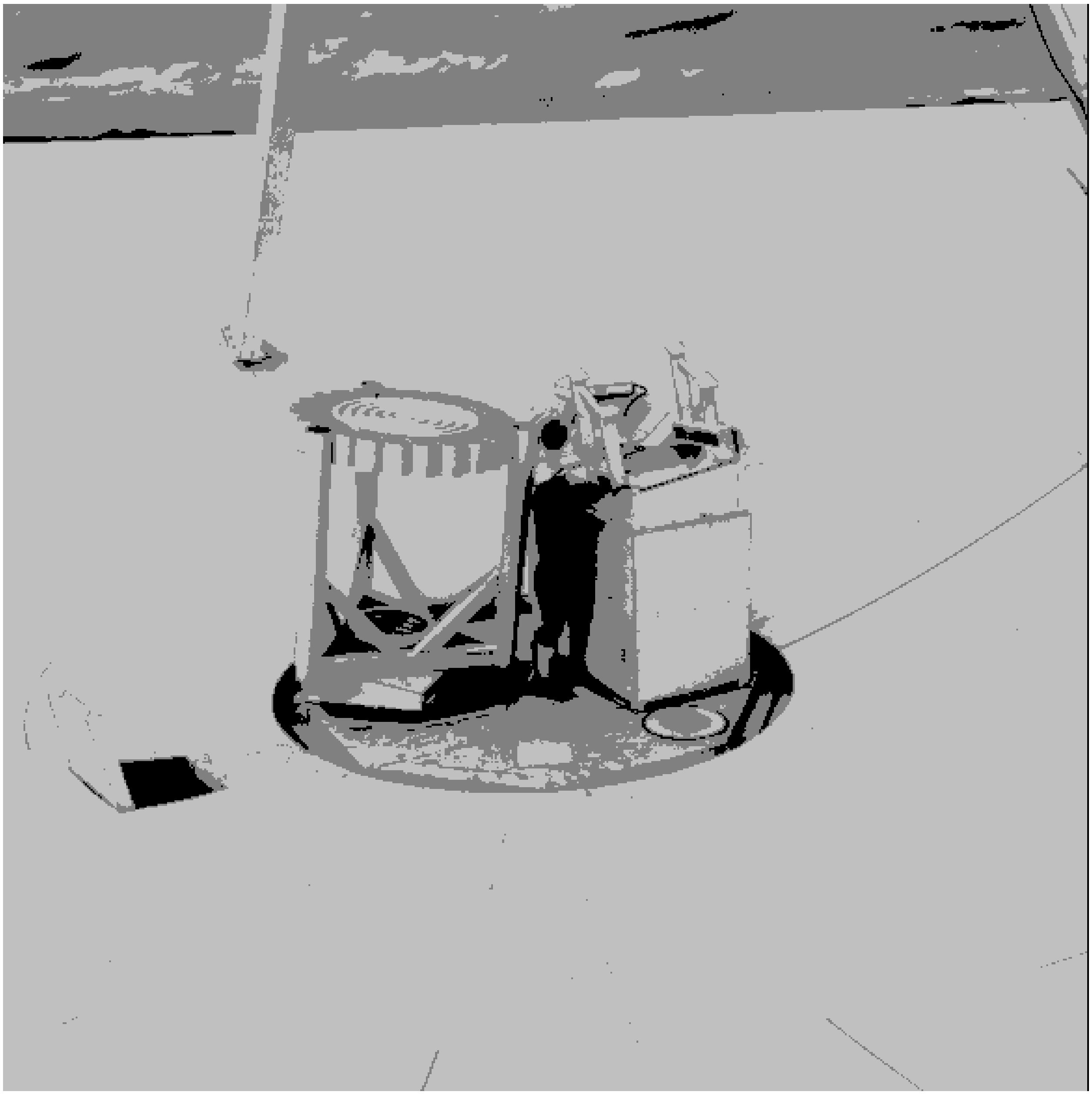

Figure 1 - 5. Photograph of a VLA feed system with 18-21 cm lens and feed at the left and a man working on the area where 6 cm, 2cm, and 1.3 cm feeds are located at the right.

Table 1 - 2
VLA Observing Bands and Associated Lines

VLA Band		Protected Band	Atomic and Molecular Lines
Frequency	Wavelength		
1340-1730 MHz	18-21 cm	1400-1427 MHz	Neutral H (Hydrogen) 1420.4 MHz
			H, He, etc. recombination lines
			$HCONH_2$ (Formamide) 1538-1542 MHz
			OH 1612, 1665, 1667, 1721 MHz
			HCOOH (Formic Acid) 1639 MHz
4500-5000 MHz	6 cm	4990-5000 MHz	$HCONH_2$ 4617-4620 MHz
14.4-15.4 GHz	2 cm	15.35-15.4 GHz	H_2CO 14.489 GHz
22.0-24.0 GHz	1.3 cm	23.6-24.0 GHz	H_2O 22.35 GHz
			NH_3 (Ammonia) 22.834-23.870 GHz

Table 1 - 3
Relationship Between Configurations and Stations

Configuration	Station Number (n)		
D	n = 1, 2, 3, 4, 5, 6, 7, 8, 9	= m	
C	n = 2, 4, 6, 8, 10, 12, 14, 16, 18	= 2 m	m = 1, 2, . . . 9
B	n = 4, 8, 12, 16, 20, 24, 28, 32, 36	= 4 m	
A	n = 8, 18, 24, 32, 40, 48, 56, 64, 72	= 8 m	

In Tables 1-4, 1-5 and 1-6 the vector (L_x, L_y, L_z) describes a station location in nanoseconds (ns) and R(m) is the radial distance (in meters) from the center of the array to the station position. Baseline vectors, denoted by (B_x, B_y, B_z) are defined by $(B_{jk})_i = (L_k)_i - (L_j)_i$ where j and k are station numbers ($k > j$ by convention) and i = 1, 2, 3, for x, y, z. The coordinates in these tables are accurate to within ± 0.04 ns.

A few modifications of the ideal station positions have been made: (1) The north arm was scaled down by 19/21 to avoid a dry lake; (2) the outermost stations on the southeast arm deviate slightly to the north to avoid a ravine; (3) the D configuration station locations are slightly modified to avoid congestion near the array center by (a) putting the n = 1 stations of the southeast and southwest arms on a short southern extension of the north arm called the north arm spur, and (b) modified locations for stations N1 to N4; and (4) station N24 is moved 100 meters north to be farther from Highway US 60.

The azimuths of the arms are:

north arm	$354°59'48''$
southeast arm	$114°59'42''$
southwest arm	$236°00'05''$

The geodetic coordinates of the center of the array are:

latitude	$34°04'43.497''$ north
longitude	$107°37'03.819''$ west.

The height of the center point of the array is 2124 m above sea level and the height variations lie within ±32 m of this altitude.

1.6 Location of Major System Components

Although we will discuss the electronics and waveguide systems in greater detail in later sections, let us briefly introduce some of the major components of the system.

Figure 1-7 illustrates some of the major components of each antenna, the waveguide communications system and the electronics located at the antennas and in the control building. Rack A contains the front end and cryogenic cooling system for the front ends. Rack B contains portions of the local oscillator (LO) and IF equipment. Both Racks A and B are suspended from the central portion of the main reflector inside a temperature-controlled vertex room. Waveguide from the feeds connect directly to Rack A. Rack C is the antenna control unit (ACU) located in the antenna pedestal room at the base of the antenna. It accepts position commands passed by Rack B and controls the antenna drive motors. Each antenna communicates back and forth to the control building via a 20-mm waveguide connected from Rack B to a buried 60-mm waveguide. Each arm of the array has a single section of buried 60-mm waveguide in which control information and antenna data are transmitted for up to eleven antennas. /vfill/eject

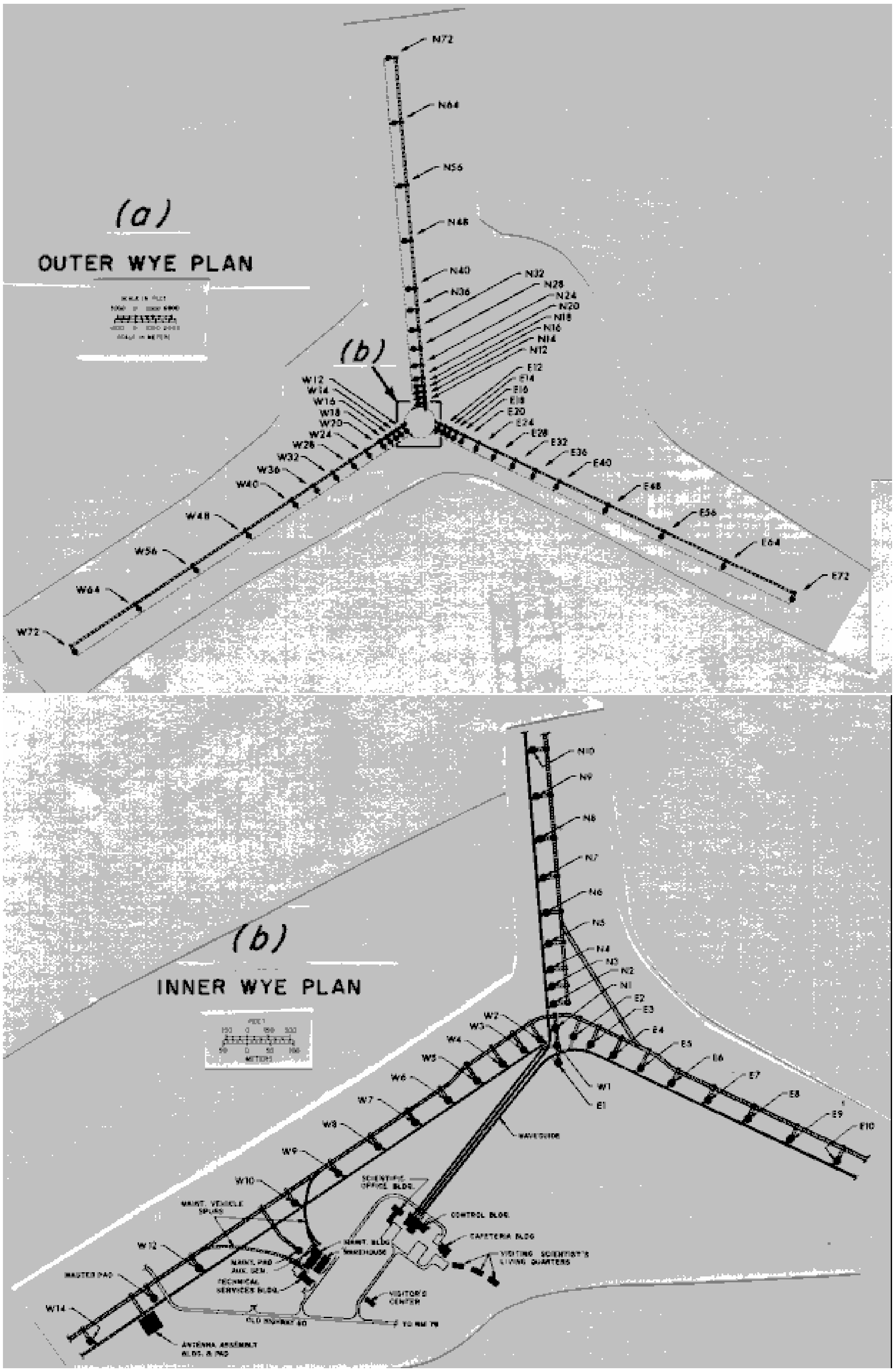

Figure 1 - 6. The outer (a) and inner (b) parts of the VLA.

Table 1 - 4
Station Positions for the Southwest Arm

Station Name	A	B	C	D	L_x (ns)	L_y (ns)	L_z (ns)	R(m)
W1				x	76.69	11.67	-108.36	39.95
W2			x	x	49.29	-123.87	-67.42	44.79
W3				x	96.46	-248.46	-136.94	89.83
W4		x	x	x	156.49	-407.06	-225.51	147.19
W5				x	228.83	-597.84	-331.98	216.18
W6			x	x	311.96	-817.22	-454.39	295.51
W7				x	405.70	-1064.49	-592.36	384.93
W8	x	x	x	x	509.53	-1338.54	-745.23	484.02
W9				x	623.12	-1638.19	-912.51	592.39
W10			x		747.12	-1962.88	-1093.09	709.81
W12		x	x		1021.28	-2683.76	-1494.63	970.49
W14			x		1328.35	-3496.20	-1948.61	1264.29
W16	x	x	x		1667.27	-4396.35	-2452.41	1589.80
W18			x		2040.62	-5381.34	-3002.15	1946.02
W20		x			2446.13	-6447.72	-3596.19	2331.63
W24	x	x			3353.71	-8816.08	-4910.74	3188.05
W28		x			4391.16	-11485.64	-6382.93	4153.44
W32	x	x			5470.50	-14443.13	-8061.25	5222.88
W36		x			6671.47	-17678.17	-9883.19	6392.71
W40	x				7988.65	-21181.36	-11844.80	7659.49
W48	x				10925.70	-28961.66	-16194.06	10473.00
W56	x				14206.44	-37731.09	-21114.62	13643.97
W64	x				17842.85	-47447.29	-26566.65	17157.45
W72	x				21802.57	-58074.16	-32540.96	21000.19

Table 1 - 5
Station Positions for the Southeast Arm

Station Name	Configuration A	B	C	D	Coordinates with array center as origin L_x (ns)	L_y (ns)	L_z (ns)	R(m)
E1				x	151.26	23.33	-218.44	79.96
E2			x	x	37.71	135.65	-50.59	44.85
E3				x	73.37	271.95	-103.23	89.94
E4		x	x	x	118.76	445.77	-170.46	147.44
E5				x	173.02	653.27	-250.51	216.07
E6			x	x	235.66	893.16	-343.18	295.42
E7				x	305.29	1163.76	-448.46	384.93
E8	x	x	x	x	381.68	1463.33	-565.35	484.02
E9				x	465.79	1790.89	-692.95	592.38
E10			x		558.29	2145.87	-830.16	709.79
E12		x	x		765.39	2933.01	-1133.62	970.21
E14			x		999.66	3822.35	-1475.27	1264.33
E16	x	x	x		1257.45	4806.65	-1855.04	1589.92
E18			x		1548.02	5883.17	-2264.55	1946.03
E20		x			1868.27	7049.02	-2704.15	2331.68
E24	x	x			2552.45	9638.20	-3698.88	3188.13
E28		x			3331.17	12556.45	-4814.90	4153.44
E32	x	x			4180.34	15789.68	-6060.60	5222.93
E36		x			5118.75	19326.37	-7416.80	6392.82
E40	x				6127.38	23156.24	-8890.33	7659.65
E48	x				8324.92	31661.66	-12190.73	10472.93
E56	x				10813.96	41248.78	-15902.56	13644.00
E64	x				13620.16	51870.75	-19982.12	17157.37
E72	x				16204.22	63678.31	-24269.82	20999.45

Table 1 - 6
Station Positions for the North Arm

Station Name	Configuration A	B	C	D	Coordinates with array center as origin L_x (ns)	L_y (ns)	L_z (ns)	R(m)
N1				x	2.24	0.05	1.71	0.84
N2			x	x	-100.24	-15.93	152.45	54.91
N3				x	-174.91	-27.56	262.39	94.90
N4		x	x	x	-249.59	-39.15	372.31	134.89
N5				x	-361.68	-56.66	537.09	194.86
N6			x	x	-495.22	-77.43	733.79	266.41
N7				x	-645.82	-100.90	955.52	347.07
N8	x	x	x	x	-812.58	-126.88	1200.98	436.37
N9				x	-995.39	-155.53	1469.71	534.19
N10			x		-1193.00	-186.06	1760.66	640.03
N12		x	x		-1632.09	-254.47	2406.72	875.11
N14			x		-2126.47	-331.52	3135.28	1140.07
N16	x	x	x		-2673.19	-416.88	3943.10	1433.62
N18			x		-3271.25	-510.29	4826.72	1754.71
N20		x			-3917.13	-611.39	5784.82	2102.44
N24	x	x			-5538.93	-865.16	8187.02	2974.68
N28		x			-6976.44	-1089.30	10305.16	3745.05
N32	x	x			-8769.76	-1369.81	12961.02	4709.44
N36		x			-10732.66	-1677.65	15864.79	5764.25
N40	x				-12857.81	-2009.03	19009.59	6906.45
N48	x				-17583.09	-2747.09	25991.26	9443.50
N56	x				-22918.88	-3578.90	33852.66	12302.77
N64	x				-28827.03	-4500.61	42565.13	15470.70
N72	x				-35282.55	-5508.69	52098.85	18935.62

Inside the control building the waveguide signals are distributed to Racks D such that each Rack D communicates with the corresponding Rack B at an antenna through the waveguide system. All local oscillator, IF, control and monitor signals are transmitted back and forth by way of this system. IF signals for each antenna are sent from a Rack D, by cable, to the shielded room where the sampler and delay and multiplier racks are located. The resulting cross-correlated signals from the multipliers are transmitted to the computer room where they are processed into ten-second visibility measurements in the on-line computers. The same on-line computer system controls the array by sending signals to each antenna via the waveguide communications system. The computer room in the control building contains, in addition to the on-line computer system, an off-line computer system for subsequent display, editing, correcting, and calibration of visibility data, plus capabilities to prepare maps and display them.

Further details on this system and the remaining equipment not yet mentioned will be discussed in later chapters.

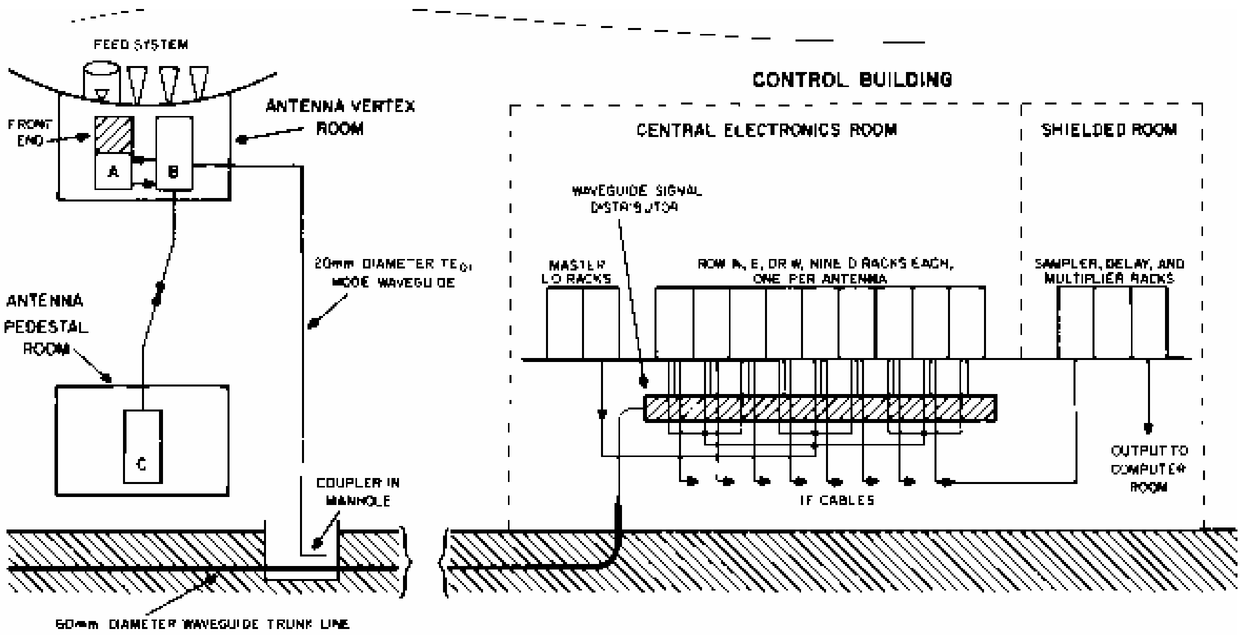

Figure 1 - 7. Schematic diagram showing the major locations of VLA electronics equipment, including details of the waveguide communications system and the signal distribution system located under the racks in the control building.

2 The Theory of the Instrument

Abstract

The theoretical, geometrical, and mathematical basis of the VLA is discussed. The major goal of this Chapter is to derive or define the basic equations describing the properties of the instrument, particularly the equations of calibration and image construction.

2.1 Introduction

An astronomer who wishes to use the VLA to study radio sources needs to know the basic principles of interferometry and aperture synthesis. The purpose of this chapter is to provide a basic introduction to these subjects with specific application to the VLA interferometers and aperture synthesis. The approach in this chapter will be dominantly theoretical. Further practical aspects of VLA interferometry and aperture synthesis are discussed in other chapters.

The basic process of interferometry is the cross-correlation of signals from two antennas observing the same source. A pair of antennas operated in this manner is called an interferometer. The signal output is analogous to the interference pattern created by a light wave passing through two slits. With N antennas there are N(N-1)/2 possible interferometers; therefore, there are 351 simultaneous interferometers in the full 27-antenna VLA. Radio interferometric measurements are considerably more complicated than the simple measurement of the radio frequency (RF) power received by the antennas. The cross-correlation of the signals from two antennas produces partial information about not only the intensities of all sources in the beams of the antennas, but also information about their positions in the sky relative to the position at which the interferometers are being "pointed". Because of the importance of time delays, antenna locations, and source position information, we will be very concerned with the geometry and coordinate systems involved in observing.

Any distribution of radio emission in an antenna beam can be considered to be the superposition of a large number of components of different size scales, locations and orientations. Because the relation between intensity distributions and the components can be described in terms of a Fourier integral relationship, it is useful to keep in mind that a single interferometer pair is at any instant measuring a single Fourier component of the apparent angular distribution of sources in the antenna beam. The essential characteristic of aperture synthesis in radio astronomy is the measurement of a large number of Fourier components of a radio source needed to reconstruct an image of the spatial intensity distribution of a source. The changing geometric relationship between the antenna pairs on the rotating earth and the radio source in the sky, allows us to measure N(N-1)/2 different Fourier components (for N antennas) each instant, for many instants. Due to the importance of earth rotation in allowing a large number of Fourier components to be sampled without adding more antennas, or moving antennas around physically, this technique is frequently called earth-rotation aperture synthesis.

The statements made so far about interferometry and aperture synthesis will be readily understood only by those experienced in these areas. Consequently, the purpose of Chapter 2 is to provide a thorough basis for understanding these subjects. We will begin by defining some fundamental concepts and continue by covering most of the things that are essential to an understanding of interferometry and aperture synthesis with the VLA. An excellent reference to most of the subjects in this chapter is the article on "Interferometry and Aperture Synthesis" by E. B. Fomalont and M. H. Wright ["Galactic and Extragalactic Radio Astronomy", ed. G. L. Verschuur and K. I. Kellermann, Springer-Verlag (New York), 1974, Chapter 10].

2.2 Some Definitions

In observing with N(N-1)/2 interferometer pairs, we point each of the N antennas at a particular point in the sky with a specified right ascension (α_o) and declination, (δ_o). This position is normally both the *antenna pointing position* and what we will call the *reference position*. This reference position is defined as the position in the sky with respect to which all timing and compensation for the delay in arrival of the same wavefront is referred. The position of a general point in the field of view, (α, δ), is frequently described with respect to the reference position in terms of a vector displacement ($\alpha - \alpha_o$, $\delta - \delta_o$) = (x, y, z). The z component is along the line of sight. Note that we have used the phrase "field of view" to describe the primary region of the sky to which the antennas are sensitive; this is important because we are not just collecting information about the total radiation in the antenna beam; rather we are collecting information about the strengths and positions of all radio sources in the field of view. We will discuss the field of view mainly in terms of the antenna half-power beamwidth (θ_{HPBW}) , which is approximately

$$\theta_{\rm HPBW} \;\simeq\; \lambda_{\rm cm}\ (\pm 5\%)\ \ \text{arcminutes} \qquad (2-1)$$

where $\lambda_{\rm cm}$ is the observing wavelength, and we have used the fact that all the VLA antennas are 25 meters in diameter. Another relevant angle is the beamwidth between first nulls (θ_{BWFN}) approximately given by

$$\theta_{\mathrm{BWFN}} \;\simeq\; 2.4\,\theta_{\mathrm{HPBW}} \;\simeq\; 3.6\,\lambda_{\mathrm{cm}} \;\;\text{arcminutes} \qquad (2-2)$$

A schematic representation of these angles with respect to the antenna beam pattern is shown in Figure 2-1 where we show an antenna beam with its radiation axis aligned with the unit vector $\mathbf{s}_o$, pointing to the reference position (α_o, δ_o) on the celestial sphere. (Unit vectors will be denoted by small letters.) We also show in Figure 2-1 a section of the celestial sphere, the tangent plane at the reference position and a general point on the celestial sphere. This is because, for the VLA operating at its larger dimensions, the deviations of the tangent plane from the celestial sphere will be significant in the outer regions of the antenna field of view. For a unit vector $\mathbf{s}$ pointing at a general point in the field of view, we must in general write $\mathbf{s}$ = (x,y,z) in a Cartesian representation, and only when deviations of the tangent plane from the celestial sphere can be neglected, can the usual

$$\mathbf{s} \;\simeq\; [(\alpha - \alpha_{\mathrm{o}})\cos\delta_{\mathrm{o}}, \delta - \delta_{\mathrm{o}}, 0] \qquad (2-3)$$

be written. The more general Cartesian expression for $\mathbf{s}$ will be discussed after coordinate systems have been more explicitly defined.

During normal observing the antennas are pointed under computer control to track the reference position $\mathbf{s}_o$. All observing consists of tracking a particular α_o and δ_o as a function of time. The fundamental time used at the VLA is International Atomic Time, abbreviated IAT, and all other times, including local apparent sidereal time (LAST or LST), are derived from IAT. The hour angle (H) for a source at right ascension α is defined as

$$\mathrm{H} \;=\; \mathrm{LST} - \alpha \qquad (2-4)$$

so a point east of the local meridian has a negative H and a source west of the local meridian has a positive H.

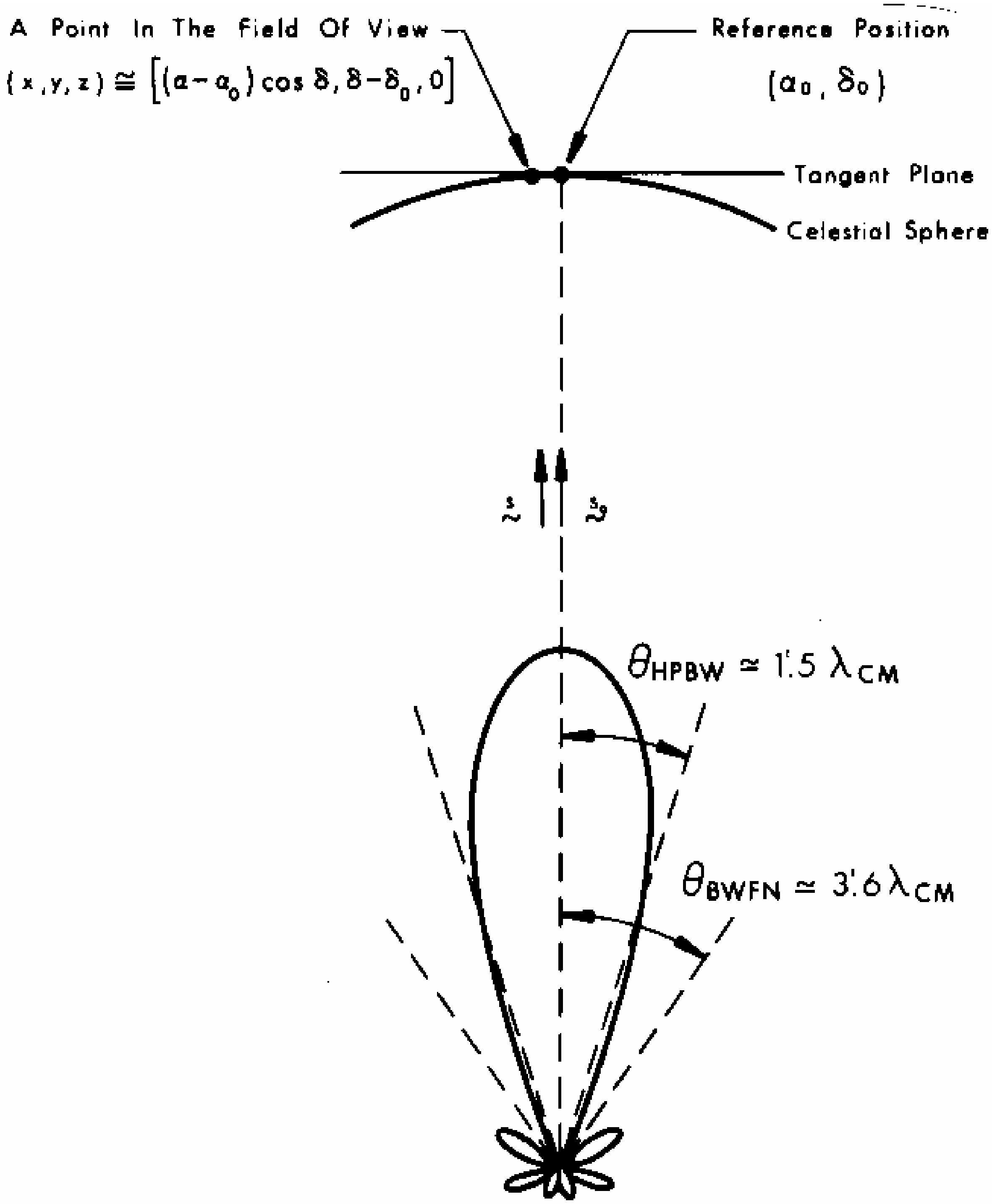

Figure 2 - 1. A schematic diagram showing the relation between an antenna beam pattern, pointed at the reference position, and positions on the celestial sphere and its tangent plane.

All earth-oriented coordinates are referred to with respect to the center of the array at geodetic coordinates

$$34°04'43.497'' \text{ north latitude}$$
$$107°37'03.819'' \text{ west longitude}$$

or a local zenith with a declination $34°04'43.497''$ on a local meridian at $7^h10^m28.2546^s$. Local MST (Mountain Standard Time) = GMT - $7^h \simeq$ UT $- 7^h$.

2.3 Interferometer Response to a Point Source

We begin with a discussion of the special case where VLA antennas track a region of the sky containing a strong point source which completely dominates the radiation received by the antennas. Let us define

$\mathbf{s}_o$	= unit vector pointing along the radiation axis of each telescope to the reference position (α_o, δ_o)
$\mathbf{s}$	= unit vector pointing to the position of a point source at (α, δ)
Δ s	= (s - s_o) = vector displacement on celestial sphere $\{\approx [(\alpha - \alpha_o) \cos \delta_o, \delta - \delta_o, 0]$ on tangent plane$\}$
$\upsilon,\ \lambda,\ \omega$	= frequency, wavelength and angular frequency of radiation
$\upsilon_o,\ \lambda_o,\ \omega_o$	= frequency and angular frequency used for radio frequency (RF) to intermediate frequency (IF) conversion
$\mathbf{L}_\mathrm{j}$	= vector position of the j^{th} antenna with respect to the center position of the array, units in seconds of time
$\mathbf{B}_{\mathrm{jk}}$	= $\mathrm{L}_\mathrm{k} - \mathrm{L}_\mathrm{j}$ = baseline vector between the j^{th} and k^{th} antennas where $\mathrm{j} < \mathrm{k}$, units in seconds of time

In Figure 2-2 we show a schematic representation of two VLA antennas intercepting a wavefront from a point source at $\mathbf{s}$ while tracking a position $\mathbf{s}_o$. The fundamental basis of interferometry is the fact that wavefronts which leave a point source at the same time arrive at slightly different times at different telescopes. In particular, for an orientation as shown in Figure 2-2, a wavefront reaches the j^{th} antenna at a time

$$\tau_{\mathrm{jk}} \;=\; \mathbf{B}_{\mathrm{jk}} \cdot \mathbf{s} \;=\; (\mathbf{L}_\mathrm{k} - \mathbf{L}_\mathrm{j}) \cdot \mathbf{s} \qquad (2-5)$$

later than it arrives at the k^{th} antenna. This corresponds to a phase difference $\omega\tau_{jk}$, thus the phase of wavefronts from the point source at $\mathbf{s}$ is given by $\omega\mathbf{B}_{jk} \cdot (\mathbf{s} - \mathbf{s}_o)$ since phase is measured with respect to the reference position. The maximum antenna separation of 35 km for the full A-array VLA means the delays will be from 0 to ≈ 120 microseconds. The process by which incoming signals are converted to measurements of the amplitude and phase of a wavefront is very complicated for the VLA because of the complex electronics system. However, in order to stress the more important aspects of this, let us discuss this process in terms of a couple of simple models. Those who do not wish to follow this discussion can proceed to Equation 2-15, taking the results on faith.

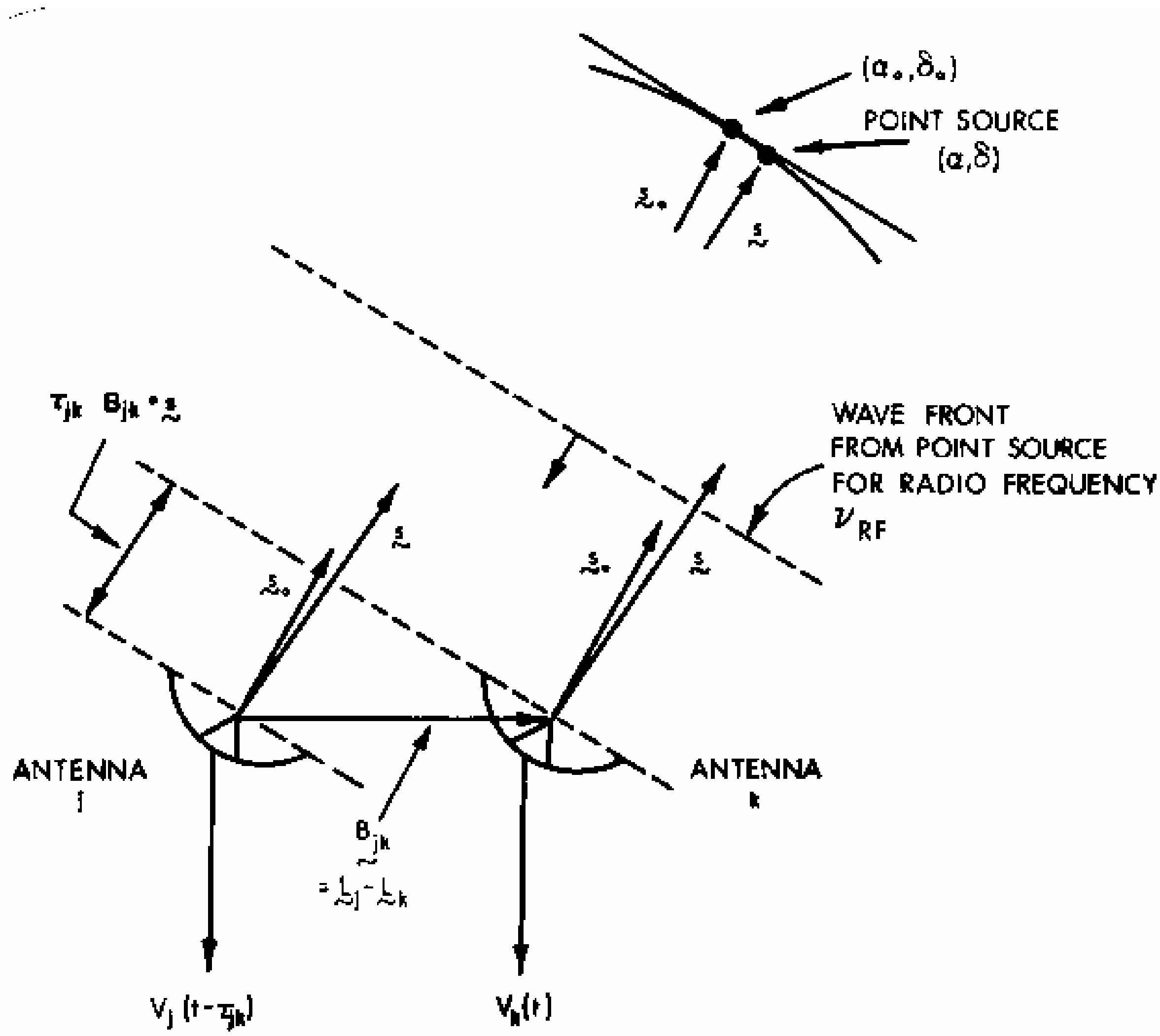

Figure 2 - 2. The geometry of a single interferometer pair with respect to wavefronts arriving from a point (α, δ) on the celestial sphere.

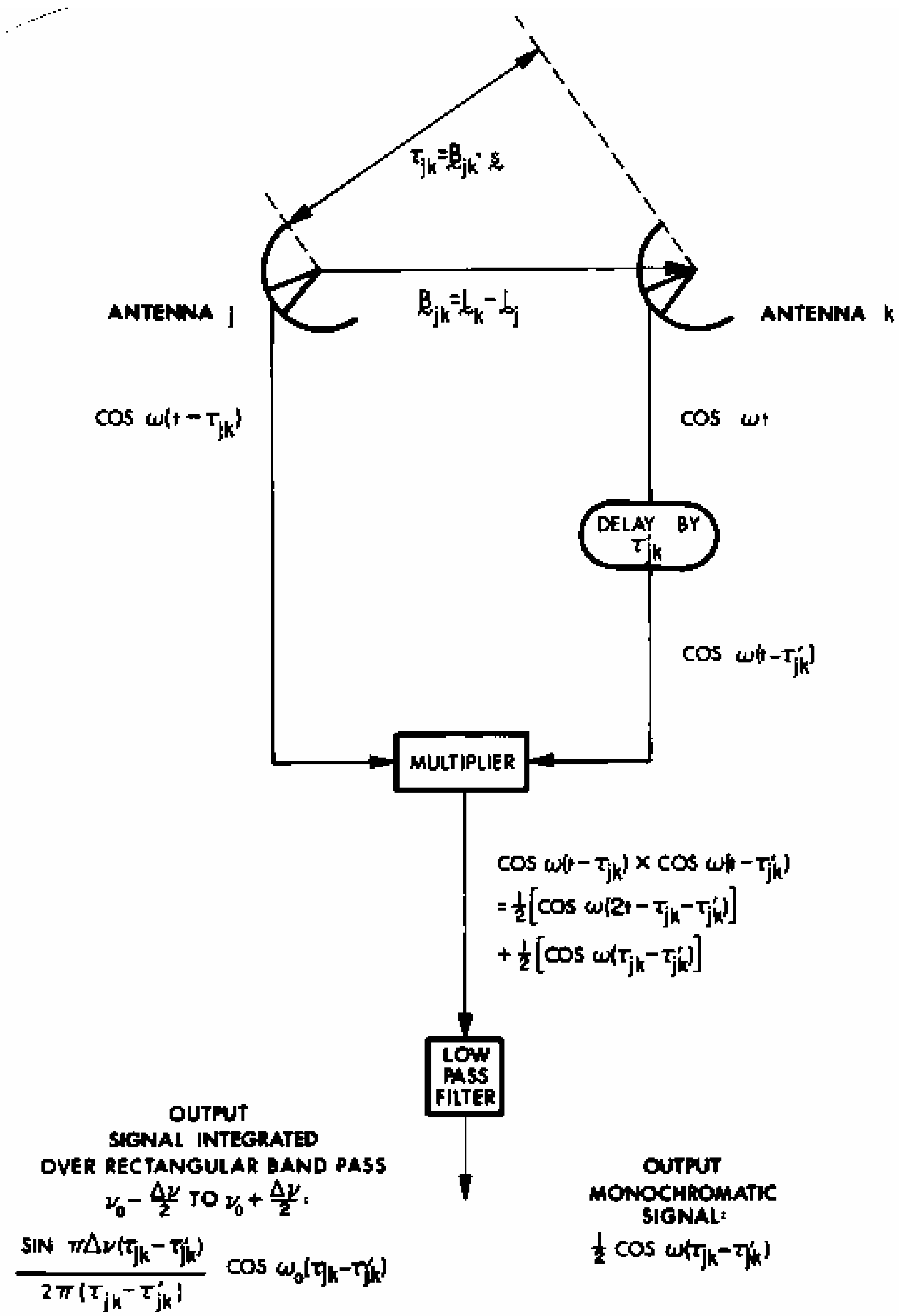

Figure 2 - 3. A simplified block diagram of the processing of pure RF signals from an interferometer pair.

Let E be the electric field strength of the incoming wavefront schematicized in Figure 2-2, and $G_j(v)$ and $G_k(v)$ be the multiplicatively accumulative amplifier power gains for frequencies between v and $v + \Delta v$ for telescopes j and k. These gains will represent everything that affects the amplitudes of the voltages propagating in the system. The output voltages for telescopes j and k, due to radiation in the RF range v to $v + \Delta v$ to when the same wavefront is producing the voltage response, can be represented in a quasimonochromatic form as

$$V_k(t) = \sqrt{\frac{1}{2} G_k(v) \Delta v} \; E \cos \omega t \qquad (2-6)$$

and

$$V_j(t) = \sqrt{G_j(v) \Delta v} \; E \cos \omega (t - \tau_{jk}) \qquad (2-7)$$

where the factors of 1/2 represent the fraction of the assumed unpolarized signal received by a single feed.

The representation of the cross-correlation output for antennas j and k is much more complicated than one would get by multiplying Equations 6 and 7. In order to illustrate this, let us first consider an unrealistically simplified model of how the signals from the two antennas could be processed. This model is shown in Figure 2-3 where cross-correlation (multiplication and filtering) is performed with the time dependent factors only after a simple delay compensation τ'_{jk} . All frequencies are RF. The multiplier output contains the sum of high- and low-frequency components, of which only the low frequencies are desired. A low-pass filter suppresses the high frequencies and producing a filter output proportional to cos $\omega(\tau_{jk} - \tau'_{jk})$ for a single monochromatic component. However, the antenna electronics actually pass a range of frequencies corresponding to a designated passband. The actual output voltages are, therefore, obtained by integrating the monochromatic output signal over the range v_o $\Delta v/2$ to $v_o + \Delta v/2$ (assuming uniform signal in this range and zero signal elsewhere) to obtain an output voltage from the low-pass filter proportional to

$$\mathrm{sinc}[\Delta v(\tau_{jk} - \tau'_{jk})] \cos \omega_o (\tau_{jk} - \tau'_{jk})$$

where sinc x = (sin π x)/x. A schematic representation of this idealized output signal is shown in Figure 2-4 for the case where $\mathbf{s} = \mathbf{s}_o$. We see that, if $(\tau_{jk} - \tau'_{jk})$ can be kept small enough, the signal can be kept on the strongest positive maximum of the envelope.

To show why we can simply integrate the monochromatic output over frequency to get the broadband output, we repeat the above procedure on a more generalized level. The signal from the radio source will be designated as m(t). Thus the two signals to the multiplier will be m(t-τ_{jk}) and m(t-τ'_{jk}). Multiplying these two signals in the time domain is the same as convolving the Fourier transform of each signal in the frequency domain. Mathematically,

$$\mathrm{F}[\mathrm{m}(\mathrm{t} - \tau_{\mathrm{jk}})\mathrm{m}(\mathrm{t} - \tau'_{\mathrm{jk}})] = [\mathrm{e}^{-\mathrm{i}2\pi\upsilon\tau_{\mathrm{jk}}}\mathrm{M}(\upsilon)] * [\mathrm{e}^{\mathrm{i}2\pi\upsilon\tau'_{\mathrm{jk}}}\mathrm{M}(\upsilon)]$$

where M(υ) is the Fourier transform of m(t), and the asterisk designates convolution. The phase terms are obtained with the shift theorem. Writing out the convolution gives

$$\mathrm{e}^{-\mathrm{i}2\pi\upsilon(\tau'_{\mathrm{jk}} - \tau_{\mathrm{jk}})} \int_{-\infty}^{\infty} \mathrm{M}(\upsilon')\mathrm{M}(\upsilon - \upsilon')\mathrm{e}^{-\mathrm{i}2\pi\upsilon'(\tau_{\mathrm{jk}} - \tau'_{\mathrm{jk}})}\mathrm{d}\upsilon'$$

The celestial signal is stochastic and can ideally be thought of as white noise over the bandwidth of the instrument. The expectation operator of the multiplier output can be carried inside the integral to the product of M functions because no other factor is stochastic. The expectation of M(υ')M($\upsilon - \upsilon'$) is zero everywhere except where $\upsilon = \upsilon'$ since the frequency components are not correlated with each other. Let E[M(υ)M(υ)] = I (an even function). Assuming the frequency response of the expectation process is unity over the bandwidth allows us to write the output as

$$\mathrm{I}\ \mathrm{e}^{[-\mathrm{i}2\pi\upsilon(\tau_{\mathrm{jk}} - \tau'_{\mathrm{jk}})]}\ 2\int_{\upsilon_o-(\Delta\upsilon/2)}^{\upsilon_o+(\Delta\upsilon)/2} \cos 2\pi\upsilon'(\tau_{\mathrm{jk}} - \tau'_{\mathrm{jk}})\mathrm{d}\upsilon'$$

and we now have an integral expression which is the same as that previously found by simply integrating the sinusoidal fringe expression over the bandwidth. The factor out front is an arbitrary phase shift. The important concept demonstrated here is that for an incoherent signal, a convolution of that signal with itself in the frequency domain reduces to an integral over the product with no frequency shift. We will use this concept again in future developments.

Extended radio sources, which have components at a position other than $\mathbf{s}_o$, are distorted in the mapping process. If $\tau'_{jk} = \tau_{jk}$ for $\mathbf{s} = \mathbf{s}_o$, outer source components do not have the proper delay compensation. Thus they will be attenuated. For the maximum baseline of 35 km the angular width between first nulls is 1.1 arcmin, which is defined as the field of view for 50-MHz bandwidth. Effects of this loss on the mapping process will be discussed later in this chapter.

The delay τ_{jk} can be as big as 120 μsec for a 35-km baseline, and for 1% accuracy we need to keep timing errors in delay compensation less than 0.01 v_o which is 0.5 ps (picoseconds) at 20 GHz. Timing accuracy of this order, 1 part in 2×10^{12}, is too hard to achieve, so a different approach is necessary. By mixing the RF signals from each antenna with an LO signal, one can convert the signals to intermediate frequencies (IF) before delay and multiplication. Phase is preserved in mixing so accuracy of timekeeping in delays need be only of the order of 0.01 Δv (for a baseband system) which is 0.2 nanosec for $\Delta v \sim 50$ MHz.

In actuality the VLA has a phase shifting network plus a delay network as shown in Figure 2-5. The phase shifters $\phi_{\mathrm{j}}(\mathrm{t})$ and $\phi_{\mathrm{k}}(\mathrm{t})$ in the LO signal paths keep the output signal within the time range of the central fringe (largest cycle) shown in Figure 2-4. The process of constantly changing the phases to "stop" the fringes is called lobe rotation since it is in effect moving the lobes of an antenna array. The "fine tuning" of the delay system to put the output signal on the peak of the central fringe is accomplished by the delays τ'_{j} and τ'_{k} in the IF paths.

In Figure 2-5 we show phase shifting in the RF signal and delay in the IF signal paths for *each* antenna. This is representative of the fact that the cross-correlated signals from each antenna pair will automatically have the correct delay compensation since delaying and phase shifting are done with respect to an arbitrary position at the center of the array for all N antennas. This is the first instance of the dominantly antenna-based treatment of VLA signal processing that the reader will encounter throughout this Introduction.

Figure 2-5 omits the many amplification stages in the system and the imperfections that may affect the signal phase. However, it does illustrate the essential aspects of the way phase information is handled for a plane wave observed as cos $(\omega t - \tau_{\mathrm{jk}})$ at the $\mathrm{j^{th}}$ antenna and cos ωt at the $\mathrm{k^{th}}$ antenna. The conversion of these signals to IF frequencies is accomplished by mixing them with an LO frequency v_o. By mixing with a phase shifted signal cos $(\omega \mathrm{t} + \phi_{\mathrm{j}})$ for the $\mathrm{j^{th}}$ antenna and cos $(\omega_{\mathrm{o}}\mathrm{t} + \phi_{\mathrm{k}})$ for the $\mathrm{k^{th}}$ antenna, one introduces not only the delay discussed previously, but also any other antenna-dependent phase corrections that can be computed and applied in real time. After filtering to eliminate all but the IF frequencies, the two signals proportional to cos $[(\omega - \omega_o)t - \omega\tau_{\mathrm{jk}} - \phi_j(t)]$ and cos $[(\omega - \omega_o)t - \phi_k(t)]$ are time delayed by $\tau'_j = \mathbf{L} \cdot \mathbf{s}_o$ and $\tau'_k = \mathbf{L}_k \cdot \mathbf{s}_o$. After multiplication together and passage through a low-pass filter, the IF signal response at frequency v is proportional to

$$\cos\{(\omega - \omega_{\mathrm{o}})[\tau_{\mathrm{jk}} - (\tau'_{\mathrm{k}} - \tau'_{\mathrm{j}})] + \omega_{\mathrm{o}}\tau_{\mathrm{jk}} - [\phi_{\mathrm{k}}(\mathrm{t} - \tau'_{\mathrm{k}}) - \phi_{\mathrm{j}}(\mathrm{t} - \tau'_{\mathrm{j}})]\}.$$

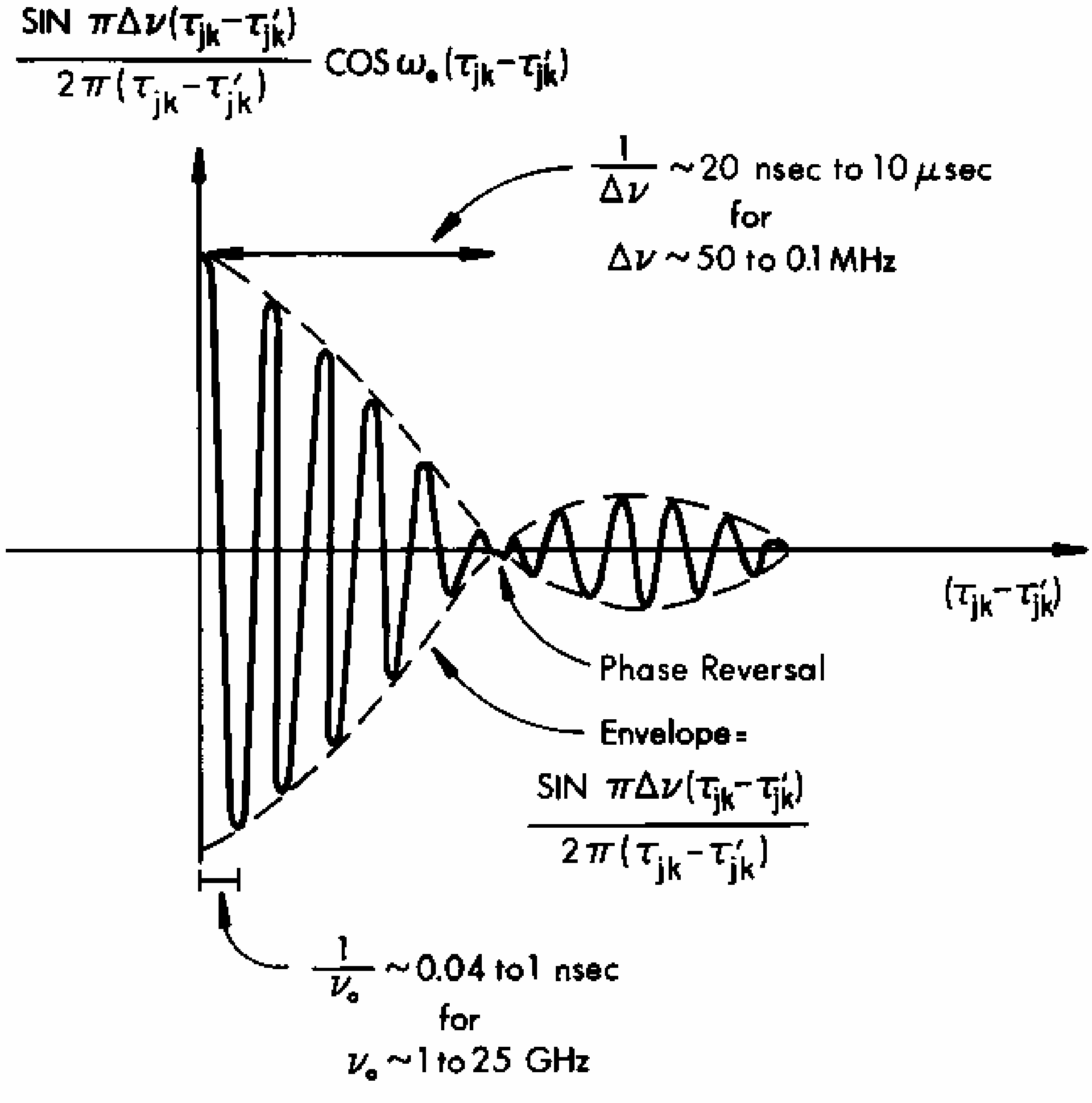

Figure 2 - 4. The theoretical signal output from the system shown in Figure 2-3. The location of the first null of the envelope defines one-half of the field of view.

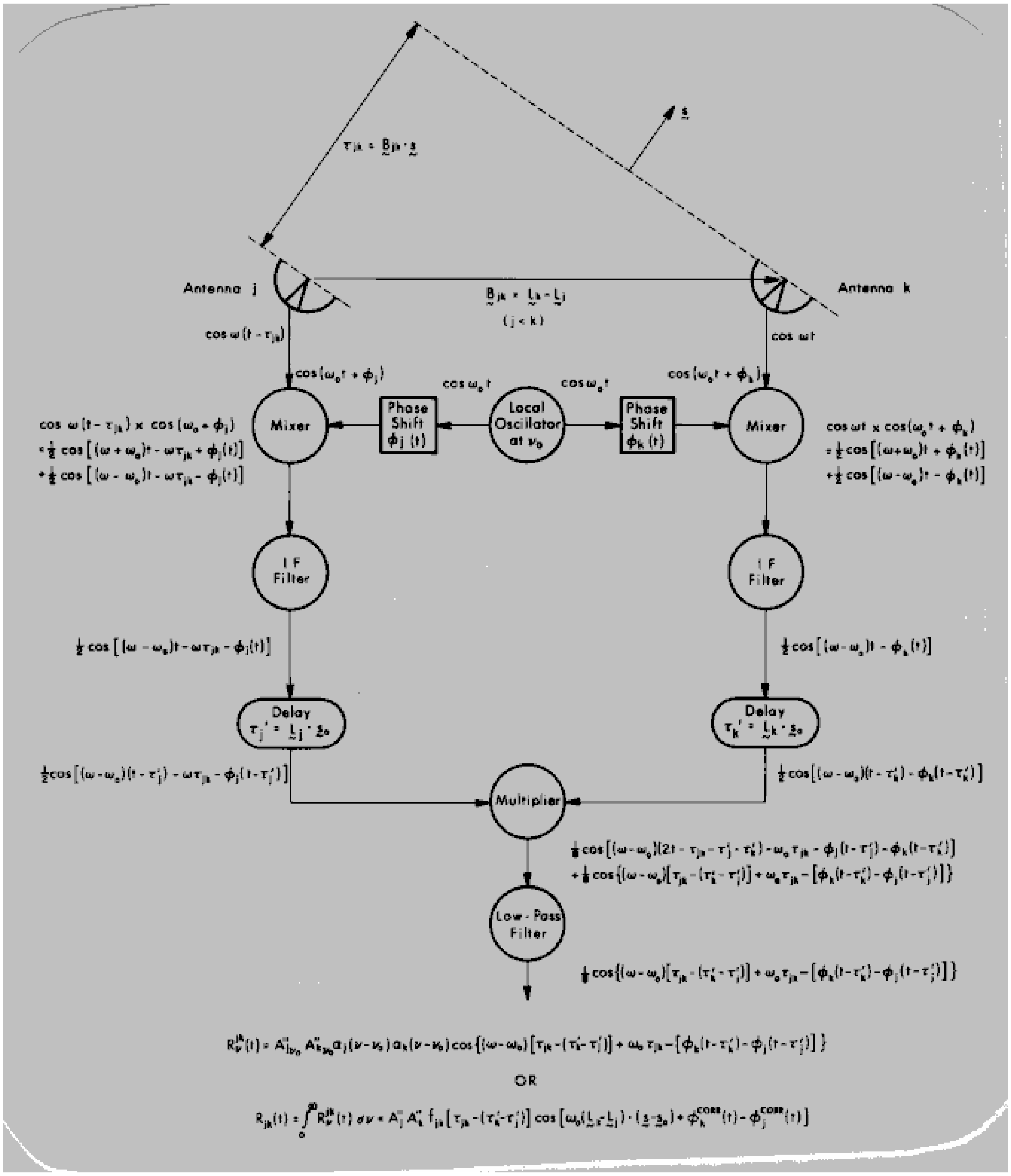

Figure 2 - 5. A simplified schematic of the signal path for a VLA interferometer pair.

Attaching the amplitude to this, the instantaneous response at frequency υ can then be written as

$$\mathrm{R}_{\upsilon}^{\mathrm{jk}}(\mathrm{t}) = \mathrm{A}''_{\mathrm{j}\upsilon_{\mathrm{o}}}\alpha_{\mathrm{j}}(\omega-\omega_{\mathrm{o}}) \cdot \cos\{(\omega-\omega_{\mathrm{o}})[\tau_{\mathrm{jk}}-(\tau'_{\mathrm{k}}-\tau'_{\mathrm{j}})] + \omega_{\mathrm{o}}\tau_{\mathrm{jk}} + [\phi_{\mathrm{k}}(\mathrm{t}-\tau'_{\mathrm{k}})-\phi_{\mathrm{j}}(\mathrm{t}-\tau'\mathrm{j})]\} \quad (2-8)$$

where

$$\mathrm{A}''_{\mathrm{j}\upsilon\mathrm{o}} = \sqrt{\mathrm{G}_{\mathrm{j}}(\upsilon_{\mathrm{o}})\Delta\upsilon}\ \mathrm{E} \quad (2-9)$$

[the amplitude from Equation 6 at frequency υ] is the band-pass function for the j[th] antenna. It is normalized such that $\int \alpha_j(\omega - \omega_o)\ d(\omega - \omega_o) = 1$. The total signal response is obtained by integrating $\mathrm{R}_{\upsilon}^{\mathrm{jk}}(\mathrm{t})$ over all frequencies. Letting $\omega' = \omega - \omega_o$ and $\Delta\tau = [\tau_{\mathrm{jk}} - (\tau'_{\mathrm{k}} - \tau'_{\mathrm{j}})]$, the phase dependent factor can be expanded as

$$\cos[\omega'\Delta\tau]\cos[\omega_{\mathrm{o}}\tau_{\mathrm{jk}} + (\phi_{\mathrm{k}} - \phi_{\mathrm{j}})] + \sin[\omega'\Delta\tau]\sin[\omega_{\mathrm{o}}\tau_{\mathrm{jk}} + (\phi_{\mathrm{k}} - \phi_{\mathrm{j}})].$$

If the band-passes are sufficiently symmetrical, only the even-function term contributes in the integral over frequency and one obtains

$$\mathrm{R}_{\mathrm{jk}}(\mathrm{t}) = \mathrm{A}''_{\mathrm{j}}\mathrm{A}''_{\mathrm{k}}\ \mathrm{f}[\tau_{\mathrm{jk}} - (\tau'_{\mathrm{k}} - \tau'_{\mathrm{j}})]\cos[\omega_{\mathrm{o}}\tau_{\mathrm{jk}} + \phi_{\mathrm{k}}(\mathrm{t}-\tau'_{\mathrm{k}}) - \phi_{\mathrm{j}}(\mathrm{t}-\tau'_{\mathrm{j}})] \quad (2-10)$$

where

$$\mathrm{f}_{\mathrm{jk}}[\tau_{\mathrm{jk}} - (\tau_{\mathrm{k}} - \tau_{\mathrm{j}})] = \int_{\mathrm{IF\ range}} \alpha_{\mathrm{j}}(\omega')\alpha_{\mathrm{k}}(\omega')\cos(\omega'\Delta\tau)\mathrm{d}\omega' \quad (2-11)$$

is the so-called *fringe-washing function* which is unity for identical, symmetrical band-pass under conditions of good delay tracking. Under these conditions, which should be valid for normal VLA operation, the output signal response is

$$\mathrm{R}_{\mathrm{jk}}(\mathrm{t}) = \mathrm{A}''_{\mathrm{j}}\mathrm{A}''_{\mathrm{k}}\cos\{\omega_{\mathrm{o}}\tau_{\mathrm{jk}} + [\phi_{\mathrm{k}}(\mathrm{t}-\tau'_{\mathrm{k}}) - \phi_{\mathrm{j}}(\mathrm{t}-\tau'_{\mathrm{j}})]\}. \quad (2-12)$$

Using $\tau_{jk} = (\mathbf{L}_k - \mathbf{L}_j) \cdot \mathbf{s}, \tau_j = \mathbf{L}_j \cdot \mathbf{s}_o$, and noting that the general form of the phase shift applied before RF to IF conversion is

$$\phi_j(t) = \omega_o \mathbf{L}_j \cdot \mathbf{s}_o - n(2\pi) + \phi_j^{corr}(t) \qquad (2-13)$$

where $\phi_j(t)$ Equation 12 then becomes

$$R_{jk}(t) = A_j'' A_k'' \cos\{\omega_o(\mathbf{k} - \mathbf{j}) \cdot (\mathbf{s} - \mathbf{s}_o) + [\phi_k^{corr}(t) - \phi_j^{corr}(t)]\} \qquad (2-14)$$

In the above equation, A_j'' is a constant proportional to the square root of the flux density of the point source being tracked for the i^{th} antenna system. In practice, when measuring and processing the interferometer response output, it is most convenient to deal with the amplitude and phase of a complex representation of the response function; thus, Equation 15 becomes

$$V'' = A_{jk}'' e^{i} \phi_{jk} = A_j'' A_k'' e^{\{i\omega_o(\mathbf{L} - \mathbf{L}_j) \cdot (\mathbf{s} - \mathbf{s}_o) + i[\phi_k^{corr} - \phi_j^{corr} + \phi_k^o - \phi_j^o]\}} \qquad (2-15)$$

where we now have system phase constants ϕ_i^o for the i^{th} antenna. The measured

$$A_{jk}'' \text{ and } \phi_{jk}'' = \phi_k'' - \phi_j'' \qquad (2-16)$$

are raw amplitude and phase measured as a function of time.

2.4 System Correction and Calibration

Because the correction and calibration of data from the VLA interferometers play such a major role in using the instrument, we will adopt a notation to describe these processes. Let the raw signal derived from the correlator output by the on-line computer system be described by double-primed quantities, such as

$$V_{jkp} = A_{jkp}'' e^{(i\phi_{jkp}'')} \qquad (2-17)$$

where p represents the polarization of the visibility data. The V''_{jkp} will have had the phase corrections (ϕ_j^{corr} and ϕ_k^{corr}) applied as part of the RF to IF conversion process.

The on-line, real time computer system can apply further corrections and calibration, as will be discussed in more detail later, before sending the visibility data on to the off-line computer system. We denote data corrected and calibrated on-line by single-primed quantities, such as

$$V'_{\mathrm{jkp}} = A'_{\mathrm{jkp}} e^{(i\phi'_{\mathrm{jkp}})}. \qquad (2-18)$$

These data are passed from the on-line computer system via fixed-head disk and magnetic tape to the off-line computer system where further corrections and calibration are applied. Let us denote data that have been corrected and calibrated by the off-line system by unprimed quantities as

$$V_{\mathrm{jkp}} = A_{\mathrm{jkp}} e^{(i\phi_{\mathrm{jkp}})}. \qquad (2-19)$$

Each VLA antenna has two feeds of orthogonal polarizations for each frequency. The 18-21 cm, 6, 2, and 1.25 cm band feeds are normally followed by circular polarizers, but linear polarizers can be inserted in the signal path to convert to linear polarization. We will be concerned with circular polarizations and will use the symbols L and R to represent left and right, respectively.

Any electromagnetic wave can be represented as left and right circularly-polarized components. Thus

$$\begin{aligned} E_L &= E_\ell e^{i\omega t} \\ E_R &= E_r e^{-i(\omega t + \theta)} \end{aligned} \qquad (2-20)$$

where ω is the phase difference between the two components. There are various ways of representing the information in a polarized wave, but the most common one in radio astronomy is Stokes parameters which are defined as follows:

$$\begin{aligned} I &= E_L E_L^* + E_R E_R^* = E_\ell^2 + E_r^2 \\ Q &= E_L E_R^* + E_R E_L^* = 2E_\ell E_r \cos\theta \\ U &= i(E_L E_R^* - E_R E_L^*) = 2E_\ell E_r \sin\theta \\ V_c &= E_L E_L^* - E_R E_R^* = E_\ell^2 - E_r^2 \end{aligned} \qquad (2-21)$$

The asterisk denotes complex conjugation. The advantage of this representation is that each product in the parenthesis corresponds to a quantity measurable with the interferometer.

Inverting the expressions we get

$$\begin{aligned} E_L E_L^* &= 1/2(I + V_c) = V_{jkLL} \\ E_R E_R^* &= 1/2(I - V_c) = V_{jkRR} \\ E_L E_R^* &= 1/2(Q - iU) = V_{jkLR} \\ E_R E_L^* &= 1/2(Q + iU = V_{jkRL}) \end{aligned} \qquad (2-22)$$

where the L and R subscript notation has been attached to the interferometer response, V_{jk}. Now that we have these relationships between the calibrated polarization data, we will derive the polarization version of the raw correlator visibilities V'_{jkp}.

The complex voltage, before cross-correlation of the j^{th} telescope, can be described as

$$\begin{aligned} R_j &= G_{jR} \cdot (E_R e^{-i\phi_p} + D_{jR} E_L e^{i\phi_p}) \\ L_J &= G_{jL} \cdot (E_L e^{i\phi_p} + D_{jL} E_R e^{-i\phi_p}) \end{aligned} \qquad (2-23)$$

where G_{jR} and G_{jL} are complex gains describing all the amplification and phase modification aspects of the j^{th} antenna, D_{jR} and D_{jL} describe the coupling between polarizations. ϕ_p is the parallactic angle which can be obtained from

$$\phi_p = \tan^{-1}\left[\frac{\cos\lambda_{lat}\sin H}{(\sin\lambda_{lat}\cos\delta - \cos\lambda_{lat}\sin\delta\cos H)}\right] \qquad (2-24)$$

where λ_{lat} is the VLA latitude. The parallactic angle (shown in Figure 2-6) is the angle between the source meridian and the elevation great circle of the VLA alt-az antennas.

An alternate technique for describing the instrumental polarization is to introduce Stokes parameters for the antennas. However, the above approach is more straightforward for instrumental calibration.

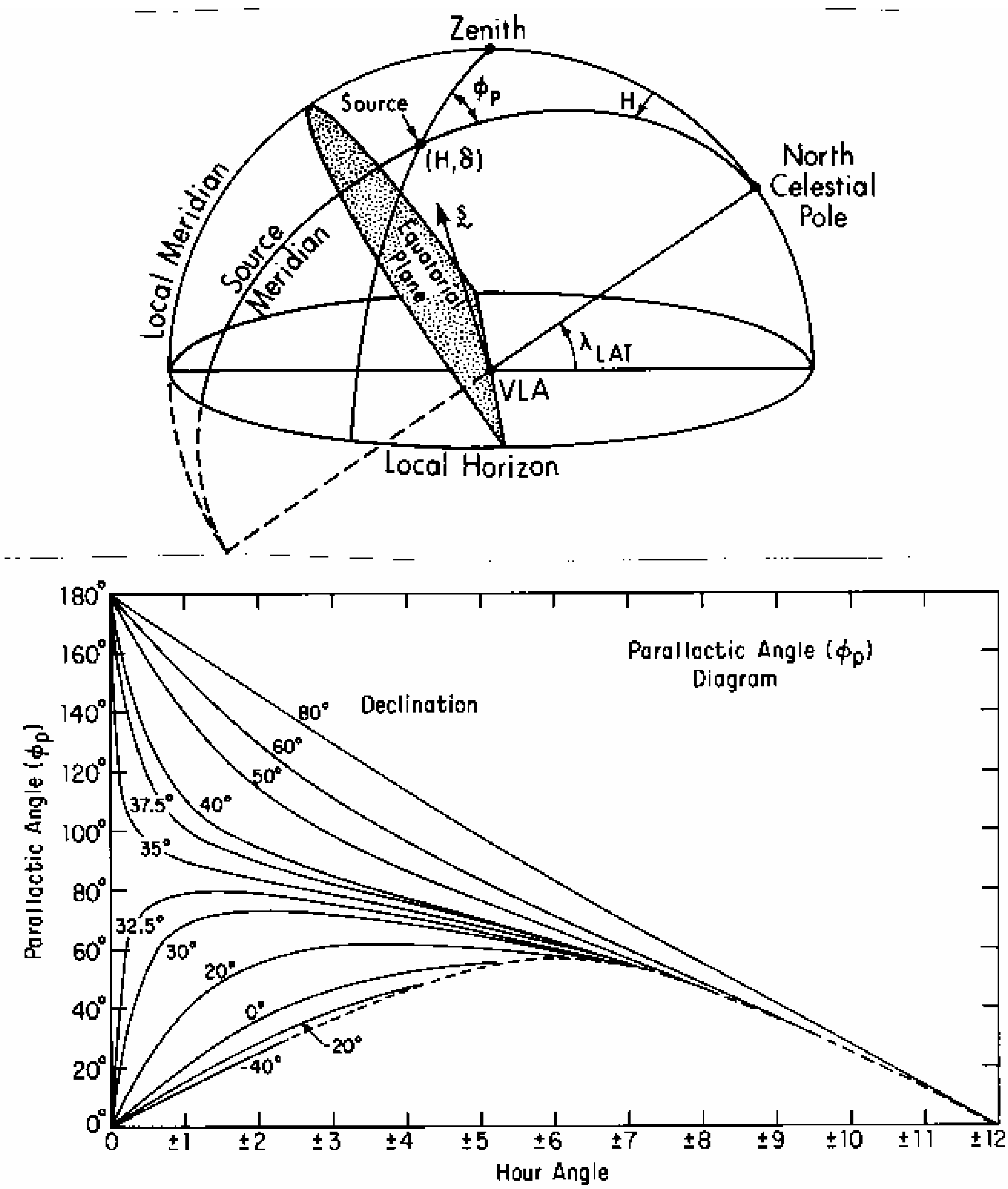

Figure 2 - 6. Parallactic angle ϕ_p is shown as the angle between the source meridian and the elevation great circle.

The measured correlator outputs are then represented as

$$\begin{aligned} V''_{\mathrm{jkLL}} &= L_j L_k^* \\ V''_{\mathrm{jkRR}} &= R_j R_k^* \\ V''_{\mathrm{jkLR}} &= L_j R_k^* \end{aligned} \qquad (2-25)$$

and

$$V''_{\mathrm{jkRL}} = R_j L_k^*$$

carrying out the multiplication for V''_{jkRR}, we get

$$V''_{\mathrm{jkRR}} = G_{\mathrm{jR}} \cdot G^*_{\mathrm{kR}} \cdot (E_R E_R^* + E_L E_L^* D_{\mathrm{jR}} e^{2i\phi_p} + E_R E_L^* E^*_{\mathrm{kR}} e^{-2i\phi_p} + D_{\mathrm{jR}} D^*_{\mathrm{kR}} E_L E_L^*)$$

and for $V''_{j\mathrm{kLR}}$, we get

$$V''_{\mathrm{jkLR}} = G_{\mathrm{jL}} \cdot G^*_{\mathrm{kR}} \cdot (E_L E_R^* e^{2i\phi_p} + E_L E_L^* D^*_{\mathrm{kR}} + E_R E_R^* D_{\mathrm{jL}} + E_R E_L^* D^*_{\mathrm{jL}} D_{\mathrm{kR}} e^{-2i\phi_p}).$$

In practice, the D's are less than 10% and the linear polarization of sources is typically 10% or less; therefore, $E_R E_L^*$ and $E_L E_R^*$ are 10% or less of $E_L E_L^*$ and $E_R E_R^*$. We can, therefore, neglect second and higher-order terms to obtain, after also using Equation 23,

$$\begin{aligned} V''_{\mathrm{jkLL}} &= G_{\mathrm{jL}} \cdot G^*_{\mathrm{kL}} \cdot V_{\mathrm{jkLL}} && (2-26) \\ V''_{\mathrm{jkRR}} &= G_{\mathrm{jR}} \cdot G^*_{\mathrm{kR}} \cdot V_{\mathrm{jkRR}} && (2-27) \\ V''_{\mathrm{jkLR}} &= G_{\mathrm{jL}} \cdot G^*_{\mathrm{kR}} \cdot (V_{\mathrm{jkLR}} e^{2i\phi_p} + V_{\mathrm{jkLL}} D^*_{\mathrm{kR}} + V_{\mathrm{jkRR}} D_{\mathrm{jL}}) && (2-28) \\ V''_{\mathrm{jkRL}} &= G_{\mathrm{jR}} \cdot G^*_{\mathrm{kL}} \cdot (V_{\mathrm{jkRL}} e^{-2i\phi_p} + V_{\mathrm{jkRR}} D^*_{\mathrm{kL}} + V_{\mathrm{jkLL}} D_{\mathrm{jR}}). && (2-29) \end{aligned}$$

Equations 27 - 30 describe how a set of four complex constants per antenna, G_{jR}, G_{jL}, D_{jR}, and D_{jL}, are sufficient to completely describe the relation between the true visibilities, V_{jkp} and the raw instrumental visibilities, V''_{jkp}. If one is not interested in linear polarization,only the V_{jkRR} and V_{jkLL} visibilities are relevant and the two complex constants, G_{jR} and G_{jL} are sufficient.

In practice, one observes point-source calibrators with known values of I, Q, U, V_c so the V_{jkp}'s can be obtained from the right-hand equalities in Equations 21. Then from measured V''_{jkp} one can solve Equations 26 - 29 for G_{jR}, G_{jL}, D_{jR}, and D_{jL}. Once these are known, we define

$$g_{jR} = 1/G_{jR}$$

and

$$g_{jL} = 1/G_{jL} \qquad (2-30)$$

and Equations 26 - 29 can be rearranged to give

$$\begin{aligned}
V_{jkLL} &= g_{jL} g^{*}_{kL} V''_{jkLL} && (2-31)\\
V_{jkRR} &= g_{jR} g^{*}_{kR} V''_{jkRR} && (2-32)\\
V_{jkLR} &= (g_{jL} \cdot g^{*}_{kR} V_{jkLR} - D_{jL} V_{jkRR} - D^{*}_{kR} V_{jkLL}) e^{-2i\phi_p} && (2-33)\\
V_{jkRL} &= (g_{jR} \cdot g^{*}_{kL} V_{jkRL} - D_{jR} V_{jkLL} - D^{*}_{kL} V_{jkRR}) e^{2i\phi_p} && (2-34)
\end{aligned}$$

as a set of equations by which V''_{jkp} data can be transformed into corrected and calibrated V_{jkp} data.

In practice, the VLA data processing system has both on-line and off-line application of corrections and calibration. Let us denote the on-line correction and calibration parameters as

$$g'_{jR}, g'_{jL}, D'_{jR}, D'_{jL}$$

and reserve double-primed parameters

$$g''_{jR}, g''_{jL}, D''_{jR}, D''_{jL}$$

for off-line correction and calibration parameters. However, since corrections like that of parallactic angle are not made twice, we assume that, if ϕ_p is applied in the on-line system, $\phi_p = 0$ in the off-line system, and vice versa.

The on-line computer system correction and calibration process can then be described as

$$\begin{aligned}
V'_{jkLL} &= g'_{jL} g'^{*}_{kL} V''_{jkLL} && (2-35)\\
V'_{jkRR} &= g'_{jR} g'^{*}_{kR} V''_{jkRR} && (2-36)\\
V'_{jkLR} &= (g'_{jL} \cdot g'^{*}_{kR} V''_{jkLR} - D'_{jL} V''_{jk} - D'^{*}_{kR} V'_{jkLL}) e^{-2i\phi_p} && (2-37)\\
V'_{jkRL} &= (g'_{jR} \cdot g'^{*}_{kL} V''_{jkRL} - D'_{jR} V''_{jkLL} - D'^{*}_{kL} V'_{jkRR}) e^{2i\phi_p} && (2-38)
\end{aligned}$$

and the off-line computer system correction and calibration process can be described as

$$
\begin{aligned}
\mathrm{V_{jkLL}} &= \mathrm{g''_{jL}\ g''^{*}_{kL}\ V'_{jkLL}} && (2-39)\\
\mathrm{V'_{jkRR}} &= \mathrm{g''_{jR}\ g''^{*}_{kR}\ V'_{jkRR}} && (2-40)\\
\mathrm{V_{jkLR}} &= \mathrm{(g''_{jL}g''^{*}_{kR}V'_{jkLR} - D''_{jL}V_{jk} - D''^{*}_{kR}V_{jkLL})e^{-2i\phi_p}} && (2-41)\\
\mathrm{V_{jkRL}} &= \mathrm{(g''_{jR}g''^{*}_{kL}V'_{jkRL} - D''_{jR}V_{jkLL} - D''^{*}_{kL}V_{jkRR})e^{2i\phi_p}} && (2-42)
\end{aligned}
$$

The corrected and calibrated V_{jkp} for a point source at a position s which has Stokes parameters I, Q, U, V_c will be described by

$$
\begin{aligned}
\mathrm{V_{jkLL}} &= \mathrm{(I + V_c + I_{noise} + V_{c,noise})\exp[i\omega_o(\mathbf{L}_k - \mathbf{L}_j)\cdot(\mathbf{s} - \mathbf{s}_o) + \phi_{noise}]} && (2-43)\\
\mathrm{V_{jkRR}} &= \mathrm{(I - V_c + I_{noise} - V_{c,noise})\exp[i\omega_o(\mathbf{L}_k - \mathbf{L}_j)\cdot(\mathbf{s} - \mathbf{s}_o) + \phi_{noise}]} && (2-44)\\
\mathrm{V_{jkLR}} &= \mathrm{(Q - iU + Q_{noise} - iU_{noise})\exp[i\omega_o(\mathbf{L}_k - \mathbf{L}_j)\cdot(\mathbf{s} - \mathbf{s}_o) + \phi_{noise}]} && (2-45)\\
\mathrm{V_{jkRL}} &= \mathrm{(Q + iU + Q_{noise} + iU_{noise})\exp[i\omega_o(\mathbf{L}_k - \mathbf{L}_j)\cdot(\mathbf{s} - \mathbf{s}_o) + \phi_{noise}]} && (2-46)
\end{aligned}
$$

In Equations 44 to 47 we have for the first time taken note of the fact that noise will be present in completely corrected and calibrated data by introducing a phase noise function (ϕ_{noise}) and a noise function for each Stokes parameter. In most equations these will not be included, but the user should be aware of their presence in all data.

In theory, the determination of calibration constants and their application to uncalibrated data to achieve calibration is very straight- forward. Observations of point sources with known values of $I = S_\upsilon$, Q, U, and V_c, which are relatively constant, are used in conjunction with Equations 26 - 30 and 21 to determine the complex functions

$$\mathrm{g_{jR},\ g_{jL},\ D_{jR},\ D_{jL}}$$

as parameters that remain constants over reasonable time scales (hopefully, days or longer). Non-calibrator source data observed over the same time scale that the calibration constants are known and stable are then calibrated using Equations 31 - 34.

2.5 Amplitude and Phase Noise

Let us briefly discuss the amplitude and phase noise introduced by the electronics system. If we define

$\Delta\upsilon$ = IF bandwidth

$\mathbf{T}_{\rm sys}$ = system noise temperature

$\mathbf{D}_{\rm ant}$ = diameter of each antenna (= 25 m)

$\epsilon_{\rm a}$ = aperture efficiency

$\epsilon_{\rm c}$ = 3 level correlator efficiency ≈ 0.82

then the theoretical rms noise fluctuation in the amplitudes for a single antenna-receiver pair is

$$\begin{aligned} \sigma &= \frac{4(\sqrt{2})\mathrm{k_B T_{sys}}}{\pi\epsilon_{\rm c}\epsilon_{\rm a}\mathrm{D}^2_{\rm ant}\sqrt{\Delta\upsilon\tau}} \\ &= \frac{2.2\times 10^{-4}\ \mathrm{T_{sys}}}{\epsilon_{\rm a}\sqrt{(\Delta\upsilon)_{\rm MHz}/50(\tau_{\rm sec}/10)}}\ \ \mathrm{Jy} \end{aligned} \qquad (2-47)$$

where $\mathrm{k_B}$ is the Boltzmann constant (1.38 x 10^{-23} joule K^{-1}) and t is the length of observing time involved. Using Equation 47 and the nominal values of $\mathrm{T_{sys}}$ and ϵ_a for each standard VLA frequency, one predicts the rms noise fluctuations listed in Table 2-1 for a single ten-second record.

For N antennas,

$$\sigma = \frac{2.2\times 10^{-4}\ \mathrm{T_{sys}}}{\epsilon_{\rm a}\sqrt{(\Delta\upsilon_{\rm MHZ}/50)(\tau_{\rm sec}/10)}} \qquad (2-48)$$

in which the noise decreases as the reciprocal square root of the number of antenna pairs.

Table 2 - 1
Amplitude Noise for Ten Seconds of Data for a Single Antenna Pair

Band	ϵ_a	T_{sys}	A_{noise} (Theoretical)
90 cm	50 %	150 K	0.026 $(50/\Delta\upsilon_{MHz})^{1/2}$ Jy
18-21 cm	50 %	60 K	0.026 $(50/\Delta\upsilon_{MHz})^{1/2}$ Jy
6 cm	65 %	60 K	0.017 $(50/\Delta\upsilon_{MHz})^{1/2}$ Jy
3.6 cm	54 %	110 K	0.12 $(50/\Delta\upsilon_{MHz})^{1/2}$ Jy
1.3 cm	46 %	130 K	0.17 $(50/\Delta\upsilon_{MHz})^{1/2}$ Jy

Next we turn to the probability distributions for both amplitude and phase of the fringes. The observed quantity consists of the signal S and the noise N vectorily added. We let

S = signal with constant amplitude

A = measured amplitude = S + N

N = noise = $Re^{i\theta}$

θ = phase noise = $\phi - \phi_{true}$

ϕ_{true} = constant phase of signal

ϕ = measured phase

To determine the joint probability density function for the fringe amplitude and phase, we assume that the true fringe amplitude, S, is a constant and that the rectangular components of the noise, R cos θ and R sin θ, are each Gaussian distributed with zero mean and variance σ^2. The joint probability distribution in rectangular coordinates is

$$P(\xi,\eta) = (2\pi\sigma^2)^{-1} \exp\left\{-(\xi+S)^2/(2\sigma^2) - (\eta^2)(2\sigma^2)\right\}.$$

This is transformed to polar coordinates by setting ξ=R cos θ, η=R sin θ, and multiplying $P(\xi,\eta)$ by the Jacobian, which in this case is A. Thus, the joint probability density function in polar form is

$$P(A,\theta) = (A/(2\pi\sigma^2)) \exp\left\{-\left[(A\cos\theta + S)^2/(2\sigma^2)\right] - \left[(A^2\sin^2\theta)(2\sigma^2)\right]\right\}. \qquad (2-49)$$

To find P(A) we integrate Equation 49 over θ which gives

$$P(A) = \int_0^{2\pi} P(A,\theta)d\theta \;=\; (A/(\sigma^2)) \exp\left[-(A^2+S^2)(2\sigma^2)\right] I_\circ\,(A/S\sigma^2)\,. \qquad (2-50)$$

This is known as the Rice-Nakagami distribution in which $I_o(x)$ is the modified Bessel function of the first kind, of order zero. It is unity when the argument is zero (no signal present). Plots of P(A) as a function of A/σ are shown in Figure 2-7 for various values of signal-to-noise ratio, Note that as S/σ increases, P(A) approaches a Gaussian distribution.

The probability density function for the phase is determined in a manner similar to finding P(A). Thus

$$P(\theta) = \int_0^{\infty} P(A,\theta)dA \;=\; [1/(2\pi)]\, e^{\left[-S^2/(2\sigma^2)\right]}\left[1 + G\,\pi^{\frac{1}{2}}\, e^{G^2}\,(1+\mathrm{erf}\ G)\right]$$

where erf is the error function and $G = S\cos\theta/(\sigma\sqrt{2})$. Without the signal S, the measured system output would have a uniform phase distribution and a Rayleigh amplitude distribution. Clearly, these distributions are altered by the presence of a signal.

The probability distribution of the phase, $P(\theta)$ is plotted in Figure 2-7 as a function of $\theta = \phi - \phi_{\rm true}$, for S/σ = 0, 1, 2, 3, and 5. We see that, in the absence of a signal, the phases are uniformly distributed. As the signal-to-noise ratio increases, the phase probability distribution has less and less deviation from the true phase, as seen from Figure 2-7 and the following table:

S/σ	$(\phi - \phi_{\rm true})_{P/P_{\max}=1/2}$
1	$\pm\ 55°$
2	$\pm\ 35°$
3	$\pm\ 22°$
4	$\pm\ 13°$

For large values of S/σ ($\geq$ 2),

$$(\phi - \phi_{\rm true})_{\rm P/P_{max}=1/2} \simeq \pm\ 65°/(S/\sigma). \qquad (2-51)$$

Examination of Figures 2-6 and 2-7 reveals the basic reasons why the presence of a weak source will always show up most easily in the phase information. The difference between the phase distributions for $S/\sigma = 0$ and 1 are much more obvious than the difference between the associated amplitude distributions.

2.6 Geometry and Coordinates

In the foregoing discussions in this section we concentrated on general concepts and avoided detailed discussions of geometry and coordinates. Let us now discuss these explicitly so further equations can be considered in greater detail.

There are only two basic coordinate systems involved in the VLA. One is an earth-oriented, topocentric system that we will call the $x_e - y_e - z_e$ system, and the other is a sky-oriented system that we will call $x_s - y_s - z_s$. Both systems are right-handed. Figure 2-9 shows the geometry and relationship between these systems.

In the earth-oriented system the z_e axis points to the north pole and the y_e axis points east. The origin of this system is the position arbitrarily defined as the center of the Y for the VLA. The geometry of the two coordinate systems and one pair of antenna as is shown in Figure 2-9. An example of station positions $\mathbf{L}_j$ and $\mathbf{L}_k$, with the resultant baseline vector $\mathbf{B}_{jk}$, is also shown for the case of the j^{th} antenna on station W56 and the k^{th} antenna on station E72, where $j < k$. In the $x_e - y_e - z_e$ system the standard polar angular coordinates (θ, ϕ) are related to declination and hour angle as shown, except ϕ = H for LST > α and ϕ = 360° - H for LST < α (the latter is shown on Figure 2-9).

The sky-oriented coordinate system as shown in Figure 2-9 is defined such that the z_s-axis extends along the vector $\mathbf{s}_o$ corresponding to the reference position so that $x_s - y_s$ are in the tangent plane to the celestial sphere at this point, with the x_s-axis pointing east as seen from the center of the wye and the y_s-axis pointing north.

In the earth-oriented system,

$$\mathbf{s} = \begin{pmatrix} \cos H \cos \delta \\ -\sin H \cos \delta \\ \sin \delta \end{pmatrix}_e \qquad (2-52)$$

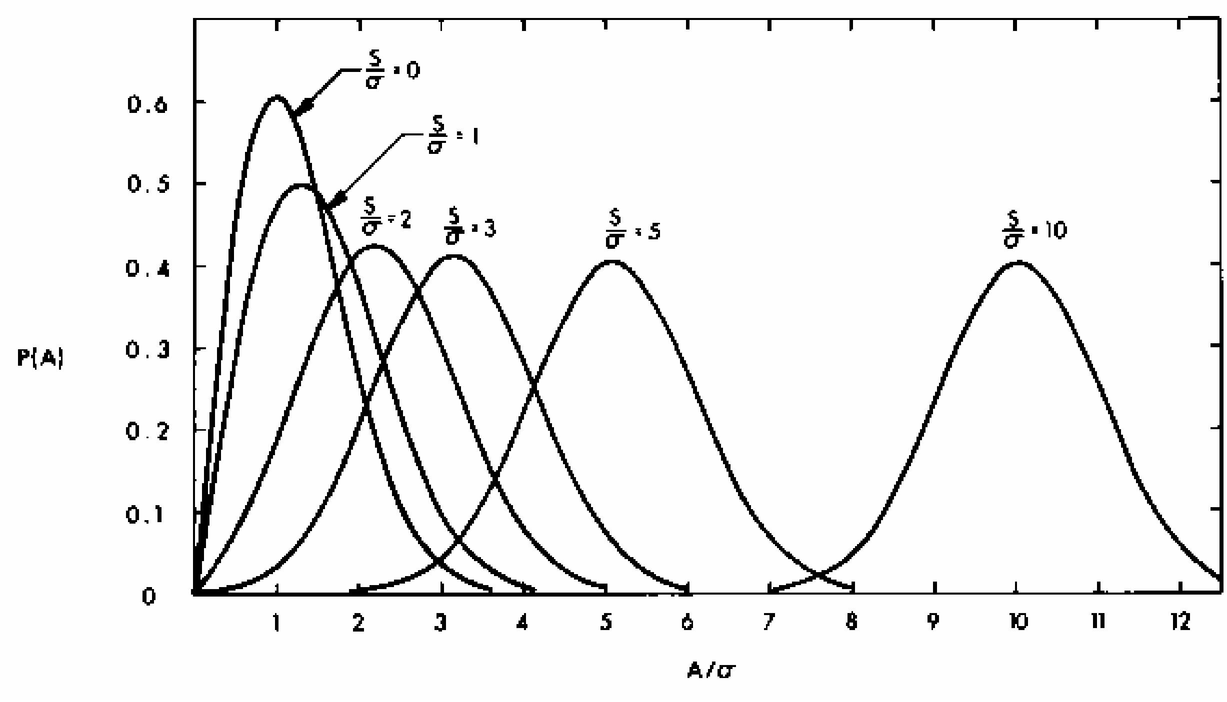

Figure 2 - 7. The probability distribution of measured amplitudes is plotted as a function of apparent signal-to-noise for a number of values of true signal-to-noise ratio.

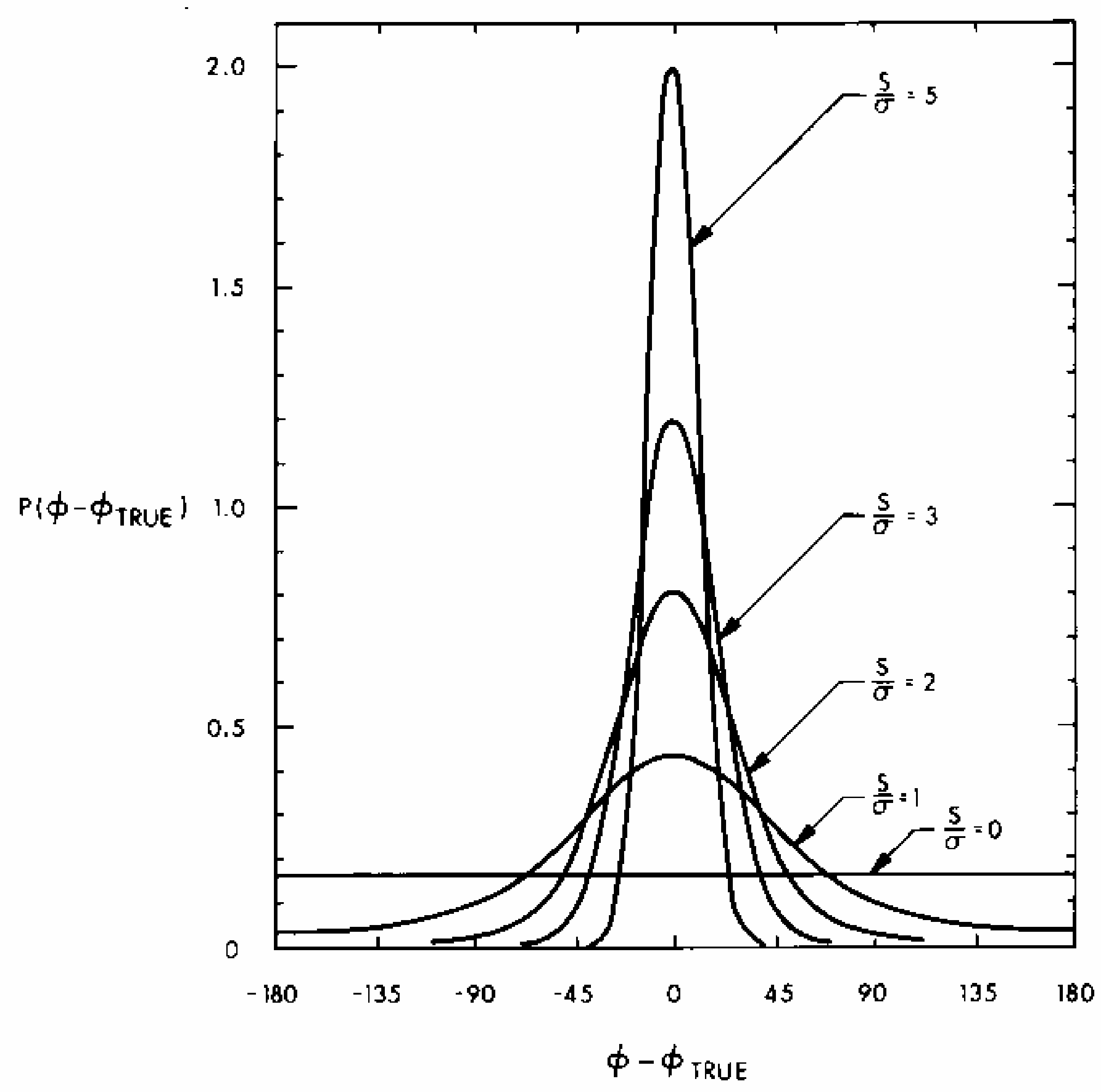

Figure 2 - 8. The probability distribution of measured phases is plotted as a function of $(\phi - \phi_{\rm true})$ for a number of values of signal-to-noise ratio.

In the earth-oriented system, the station position of

$$\mathbf{s}_{\rm o} = \begin{pmatrix} \cos \mathrm{H_o} \cos \delta_{\rm o} \\ -\sin \mathrm{H_o} \cos \delta_{\rm o} \\ \sin \delta_{\rm o} \end{pmatrix}_{\rm e}$$

where $\mathrm{H_o} = \mathrm{LST} - \alpha_{\rm o}$. In the earth-oriented system, the station position of the $\mathrm{j^{th}}$ antenna, as shown in Figure 2-9, is given by the appropriate dot products of coordinate unit vectors

$$\mathbf{L}_{\rm j} \; = \; (\mathbf{L}_{\rm jx}, \mathbf{L}_{\rm jy}, \mathbf{L}_{\rm jz})_{\rm e}. \qquad (2-53)$$

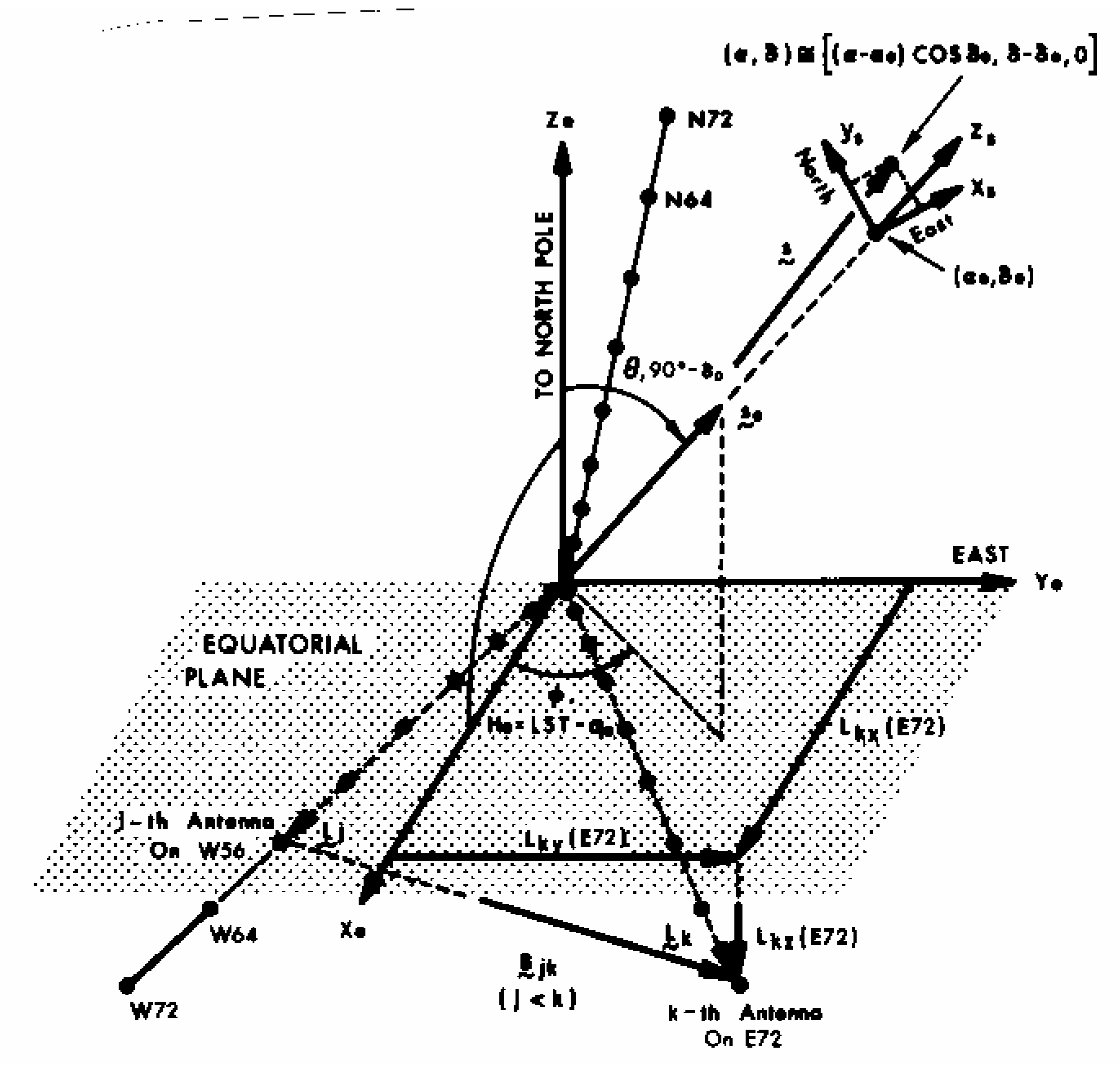

Figure 2 - 9. Geometrical relationships between the earth-oriented coordinate system (x_e, y_e, z_e) and the sky-oriented system (x_s, y_s, z_s).. $\mathbf{L}_j$ and $\mathbf{L}_k$ are vectors from the VLA wye center to two antennas on separate arms.

The transformation matrix from the earth-oriented system to the sky- oriented system is given in general by

$$M_{\mathrm{earth-sky}} = \begin{pmatrix} \mathbf{x}_e \cdot \mathbf{x}_s & \mathbf{y}_e \cdot \mathbf{x}_s & \mathbf{z}_e \cdot \mathbf{x}_s \\ \mathbf{x}_e \cdot \mathbf{y}_s & \mathbf{y}_e \cdot \mathbf{y}_s & \mathbf{z}_e \cdot \mathbf{y}_s \\ \mathbf{x}_e \cdot \mathbf{z}_s & \mathbf{y}_e \cdot \mathbf{y}_s & \mathbf{z}_e \cdot \mathbf{z}_s \end{pmatrix} \qquad (2-54).$$

The dot products appearing in each element are most easily determined from Figure 2-10 which is an altered presentation of the coordinate systems shown in Figure 2-9. The result is

$$\mathrm{M}_{\mathrm{earth-sky}} = \begin{pmatrix} \sin \mathrm{H} & \cos \mathrm{H} & 0 \\ -\sin\delta\cos\mathrm{H} & \sin\delta\sin\mathrm{H} & \cos\delta \\ \cos\delta\cos\mathrm{H} & -\cos\delta\sin\mathrm{H} & \sin\delta \end{pmatrix} \qquad (2-55).$$

The projection of the baseline vector $\mathbf{L}_j$ onto the plane of the sky tangent to **s** is a very significant vector. The length of the projection determines the resolution of the baseline (longer baseline $\sim$ better resolution), and the orientation of the projection determines the direction in which we have the resolution. u and v are the designations used for the east-west and north-south components of the projected baseline, respectively. An additional component, w, is a measure of the relative distance between the source and array center and between the source and any antenna. The u, v, w coordinates for an antenna-oriented description are determined from the transformation matrix, Equation 55, and the earth-oriented description of $\mathbf{L}_j$. Thus,

$$\mathrm{L}_j = \begin{pmatrix} u_j \\ v_j \\ w_j \end{pmatrix} = \begin{pmatrix} \sin \mathrm{H} & \cos \mathrm{H} & 0 \\ -\sin\delta\cos\mathrm{H} & \sin\delta\sin\mathrm{H} & \cos\delta \\ \cos\delta\cos\mathrm{H} & -\cos\delta\sin\mathrm{H} & \sin\delta \end{pmatrix} \begin{pmatrix} \mathrm{L}_{jx} \\ \mathrm{L}_{jy} \\ \mathrm{L}_{jz} \end{pmatrix}_e \qquad (2-56)$$

Executing the matrix product gives

$$u_j = \mathrm{L}_{jx}\sin\mathrm{H} + \mathrm{L}_{jy}\cos\mathrm{H} \qquad (2-57)$$

$$v_j = \sin\delta(-\mathrm{L}_{jx}\cos\mathrm{H} + \mathrm{L}_{jy}\sin\mathrm{H}) + \mathrm{L}_{jz}\cos\delta \qquad (2-58)$$

for the projection of the antenna position vector on the tangent plane of the sky and

$$w_j = \cos\delta(\mathrm{L}_{jx}\cos\mathrm{H} - \mathrm{L}_{jy}\sin\mathrm{H}) + \mathrm{L}_{jz}\sin\delta \qquad (2-59)$$

for the delay in time between the arrival of a wavefront from (α,δ) at the j^{th} antenna and at the center of the array.

Another necessary matrix relates a position (x, y, z,) in the sky- oriented system to the celestial coordinates (α,δ). If a surface segment of a sphere is projected onto a plane tangent to the sphere in the **s** direction we have

$$\mathbf{s} - \mathbf{s}_{\mathrm{o}} = \begin{pmatrix} \mathrm{x} \\ \mathrm{y} \\ \mathrm{z} \end{pmatrix}_{\mathrm{s}} = \begin{pmatrix} \cos\delta \sin(\alpha - \alpha_o) \\ -\sin\delta_o \cos\delta \cos(\alpha - \alpha_o) + \cos\delta_o \sin\delta \\ \cos\delta_o \cos\delta \cos(\alpha - \alpha_o) + \sin\delta_o \sin\delta - 1 \end{pmatrix} \qquad (2-60)$$

Figure 2-11 illustrates the tangent-plane geometry used in deriving Equation 60. Relationships for sin (θ) sin (A) and $\sin(\theta)$ cos(A) are determined from the law of cosines and law of sines applied to a spherical triangle defined by (α_o, δ_o), (α, δ) and the north celestial pole.

For the case in which θ is small, $\mathbf{s}$ - $\mathbf{s}_o$ can be approximated as

$$\mathbf{s} - \mathbf{s}_{\mathrm{o}} = \begin{pmatrix} \mathrm{x} \\ \mathrm{y} \\ \mathrm{z} \end{pmatrix}_{\mathrm{s}} \simeq \begin{pmatrix} (\alpha - \alpha_o)\cos\delta_o \\ (\delta - \delta_o) \\ 0 \end{pmatrix} \qquad (2-61).$$

The purpose of most of this discussion has been preparatory to writing explicit expressions for the vector projection $(\mathbf{L}_{\mathrm{k}}$ - $\mathbf{L}_{\mathrm{j}}) \cdot (\mathbf{s}$ - $\mathbf{s}_{\mathrm{o}})$, i.e.,

$$\begin{aligned} (\mathbf{L}_k - \mathbf{L}_j) \cdot (\mathbf{s} - \mathbf{s}_o) &= (\mathrm{u_k} - \mathrm{u_j}, \mathrm{v_k} - \mathrm{v_j}, \mathrm{w_k} - \mathrm{w_j}) \begin{pmatrix} \mathrm{x} \\ \mathrm{y} \\ \mathrm{z} \end{pmatrix} \\ &= \mathrm{u_{jk}x} + \mathrm{v_{jk}y} + \mathrm{w_{jk}z} \\ &= \mathrm{ux} + \mathrm{vy} + \mathrm{wz} \end{aligned} \qquad (2-62)$$

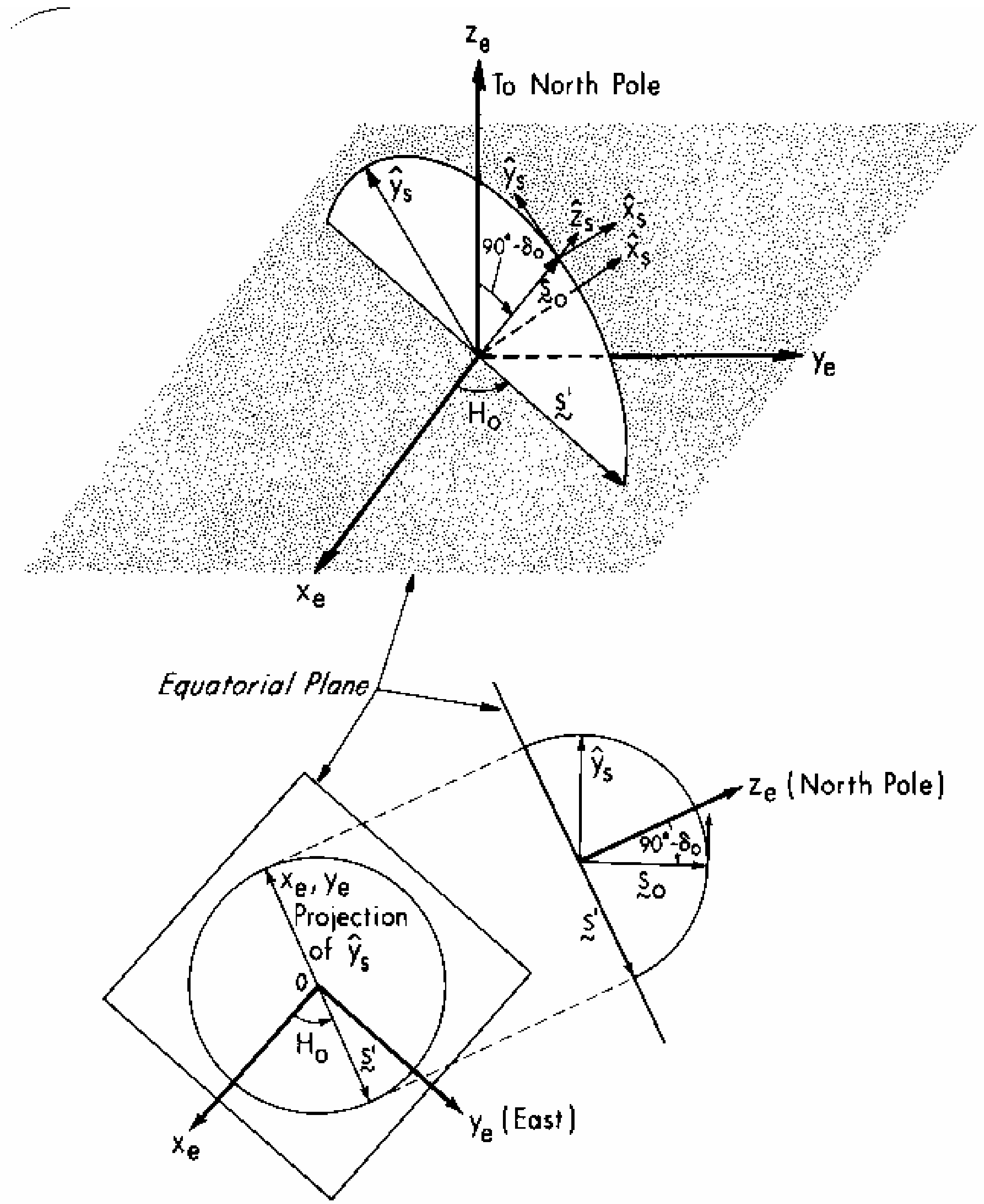

Figure 2 - 10. Geometrical presentation of earth and sky coordinate systems arranged for convenient determination of Equation (2-55).

where $u_{jk} = u_k - u_j, v_{jk} = u_k - u_j, w_{jk} = w_k - w_j$. The units of u,v,w are seconds of time. We have adopted a convention that will be used frequently whereby the lack of subscripts indicates the j-k pair; that is, (u, v, w,) = (u_{jk}, v_{jk}, w_{jk}). For the case in which the tangent plane approximation to the celestial sphere is valid, we have

$$(\mathbf{L}_k - \mathbf{L}_j) \cdot (\mathbf{s} - \mathbf{s}_o) \simeq u_{jk}x + v_{jk}y = ux + vy \qquad (2-63).$$

Because we will need to be careful about when we use Equation 62 and when the approximate Equation 63 is sufficient, let us evaluate the conditions under which the wz term can be neglected. From Figure (2-11) it can be seen that

$$z = \cos\theta - 1 \simeq \frac{-\theta^2}{2} \qquad (2-64)$$

so one can evaluate the importance of the zw term by putting it in terms of a phase

$$\phi_z = \frac{\omega_o w \theta^2}{2} \qquad (2-65)$$

is the angular radio frequency. Letting w = B/c, and putting B in units of a 35-kilometer baseline and θ in arcminutes

$$\phi = \left(\frac{53}{\lambda_{cm}}\right)\left(\frac{B_{km}}{35}\right)\ \theta^2_{arcmin} \quad \text{degrees.} \qquad (2-66).$$

B_{km} will range up to 35 and θ will typically range up to either $\theta_{HPBW/2}$ (c.f., Equation 1) or one-half the delay beamwidth caused by use of finite band-passes,

$$\theta_{delay} \simeq 1.2\left(\frac{50}{\Delta\upsilon_{MHz}}\right)\left(\frac{35}{B_{km}}\right) \quad \text{arcminutes} \qquad (2-67)$$

depending upon which is smaller. For the two cases

$$\theta^{max} = \frac{\theta_{HPBW}}{2} > \frac{\theta_{delay}}{2}, \phi_z^{max} = 38\lambda_{cm}\left(\frac{B_{km}}{35}\right) \quad \text{degrees} \qquad (2-68)$$

and

$$\theta^{\max} = \frac{\theta_{\text{delay}}}{2} < \frac{\theta_{\text{HPBW}}}{2}, \phi_{\text{z}}^{\max} = \left(\frac{18}{\lambda_{\text{cm}}}\right)\left(\frac{18}{\text{B}_{\text{km}}}\right)\left(\frac{50}{\Delta\upsilon_{\text{MHz}}}\right) \quad \text{degrees} \tag{2 – 69}$$

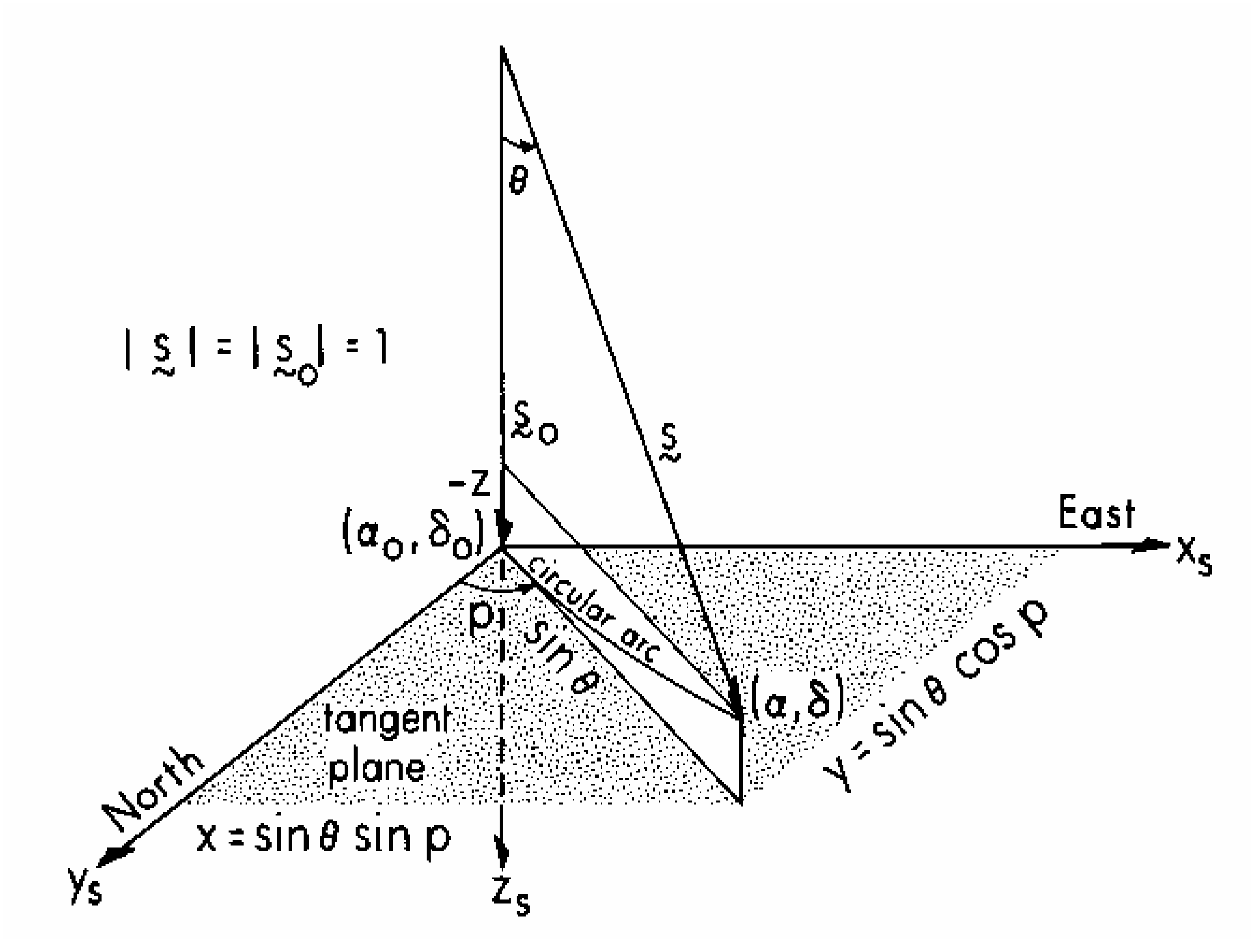

Figure 2 - 11. Inverted presentation of (x_s, y_s, z_s) coordinate system shown in Figure 2-9. Note that the line-of-sight path along s does not extend to the tangent plane

2.7 Visibility Function for a Point Source

Let I, Q, U, and V_c be the Stokes parameters for a point source located at a position **s** which is observed with a reference position **s**. Combining Equations 43 through 46 with Equation 62, the four corrected, calibrated correlator visibilities for this point source can be written as

$$V_{jkLL} = (I + V_c) \exp\left[i\omega_o(ux + vy + wz)\right] \quad (2-70)$$
$$V_{jkRR} = (I - V_c) \exp\left[i\omega_o(ux + vy + wz)\right] \quad (2-71)$$
$$V_{jkLL} = (Q - iU) \exp\left[i\omega_o(ux + vy + wz)\right] \quad (2-72)$$

and

$$V_{jkRL} = (Q + iU) \exp\left[i\omega_o(ux + vy + wz)\right] \quad (2-73)$$

neglecting noise effects, where $(\mathbf{s} - \mathbf{s}_o) = (x, y, z), \text{and}(\mathbf{L}_k - \mathbf{L}_j) = (u,v,w)$ in units of time. If we denote the visibility functions for the four Stokes parameters by V_{jkI}, V_{jkQ}, V_{jkU}, and V_{jkV}, then

$$V_{jkI} = S_\upsilon \exp\left[i\omega_o(ux + vy + wz)\right] \quad (2-74)$$
$$V_{jkQ} = Q \exp\left[i\omega_o(ux + vy + wz)\right] \quad (2-75)$$
$$V_{jkU} = U \exp\left[i\omega_o(ux + vy + wz)\right] \quad (2-76)$$

and

$$V_{jkV_c} = V_c \exp\left[i\omega_o(ux + vy + wz)\right] \quad (2-77)$$

where we explicitly identify the I Stokes parameter with the flux density S_υ. Under many circumstances we can neglect wz compared with (ux + vy), but we will carry the extra term in what follows even in those cases in which it is negligible. We will also frequently consider only the I Stokes parameter visibility, V_{jkI}, both because it is the most important and because from Equations 74 to 75 the functional forms of the others are the same. Equation 77 is strictly true only when the source does not have a large linear polarization. The treatment of polarization in this chapter, starting with Equation 34, will not handle the exceptional case of a highly elliptically polarized source.

2.8 Visibility Function for an Extended Source

We can now derive the equations for the visibility produced by observations of an extended source. We assume measured visibilities have been corrected and calibrated. Our derivation is based upon the principle that any infinitesimal region of the sky can be treated as a point source of radiation as far as any single interferometer pair is concerned. Let (α, δ) be the location of an infinitesimal solid angle $d\Omega$. By definition, the flux density S_υ for any source with an intensity distribution $I_\upsilon(\alpha, \delta)$ for the first Stokes parameter is given by

$$S_\upsilon = \int\int_{\text{source}} I_\upsilon(\alpha, \delta) d\Omega \qquad (2-78)$$

where $d\Omega = \cos\delta \; d\alpha \, d\delta$. Therefore, radiation from the infinitesimal solid angle $d\Omega$ can be considered to make an infinitesimal contribution to the flux density. If we further define $P(\alpha - \alpha_o, \delta - \delta_o)$ to be the normalized antenna power pattern, the contribution of the solid angle $d\Omega$ to the visibility function is given by the following generalization of Equation 74:

$$dV_{jkI}(\alpha, \delta) = P(\alpha - \alpha_o, \delta - \delta_o) I(\alpha, \delta) \exp\left[i\omega_o(\mathbf{L}_k - \mathbf{L}_j) \cdot (\mathbf{s} - \mathbf{s}_o)\right] d\Omega \qquad (2-79)$$

where for convenience we now drop the frequency subscripts. Integrating Equation 79 over the antenna beam, we get the integrated or total visibility

$$V_{jkI} = P(\alpha - \alpha_o, \delta - \delta_o) I(\alpha, \delta) \exp\left[i\omega_o(\mathbf{L}_k - \mathbf{L}_j) \cdot (\mathbf{s} - \mathbf{s}_o)\right] (\cos\delta) d\alpha d\delta \qquad (2-80).$$

The equations for V_{jkQ}, V_{jkU}, and V_{jkV} are altered accordingly with the $I(\alpha, \delta)$ distribution functions replaced by the spatial distribution function of the appropriate Stokes parameters.

Equation 80 is the complex Fourier transform of the apparent intensity distribution $P(\alpha - \alpha_o, \delta - \delta_o)\ I(\alpha, \delta)$. It is because of this that *we can describe any single complex visibility measurement as a single Fourier component of $P(\alpha - \alpha_o, \delta - \delta_o) I(\alpha, \delta)$.* Since Equation 80 is a Fourier integral, we can invoke all that we know about Fourier transforms to analyze and interpret interferometric data. In particular, we know how, in principle, to determine $P(\alpha - \alpha_o, \delta - \delta_o) I(\alpha, \delta)$ from VLA data by the Fourier inversion integral

$$\cos\delta \, P(\alpha - \alpha_o, \delta - \delta_o) I(\alpha, \delta) = \int\int\int V_I \exp\left[-i\omega_o(\mathbf{L}_k - \mathbf{L}_j) \cdot (\mathbf{s} - \mathbf{s}_o)\right] du\, dv\, dw \qquad (2-81).$$

The reader will note that Equation 80 is a two-dimensional integral over the celestial sphere, whereas Equation 81 is, in principal, a three- dimensional integral. Indeed, converting from (α, δ) to (x,y,z) using Equation 60 through 62 one transforms Equation 80 into

$$V_I(u,v,w) = \int\int P(x,y)I(x,y)\exp\left[-i\omega_o(ux+vy+wz)\right] dx\, dy \qquad (2-82)$$

where the integral is evaluated for on the celestial sphere, and Equation 81 becomes

$$P(x,y,z)I(x,y,z) = \int\int\int V_I(u,v,w)\exp\left[i\omega_o(ux+vy+wz)\right] du\, dv\, dw. \qquad (2-83).$$

Equation 83 needs the additional constraint $z \simeq -(1/2)(x^2+y^2)$ to get the "correct" radiation distribution on the celestial sphere.

In practice, one makes a finite number of discrete measurements of V_I(u,v,w) for finite integration times, so Equation 83 will be rewritten as the following summation equation:

$$\begin{aligned} P(x,y)I(x,y) = & \sum_{\substack{\text{measured} \\ u,v,w}} [V_I(u,v,w)\exp[-\omega_o(ux+vy+wz)] \\ & \quad + V_I^*(u,v,w)\exp[+\omega_o(ux+vy+wz)]\Delta u\Delta v\Delta w] \\ + & \sum_{\substack{\text{unmeasured} \\ u,v,w}} [V_I(u,v,w)\exp[-\omega_o(ux+vy+wz)] \\ & \quad + V_I^*(u,v,w)\exp[+\omega_o(ux+vy+wz)]\Delta u\Delta v\Delta w] \end{aligned} \qquad (2-84).$$

In Equation 84 we have invoked the Hermitian properties of V_I, V_I(-u,-v,-w) = V_I^*(u,v,w), that are required for the left-hand side of Equations 83 and 84 to be real. We have also conceptually separated measured and unmeasured visibilities.

2.9 Spectral Line Visibility

The visibility function for a spectral line system can be easily developed as an extension of the material in Section 8. We start with Equation 82 by adding a delay τ to the exponential function giving

$$\iint \mathrm{P(x,y)I(x,y)\exp -i[2\pi \upsilon\tau + 2\pi\upsilon(ux + vy + wz)]dx\,dy}.$$

In the system, this delay is located with the other delays shown in the oval in Figure 2-5. It is alternately positioned in one antenna path and then the other, so that we effectively have positive and negative lags.

Next, we integrate over the bandwidth to give

$$\mathrm{V_I(u,v,w,\tau)} = \iiint \mathrm{P(x,y,\upsilon)I(x,y,\upsilon)b(\upsilon)\cdot\exp -i[2\pi\upsilon\tau + 2\pi\upsilon(ux + vy + wz)]dx\,dy\,d\upsilon} \quad (2-85)$$

where $\mathrm{b}(\upsilon)$ is the frequency passband function.

Following the correlators, a synchronous computer and array processor calculate the Fourier transform of the visibility with respect to the delay τ. Since both positive and negative lags are used in the system only the real part of the visibility function is necessary. This will be shown below. The real part of the visibility function can be represented as

$$\begin{aligned}\mathrm{Re\{V_I(u,v,w,\tau)\}} = &\frac{1}{2}\iiint \mathrm{P(x,y,\upsilon)I(x,y,\upsilon)b(\upsilon)}\\ &\cdot\mathrm{\exp\{-i[2\pi\upsilon\tau + 2\pi\upsilon(ux + vy + wz)]\}dx\,dy\,d\upsilon}\\ &+\frac{1}{2}\iiint \mathrm{P(x,y,\upsilon)I(x,y,\upsilon)b(\upsilon)}\\ &\cdot\mathrm{\exp\{+i[2\pi\upsilon\tau + 2\pi\upsilon(ux + vy + wz)]\}dx\,dy\,d\upsilon}\end{aligned}\quad .$$

Now take the Fourier transform with respect to τ and re-arrange the integrals to integrate on τ first. Note that the limits on all integrals are over the entire range of the functions in the integrand.

$$\begin{aligned}&\int_{-\infty}^{\infty} \mathrm{Re}\{V_i(u,v,w,\tau)\}e^{\mathrm{i}2\pi\upsilon'\tau}d\tau\\ &\quad = \frac{1}{2}\iiint \mathrm{P(x,y\upsilon)I(x,y,\upsilon)b(\upsilon)e^{i2\pi\upsilon(ux + vy + wz)}}\int_{-\infty}^{\infty}\mathrm{e^{-i2\pi(\upsilon-\upsilon')\tau}d\tau\,dx\,dy\,d\upsilon}\\ &\quad + \frac{1}{2}\iiint \mathrm{P(x,y,\upsilon)I(x,y,\upsilon)b(\upsilon)e^{+i2\pi\upsilon(ux + vy + wz)}}\int_{-\infty}^{\infty}\mathrm{e^{+i2\pi(\upsilon-\upsilon')\tau}d\tau\,dx\,dy\,d\upsilon}\end{aligned}$$

The two integrals over τ give $\delta(\upsilon - \upsilon')$ and $\delta(\upsilon + \upsilon')$ respectively. Thus it is simple to integrate next with respect to υ. The result is

$$\int_{-\infty}^{\infty} \mathrm{Re}\{V_I(u,v,w,\tau)\} e^{i2\pi\upsilon\tau} d\tau$$

$$= \frac{1}{2} \iint_{-\infty}^{\infty} P(x,y,\upsilon) I(x,y,\upsilon) b(\upsilon) e^{-i2\pi\upsilon(ux + vy + wz)} dx\, dy$$

$$+ \frac{1}{2} \iint_{-\infty}^{\infty} P(x,y,-\upsilon) I(x,y,-\upsilon) b(\upsilon) e^{+i2\pi\upsilon(ux + vy + wz)} dx\, dy$$

Where the prime on υ has been dropped. P(x,y,υ) and I(x,y,υ) are even functions since their time domain counterparts are real functions. Hence our result reduces to

$$\int_{-\infty}^{\infty} \mathrm{Re}\{V_I(u,v,w,\tau) e^{i2\pi\upsilon\tau} d\tau = \iint P(x,y,\upsilon) I(x,y,\upsilon) b(\upsilon) e^{-i2\pi\upsilon(ux + vy + wz)} dx\, dy \quad (2-86)$$

The right hand side of Equation 86 appears to be the same as the right hand side of Equation 82. The difference is that Equation 82 is the visibility at the center radio frequency and Equation 86 is the visibility at one of the frequencies determined by the Fourier transform on τ. Thus the Fourier transform of the real part of V_I contains all the necessary visibility information for mapping the source at frequency υ. Theoretically, Equation 86 is an infinite continuous visibility function over all frequencies. In practice we would have a finite number of discrete frequencies determined by the number of lags in the system. Information on the number of available frequency channels versus bandwidth is given in Chapter 3. One additional requirement for spectral line work which is not necessary for continuum work is that the bandpass function b(υ) must be determined. Calibration procedures for this are discussed in Chapter 12.

2.10 U-V Plane Coverage

The values of (u,v,w) for which measurements of V_I are made, determine the quality of radio image reconstruction from visibility measurements. This is mostly a question of u-v coverage, and for the purposes of this section we will not consider the effects of w.

The ideal circumstance would be complete and uniform sampling of all (u,v) within a circular region in the so-called u-v plane. In practice,

$$u = u_k - u_j = (L_{kx} - L_{jx}) \sin H + (L_{ky} - L_{jy}) \cos H \qquad (2-87)$$

and

$$v = v_k - v_j = \sin\delta[-(L_{kx} - L_{jx}) \cos H + (L_{ky} - L_{jy}) \sin H] + (L_{kz} - L_{jz}) \cos \delta, \qquad (2-88)$$

and from these equations one can show that, for a particular antenna pair, u and v are related to each other by

$$\left(\frac{u}{a}\right)^2 + \left(\frac{v - v_o}{b}\right)^2 = 1 \qquad (2-89)$$

which is the equation for an ellipse, where

$$a = \sqrt{(L_{kx} - L_{jx})^2 + (L_{ky} - L_{jy})^2}, \qquad (2-90)$$

$$b = a \sin \delta, \qquad (2-91)$$

and

$$v_o = (L_{kz} - L_{jz}) \cos \delta. \qquad (2-92)$$

The u-v ellipse for a particular antenna pair has a center located at ($u=0, v=v_o$), with a major axis a, a minor axis b, and an eccentricity cos δ. The size of each u-v ellipse is, to first order, proportional to the physical separation between antennas, $\mathbf{B}_{jk} = \mathbf{L}_k$-$\mathbf{L}_j$. The u-v plane coverage formed by the 351 ellipses of the full 27 antenna VLA for A, B, C, or D configurations is shown for $\delta = 80°, 60°, 40°, 20°, 0°, -20°$, and $-40°$ in Figure 2-12. These ellipses are for continuous, elevation-limit-to-elevation-limit tracking for $\delta < 64°$ and 24^h tracking for $\delta > 64°$. Each measured (u-v) ellipse and the conjugate (-u,-v) ellipse are plotted, making 702 ellipses or segments of ellipses for each case in Figure 2-12.

Examination of Figure 2-12, with an eye to selecting the circular region of measurement to be used in reconstructing radio images, allows one to evaluate the location and severity of the problem of unmeasured u-v.

2.11 Radio Image Reconstruction By Direct Transform

A direct transform of measured visibilities into a radio image map can be obtained by neglecting the portion of Equation 84 dealing with nonmeasured visibilities and approximating P(x,y)I(x,y) by

$$P(x,y)\,I(x,y) \simeq \frac{\displaystyle\sum_{\substack{\text{measured}\\ u,v}} \left[V_I e^{-i\omega_o(ux+vy+wz)} + V_I^* e^{i\omega_o(ux+vy+wz)}\right] W(u,v)T(u,v)}{\displaystyle\sum_{\substack{\text{measure}\\ u,v}} W(u,v)T(u,v)} \qquad (2-93)$$

where $\Delta u \Delta v \Delta w$ has been replaced by an arbitrary weighting function W(u,v) and an arbitrary tapering function (u,v). Taking W(u,v) = 1 results in the so-called "natural" weighting, while taking W(u,v) = 1/N(u,v) results in the so-called "uniform" weighting, where N(u,v) is a function describing the relative density of measurements in the u-v plane. The tapering function T(u,v) allows an additional relative degree of emphasis of low resolution measurements vs. high resolution measurements. The most frequently used taper function is a Gaussian,

$$T(u,v) = \exp\left[-\left(\frac{u}{u_{taper}}\right)^2 - \left(\frac{v}{v_{taper}}\right)^2\right] \qquad (2-94)$$

where u_{taper} and v_{taper} are free parameters usually taken to be the same.

2.12 Point Source Images for the Full VLA

We know the visibility function for a point source from Equation 74. A point source exactly at the reference position will have $V_I = S_\upsilon$ where S_υ is the flux density. Because of this, one can evaluate the quality of a VLA radio image for any specified u-v coverage by calculating

$$P(x,y)I(x,y) \simeq \frac{\displaystyle\sum_{\substack{\text{measure}\\ u,v,w}} 2S_\upsilon \cos[\omega_o(ux+vy+wz)]W(u,v)T(u,v)}{\displaystyle\sum_{\substack{\text{measured}\\ u,v,w}} W(u,v)T(u,v)} \qquad (2-95)$$

which is obtained from Equation 93 for a point source at the reference position.

Point source image responses are sometimes called the synthesized beam or dirty beam, and sometimes called the point spread function. The synthesized beams made from uniform weighting mapping, for 27 antennas with full coverage tracking of sources as $\delta = 60°, 30°, 0°, \text{and} -30°$, are then shown in Figure 2-13. The central beams in Figure 2-13 are truncated to the 10% level.

The VLA with 27 antennas produces 351 baselines. The instantaneous u-v plane coverage, made up of the 702 points produced at any instant, is always in the form of a six-pointed star, with varying distortions for different declinations and hour angles. Figure 2-14 shows an instantaneous u-v plane distribution and synthesized beam for a source at $\delta = 30°$, $H = 0$. The principal sidelobe level in this map, made with uniform weighting, is 27%. More extensive observing of sources at this declination will result in improved beam shape and lower sidelobes. For example, Table 2-2 shows the decrease of maximum sidelobe level in the inner one-fourth and outer three-fourths of the beam as data on a source at $\delta = 30°$ increases.

Figure 2-15 shows the change in beam shape for the $\delta = 30°$, showing the map with fifteen minutes, one hour, two hours, six hours, and twelve hours of integration time.

Table 2 - 2

Sidelobe Levels for $\delta = 30°$ Buildup Map

H_{start}	H_{stop}	H_{range}	Inner 1/4 Maximum Sidelobe Level	Outer 3/4 Maximum Sidelobe Level
-6^h	-5^h45^m	15^m	27%	12%
-6^h	-5^h30^m	30^m	16	4
-6^h	-5^h	1^h	9	4
-6^h	-4^h	2^h	8	3
-6^h	-3^h	3^h	7	2
-6^h	-2^h	4^h	5	2
-6^h	0^h	6^h	3	2
-6^h	$+6^h$	12^h	3%	<1%

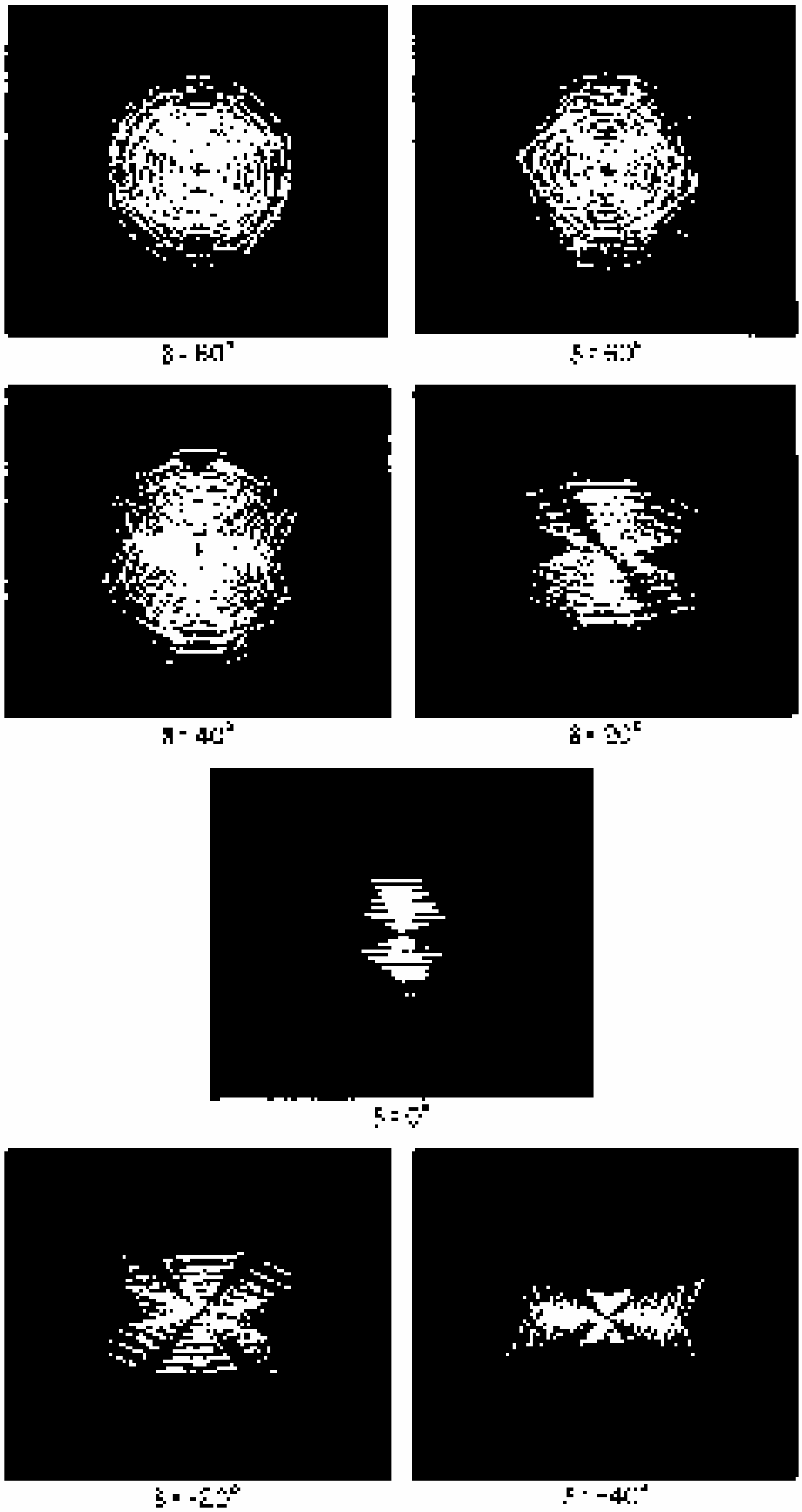

Figure 2 - 12. The possible u-v plane coverage for the 27-antenna VLA for declinations of 80°, 60°, 40°, 0°, −20°, −40°.

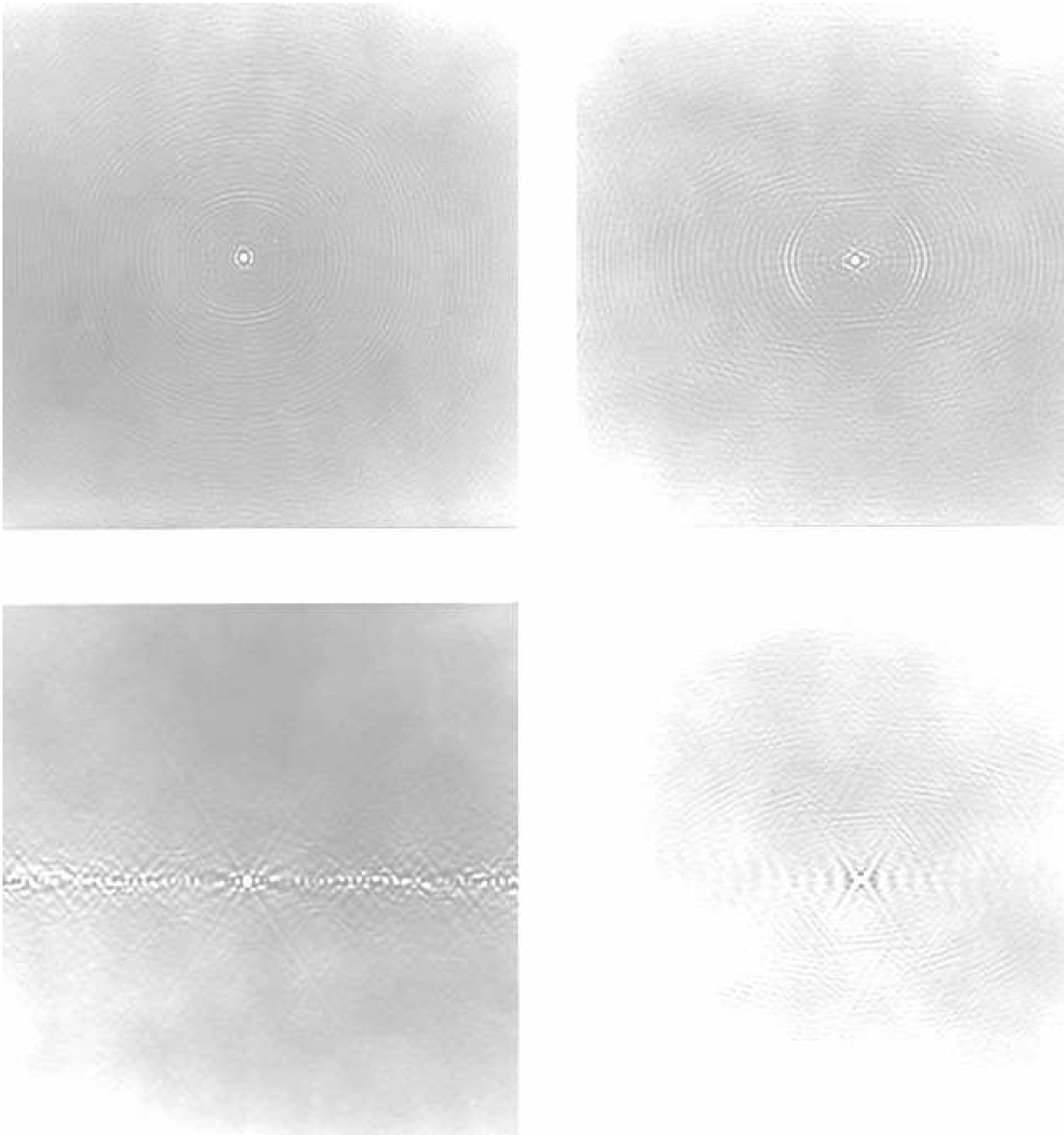

Figure 2 - 13. The synthesized beam for full tracking coverage of the 27-antenna VLA for a number of declinations. The main beam has been truncated to the 90% level to allow sidelobe patterns to be more visible

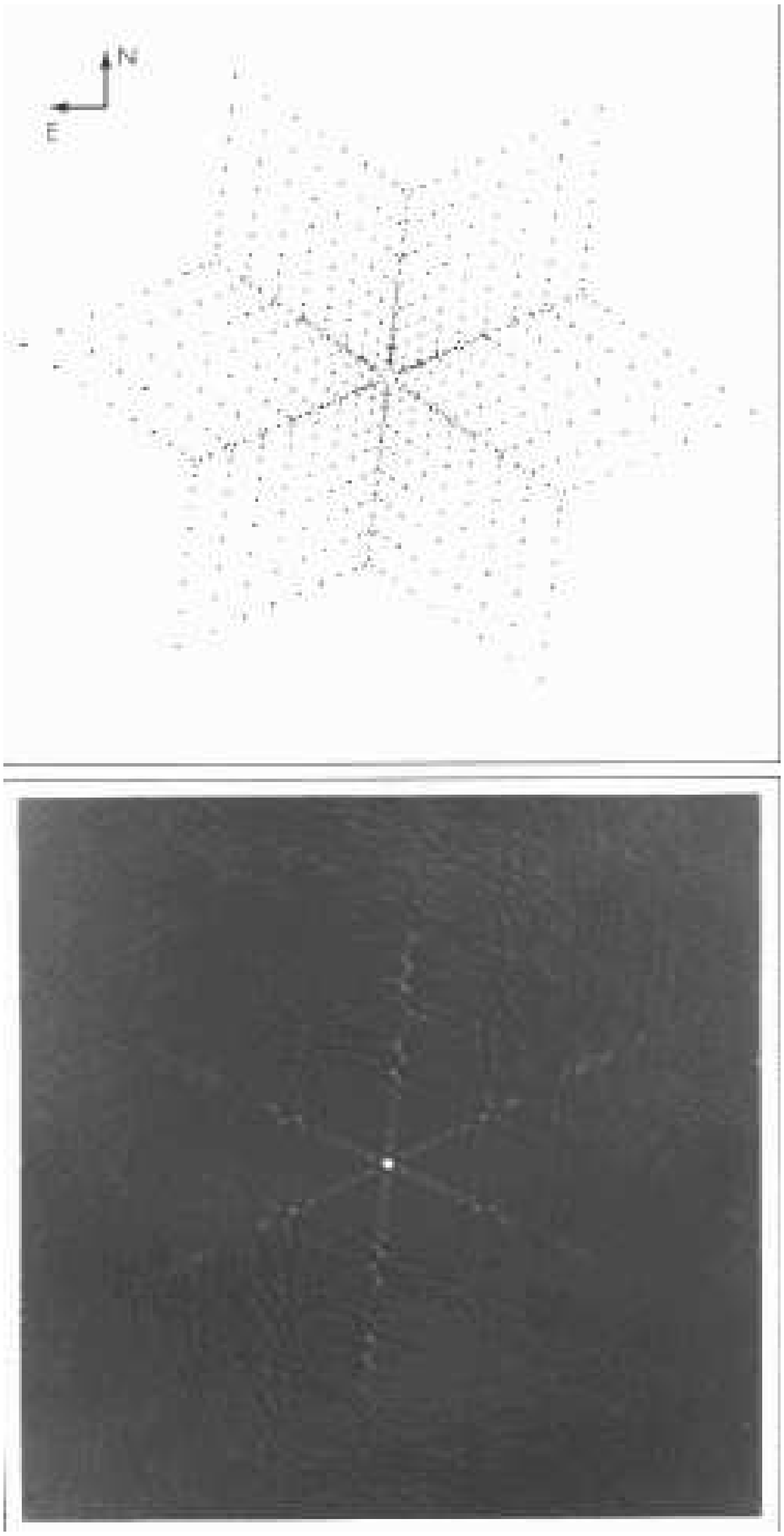

Figure 2 - 14. The u-v plane coverage an synthesized beam of an instantaneous sampling of data for a source at $\delta = 30°$ and H=0 for a 27-antenna VLA.

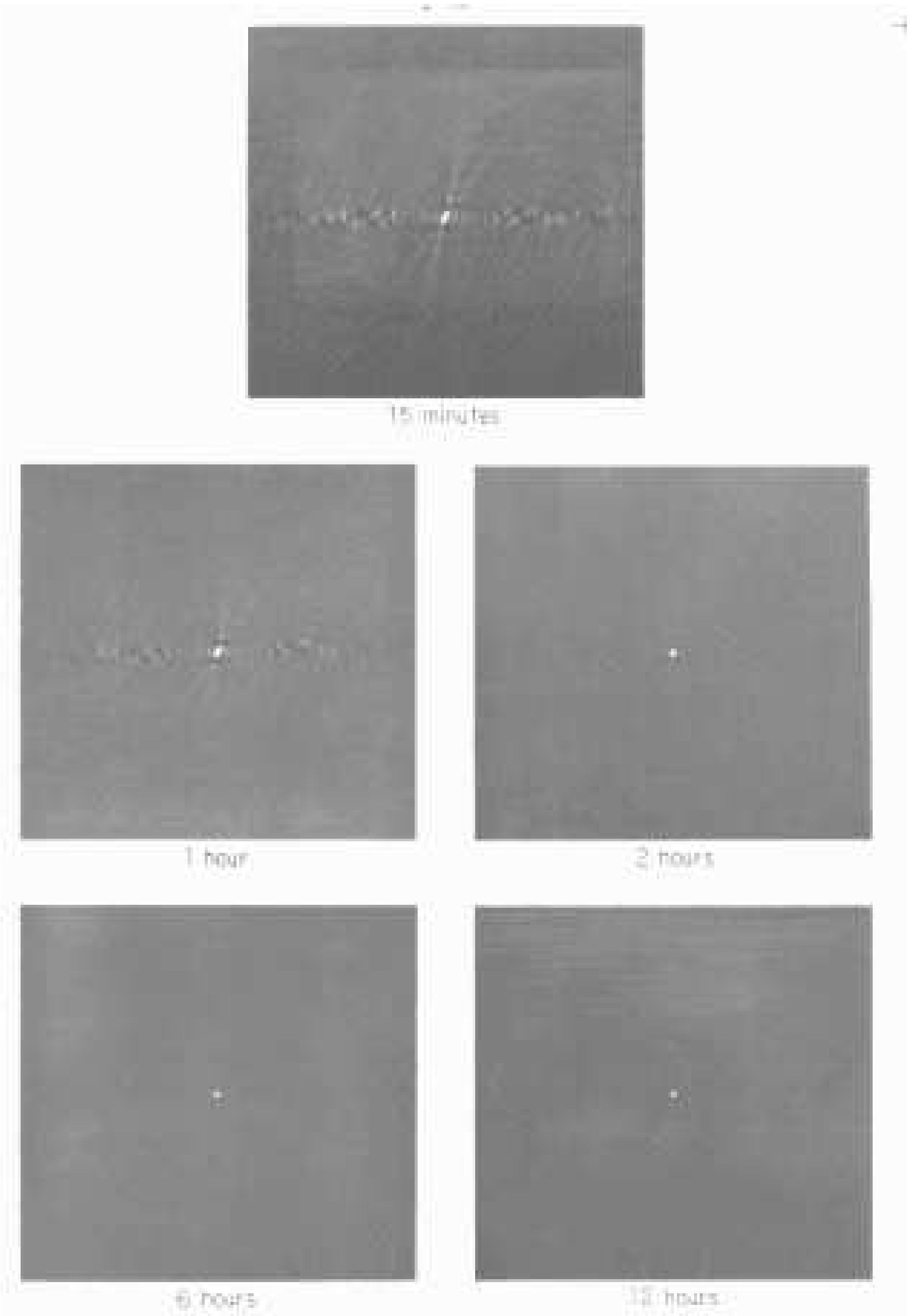

Figure 2 - 15. The changed synthesized beam patterns for a buildup map made form data continuously added to maps of a source at $\delta = 30°$, observed from H=-6^{h} to H=$+6^{h}$ with a 20-antenna VLA.

2.13 Radio Image Reconstruction with the FFT Algorithm

The direct transform method of radio image reconstruction discussed in a previous section is conceptually simple but expensive to use because the time needed to calculate an image is proportional to $N_x \cdot N_y \cdot N_{uv}$ where $N_x \times N_y$ is the size of the map and N_{uv} is the number of measured data points. The Cooley-Tukey FFT algorithm, on the other hand, takes computation time proportional to $N_x N_y \log(N_x N_y)$. For this reason most radio image reconstruction is based on the FFT algorithm.

The FFT algorithm in its most useful form requires that N_x and N_y are powers of two. It further requires that the visibility data be gridded into an $N_x \times N_y$ complex array before computation of a radio image from this rectangular (usually square) array.

In order to understand the general features of this process, let us introduce a useful way of describing the process in terms of how a true radio image, I_{true}(x,y) is affected by the major computational processes. We neglect all instrumental effects.

The true visibility function we denote by V_{true}(u,v), and denote the Fourier transform (and its inverse) by an overhead bar,

$$V_{true}(u, v) = \overline{I_{true}(x, y)} \qquad (2-96)$$

and

$$I_{true}(x, y) = \overline{V_{true}(u, v)}. \qquad (2-97)$$

If we denote the sampled or measured visibilities by V(u,v), then

$$V(u, v) = V_{true}(u, v) \cdot W(u, v), \qquad (2-98)$$

where W(u,v) is a combined sampling, weighting, and tapering function that can be described by

$$W(u, v) = \sum_{i=1}^{N_u} \sum_{j=1}^{N_v} W_{ij} T_{ij} \delta(u - u_i) \delta(v - v_j). \qquad (2-99)$$

In Equation 99 the weight W_{ij} and taper T_{ij} are those for the i,j-th point of the $N_u N_v$ measured (u_i, v_j) points in a real observing situation.

The required rectangular array of visibilities will be denoted by V_{grid}(u,v), and the process of obtaining this array can be described by

$$V_{\mathrm{grid}} = \mathrm{III}(u,v) \cdot [C(u,v) \times (V_{\mathrm{true}} \cdot W)] \qquad (2-100)$$

where * indicates convolution (in two dimensions in this case) and

$$\mathrm{III}(u,v) = \sum_{\ell=1}^{N_x} \sum_{m=1}^{N_y} \delta(u-u_\ell)\delta(v-v_m) \qquad (2-101)$$

is a two-dimensional sampling (shah) function which has nonzero values only on the grid points (u_ℓ, v_m) of a rectangular array of size $N_x \times N_y$, where both N_x and N_y are powers of two. The purpose of the convolution function, C(u,v), is to smooth the irregularly sampled data so that the result can be uniformly sampled by III(u,v).

The radio image or map is obtained from the Fourier transform of V_{grid}, so from Equations 97 and 100 we get

$$I(x,y) = \overline{\mathrm{III}} \times [\overline{C} \cdot \overline{WT\omega} \times I_{\mathrm{true}}] \qquad (2-102)$$

We used the convolution theorem for Fourier transforms

$$\overline{A \times B} = \overline{A} \cdot \overline{B} \qquad (2-103)$$

and its close relative

$$\overline{A \cdot B} = \overline{A} \times \overline{B} \qquad (2-104)$$

The point spread function or synthesized beam is found by setting $I_{\mathrm{true}}(x,y) = \delta(x)\delta(y)$ in Equation 102

$$I_{\mathrm{beam}}(x, y) = \mathrm{III} \times (\overline{C} \cdot \overline{W}) \qquad (2-105)$$

The function W is a type of point spread function obtained purely from the sampling, weighting, and tapering of original measurements. The function I_{beam}(x,y) is a modified point spread function including the effects of convolution before gridding and the gridding process itself.

The Fourier transform of the shah function is again a shah function with adjacent delta functions separated by the reciprocal of the separation in the untransformed domain. Thus, if the separation between two adjacent delta functions is four units in the uv plane, the separation is one-fourth unit in the xy plane. The result of convolving III with C W is to replicate C W about each delta function. If the sampling interval is too large in the uv plane (called undersampling), the consequentially smaller sampling interval in the xy plane will cause adjacent replications of C W to overlap. This effect is called aliasing because high frequencies can impersonate low frequencies in this overlap area. The effects of aliasing caused by real sources are reduced when the mapped area corresponds to the main antenna beam, outside of which, sensitivity to sources is greatly reduced. In addition, the convolution with C during the process of gridding causes a point outside the mapped area to be reduced in intensity by the ratio $C(x_a, y_a)C(x_m, y_m)$ when aliased into the map at the point (x_m, y_m). The ideal case where this ratio is zero would be obtained if C(u,v) were a two-dimensional sinc function, but the computing time would be very large. Under many practical circumstances C(u,v) can be taken to be a two-dimensional Gaussian with the convolution applied only over a small range of u-v points, which results in a considerable reduction in aliasing. The simplest convolution function is the so-called box convolution where all data within half a cell of a grid point are complex averaged into a single visibility. Aliasing badly attenuated when box convolution is used.

2.14 Map Sizes and the Number of Point per Synthesized Beam

An aperture with a diameter B will have a half-power beamwidth (HPBW) given by

$$\theta_{\mathrm{HPBW}} = 1.24(\lambda/B)\mathrm{radians} \qquad (2-106)$$

Let us denote the number of points per synthesized beam by N_{pts} and the size of a radio map by $N_x \times N_y$. For a map size equal to θ_{HPBW} of a VLA antenna, the number of linear points in a map can then be derived from N_{pts} times the ratio of θ_{HPBW} for a VLA antenna (Equation 1) and the θ_{HPBW} for a synthesized aperture of size B_{km} (Equation 106), e.g.,

$$N_x = 34 N_{pts} B_{km}. \qquad (2-107)$$

The values of N_{pts} that are desirable range from a minimum of 2 to a display or map cleaning oriented value of 4 or 5. In practice, Equation 107 is basically for a synthesized aperture with uniform weighting and no tapering. Natural weighting and tapering broaden the synthesized beam so that smaller map sizes (N_x, N_y) will suffice for a particular N_{pts}. Table 2-3 gives the map sizes for $N_{pts} = 2$ and 4 for the arm length of each configuration.

In practice, N_x and N_y must be powers of 2, so that reasonable maps of 4 or more points per beamwidth will be made for apertures in the A, B, C and D configurations by taking N_x or N_y equal to 8192, 2048, 1024, and 128. The trade-offs in mapping regions larger than the antenna HPBW, selecting different values of N_{pts}, or choosing u-v plane apertures larger or smaller than array arm lengths are obvious.

Table 2 - 3
Map Sizes for Different Configurations

Configuration	Arm Length, km	N_x or N_y	
		$N_{pts} = 2$	$N_{pts} = 4$
A	21	2560	5121
B	6.4	780	1560
C	1.95	237	475
D	0.60	36	72

2.15 Gridding, Cell Sizes, and the Sampling Theorem

Let us denote cell spacings or cell sizes of radio maps by $(\Delta x, \Delta y)$ of gridded u-v plane apertures by $(\Delta u, \Delta v)$. The angular size of field of view for a map is then $(N_x \Delta x, N_y \Delta y)$ and the size of the gridded u-v aperture $(N_x \Delta u, N_y \Delta v)$. The use of the FFT algorithm in radio image reconstruction imposes a constraint between the cell sizes in the u-v plane and the angular size of a map because of the sampling theorem. For an overall u range of $N_x \Delta u v_o = u_c$ in radians (u_c is called the cutoff frequency) we must sample in the x domain at an interval of $1/2u_c$. Thus we have

$$\Delta \mathrm{u} = \frac{1}{2\mathrm{N_x}\Delta \mathrm{x} \upsilon_\mathrm{o}} \qquad (2-108)$$

and similarly

$$\Delta \mathrm{v} = \frac{1}{2\mathrm{N_y}\Delta \mathrm{y} \upsilon_\mathrm{o}} \qquad (2-109)$$

where υ_o is the observing frequency, Δu and Δv are in units of time, and Δx and Δy are in units of radians. The relation between a gridded u-v plane for the full VLA observing source at $\delta = 40°$ and the corresponding radio map of a point source is shown in Figure 2-16.

If we select $\mathrm{B_{km}} \times \mathrm{B_{km}}$ to be the size of the u-v plane aperture we grid for mapping, then $\mathrm{N_y}\Delta\mathrm{vc} = \mathrm{N_x}\Delta\mathrm{uc} = 10^5\mathrm{B_{km}}$ with c in cm/s, and Equations 108 and 109 can be used to obtain

$$\Delta \mathrm{x} = \Delta \mathrm{y} = 1.03'' \left(\frac{\lambda_\mathrm{cm}}{\mathrm{B_{km}}}\right) \qquad (2-110)$$

for the map cell size.

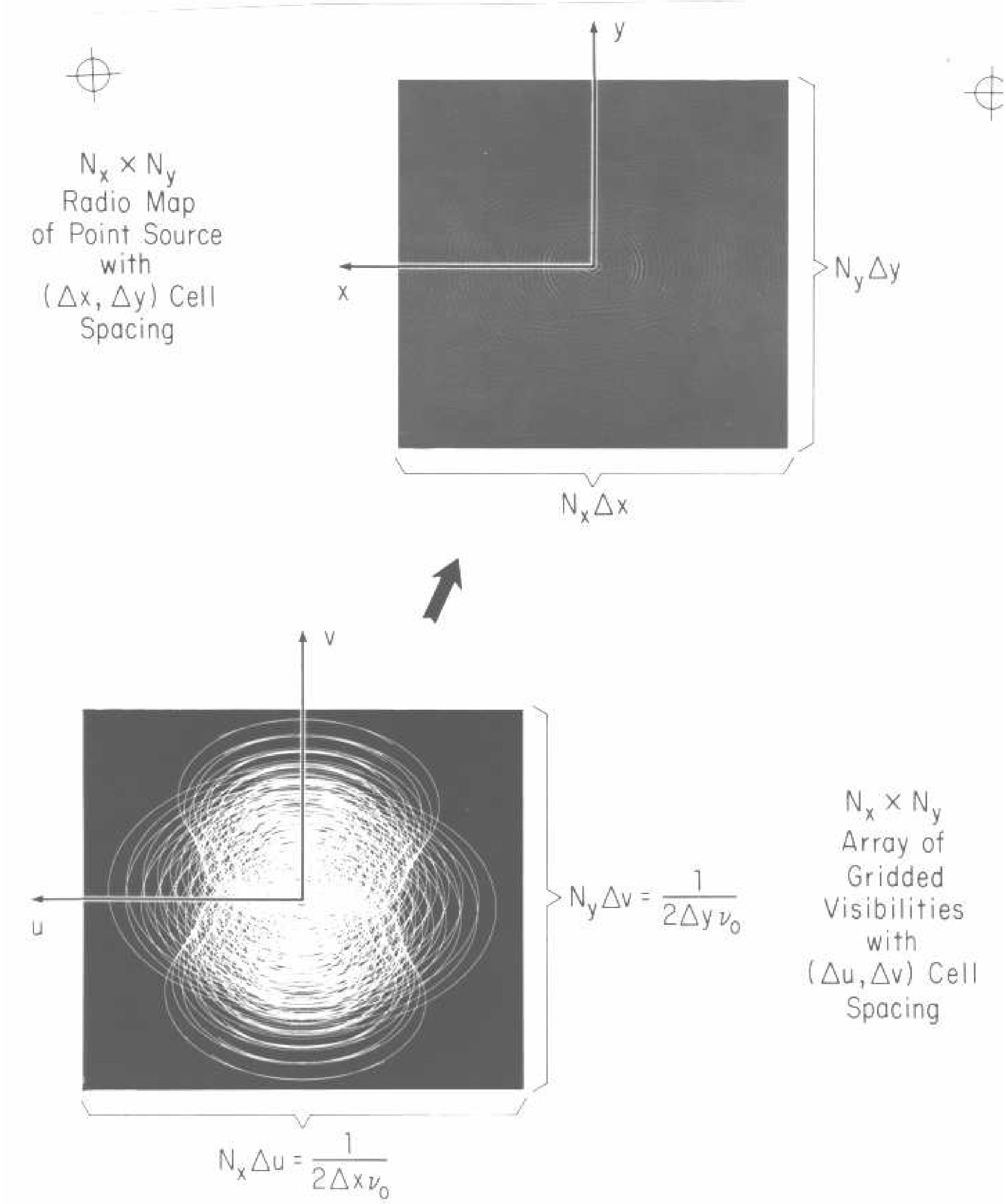

Figure 2 - 16. The relation between a gridded u-v plane, for the 27-antenna VLA observing a source at $\delta = 40°$, and the corresponding point source image map.

2.16 Bandwidth Effect *(Radial Smearing)*

2.16.1 Visibility Function for Finite Bandwidth

In Section 3 we discussed the effect of the bandwidth on the fringe amplitude if there were no delay tracking. For any map point not at the phase center, the delay tracking will not properly compensate for the geometric delay in the signal arrival time. In this section we want to discuss the effect of the bandwidth on the overall map.

Insight to the bandwidth effect can most easily be obtained from analyzing a point source located an angular distance (x_p, y_p) from the map center. Fourier transforming $\delta(x - x_p, y - y_p)$ gives $\exp[-i2\pi\upsilon(ux_p + vy_p)]$ for the complex visibility. u and v are in units of seconds of time and carry no frequency dependence. To bring in the frequency response of the system, let $\alpha(\upsilon)$ represent the frequency dependence for all the electronics from the antenna up to the correlator. As explained in Section 3 we can multiply and integrate (rather than convolve) the frequency dependent functions from two antennas since we are observing an incoherent signal. Consequently, the observed brightness for the (j,k) pair is

$$B_{jk}(ux_p + vy_p) = \int_{-\infty}^{\infty} \alpha_j(\upsilon)\alpha_k(\upsilon)e^{-i2\pi\upsilon(ux_p + vy_p)}d\upsilon \qquad (2-111)$$

For convenience, $\alpha_j(\upsilon)\alpha_k(\upsilon)$ will be replaced by $b_{jk}(\upsilon)$. Equation 111 then becomes

$$B_{jk}(ux_p + vy_p) = \int_{-\infty}^{\infty} b_{jk}(\upsilon)e^{-i2\pi\upsilon(ux_p + vy_p)}d\upsilon \qquad (2-112)$$

which is a Fourier transform of $b_{jk}(\upsilon)$

2.16.2 Radial Nature of Bandwidth Smearing

Our next step is to transform B_{jk} to the x,y plane. The integral is

$$b(x, y) = \int\int_{-\infty}^{\infty} B_{jk}(ux_p + vy_p)e^{i2\pi\upsilon_o(ux+vy)}du\,dv$$

where υ_o is the center frequency. The generality of this derivation can be continued more easily if x,y coordinates are converted to polar coordinates -r sin θ, r cos θ to give $b(x,y,x_p, y_p) =$

$$\int\int_{-\infty}^{\infty} B_{jk}[r_p(-u\sin\theta_p + v\cos\theta_p)]e^{i2\pi r\upsilon_o(-u\sin\theta + v\cos\theta)}du\,dv$$

where θ is defined counterclockwise from the y-axis as a position angle. u and v can now be rotated to simplify the integral. Let

$$u' = -u\sin\theta_p + v\cos\theta_p \qquad (2-113)$$

$$v' = v\sin\theta_p + u\cos\theta_p \qquad (2-114)$$

which gives for the unprimed coordinates

$$u = v'\cos\theta_p - u'\sin\theta_p \qquad (2-115)$$

$$v = u'\cos\theta_p + v'\sin\theta_p \qquad (2-116)$$

Substituting these expressions into the integral gives

$$b(r, \theta, r_p, \theta_p) = \int\int_{-\infty}^{\infty} B(r_p u')e^{i2\pi r\upsilon_o[\cos(\theta_p - \theta)u' + \sin(\theta_p - \theta)v']}du'\,dv'.$$

The u′,v′ variables are now separated so each may be integrated separately. Applying the similarity theorem to the u′ integration and recognizing the Dirac delta in the v′ integration gives

$$B(r, \theta, r_p, \theta_p) = \left(\frac{1}{r_p}\right) B\left[\upsilon_o\left(\frac{r}{r_p}\right)\cos(\theta_p - \theta)\right]\delta[r\upsilon_o\sin(\theta_p - \theta)]. \qquad (2-117)$$

.

The point source has been elongated in a radial direction from the map center in the shape of the frequency bandpass function. Perpendicular to this, in the azimuthal (θ) direction, there is no spreading or smearing.

2.16.3 Computation of Bandwidth Smearing in Map Plane

The previous result can be generalized to any map by multiplying together all appropriate factors in the u,v plane. Assuming all baselines have the same bandpass function, we get

$$\mathrm{V(u,v) = W(u,v)T(u,v)B(u,v)S(u,v)V_{true}(u,v)} \qquad (2-118)$$

where $\mathrm{V_{true}}$(u,v) is the Fourier transform of the true brightness distribution, S in the sampling function, and W and T are the weighting and tapering functions. The mapped brightness distribution is then

$$\mathrm{I(x,y) = w(x,y) * (t(x,y) * (b(r,\theta) * (s(x,y) * I_{true}(x,y))))} \qquad (2-119)$$

where s, w, and t are the transforms $\overline{\mathrm{S}}$, $\overline{\mathrm{W}}$, and $\overline{\mathrm{T}}$, respectively, b(r,θ) is expression 117, and the asterisk denotes two dimensional convolution. We see that the true brightness distribution is convolved with the bandpass spread function, b(r,θ). This causes all features to be elongated in a radial direction from the map (phase) center.

We can carry out a basic evaluation of the effect of various bandwidths by considering the case of a point source located at a $\mathrm{y}_p = 0$ and arbitrary y_p and the result will be completely general for radial distances $\theta = \mathrm{x_p} = \mathrm{r_p}$. We assume uniform weighting over a u-v plane sampling that will be taken to be uniform for all $|\mathrm{u}| \leq \mathrm{u_{max}}$ and $|\mathrm{v}| \leq \mathrm{v_{max}}$. The beam at radius θ is then

$$\mathrm{I_{beam}(r,\theta;\Delta\upsilon) = v(r,\theta) * I_{beam}(r,\theta;\Delta\upsilon = 0)} \qquad (2-120)$$

Computations based upon Eqn. 120 have been carried out by R. Perley in VLA Scientific Memorandum No. 138 for a number of assumptions concerning the taper and the bandwidth function. For un-distorted beams given by

$$\mathrm{I}_{\mathrm{beam}}(\mathrm{r}, \theta; \Delta v = 0) = \mathrm{sinc}\left[\frac{\eta(\mathrm{r}-\theta)}{\theta_{\mathrm{HPBW}}}\right] \text{ no taper, uniform sampling}$$

and

$$\mathrm{I}_{\mathrm{beam}}(\mathrm{r}, \theta; \Delta v = 0) = \exp\left[-\left(\frac{\gamma(\mathrm{r}-\theta)}{\theta_{\mathrm{HPBW}}}\right)^2\right], \text{ gaussian taper, uniform sampling} \qquad (2-121)$$

where $\eta = 3.79$ and $\gamma = 1.665$. If one defines functions α and β by

$$\alpha = \left(\frac{\Delta\theta}{\theta_{\mathrm{HPBW}}}\right) \qquad (2-122)$$

$$\beta = \left(\frac{\Delta v}{v_{\mathrm{o}}}\right)\left(\frac{\theta}{\theta_{\mathrm{HPBW}}}\right) \qquad (2-123)$$

where $\Delta\theta = (\mathrm{r} - \theta)$, and let I_o be the un-smeared central intensity, then the radially smeared beams for three cases are as given in Table 2-4.

Table 2 - 4
Radial Beam Shapes for Different Finite Bandwidth Models

Bandwidth	Taper	$\mathrm{I}_{\mathrm{beam}}(\alpha, \beta)/\mathrm{I}_{\mathrm{o}}$
square	none	$\mathrm{Si}[\eta(\alpha + \beta/2)] - \mathrm{Si}[\eta(\mathrm{alpha} - \beta/2)]$
square	gaussian	$\left(\frac{\pi^{\frac{1}{2}}}{2\beta\gamma}\right)\{\mathrm{erf}[\gamma(\alpha + \beta/2)] - \mathrm{erf}[\gamma(\alpha - \beta/2)]\}$
gaussian	gaussian	$\exp\left[\frac{-(\alpha\gamma)^2}{1+\beta^2}\right]/(1+\beta^2)^{\frac{1}{2}}$

In Table 2-4 we have used the standard functions

$$\mathrm{erf}(\mathrm{x}) = \left(\frac{2}{\pi^{\frac{1}{2}}}\right)\int_0^{\mathrm{x}} \exp\left(-\mathrm{t}^2\right) \mathrm{dt}$$

and

$$\mathrm{Si}(\mathrm{x}) = \int_0^{\mathrm{x}} \frac{\sin(\mathrm{t})}{\mathrm{t}} \mathrm{dt}$$

Figures 2-17, 2-18, and 2-19 show plots of I_{beam}/I_o vs. β, I_{beam}/I_o vs. α (beam shape) for various values of α, and the ratio of radial to azimuthal beam width as a function of β, respectively.

Plotted in Figures 2-17 and 2-19 are empirical measurements of the effects of finite bandwidth made for the A-array (open circles) and the C-array (filled circles). We see that the A-array data, which are most subject to band-width smearing effects, are fit quite well by the model assuming a square frequency band-pass and a gaussian taper.

In Figures 2-18 and 2-19 we also indicate an array-dependent expression for β, i.e.

$$\beta = 1.6 \left(\frac{\theta}{1'}\right) \left(\frac{\Delta v}{50\ \mathrm{MHz}}\right) \left(\frac{1}{3.285}\right)^{\mathrm{n}-1} \qquad (2-124)$$

where n = 1, 2, 3, and 4 for the A, B, C, and D arrays, respectively.

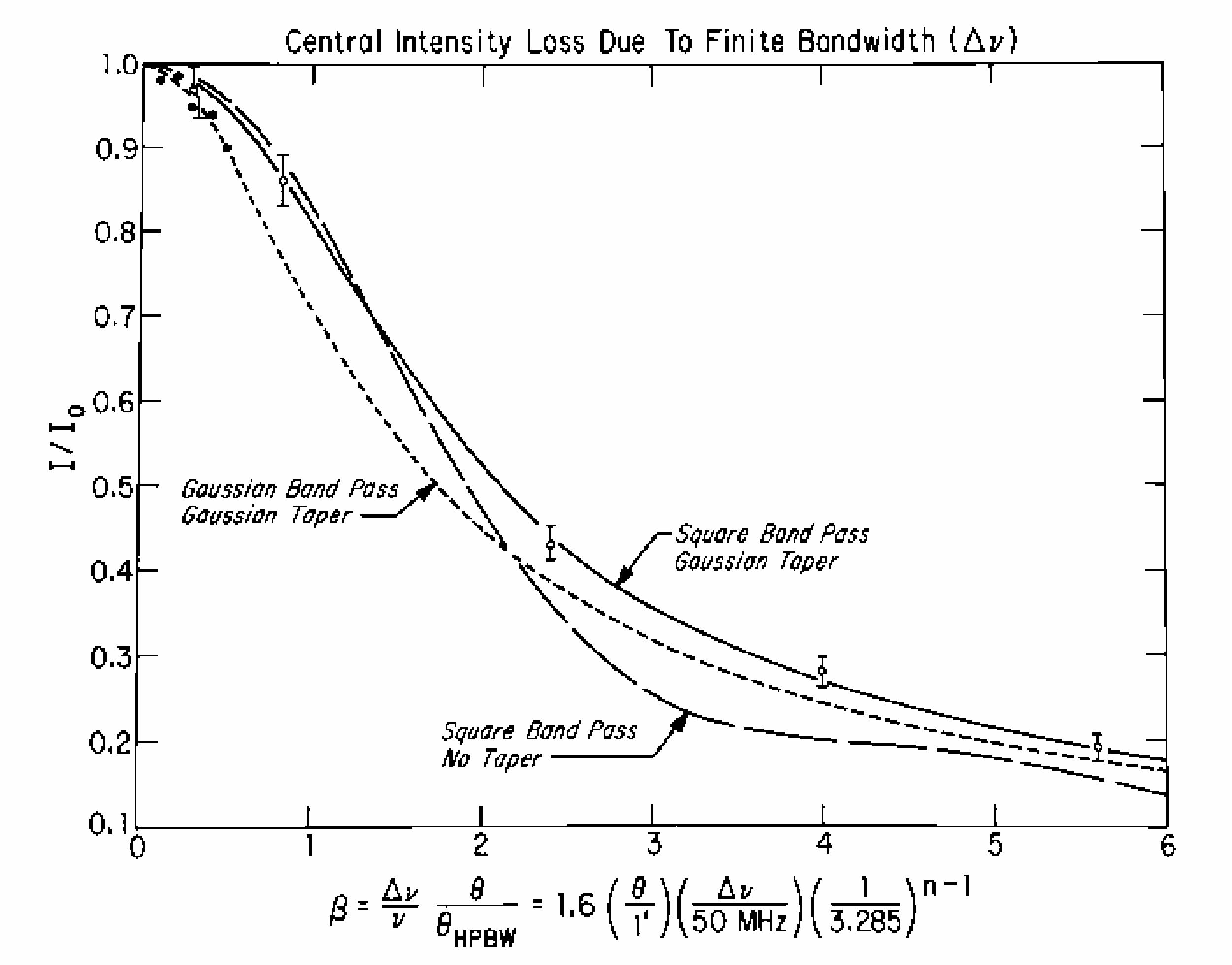

Figure 2 - 17. Central intensity loss (due to finite bandwidth Δv) plotted as a function of $\beta = beta(\theta,\ \Delta v,\ \mathrm{n})$, where θ is angular displacement from the phase center and n = 1, 2, 3, and 4 for the A, B, C, and D configurations.

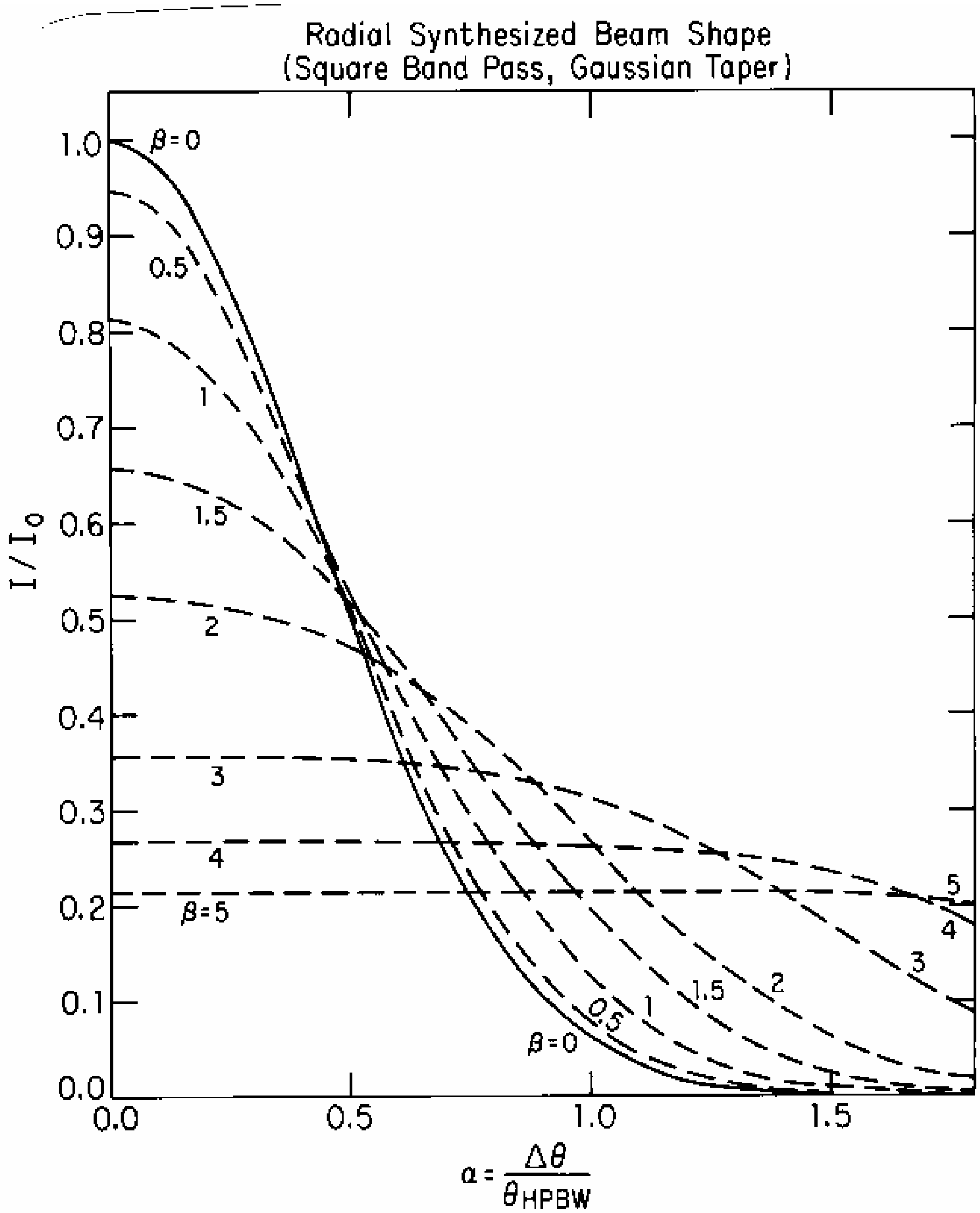

Figure 2 - 18. Beam shape due to finite bandwidth for a number of values of $\beta = \beta(\theta,\ \Delta v,\ \text{configuration})$.

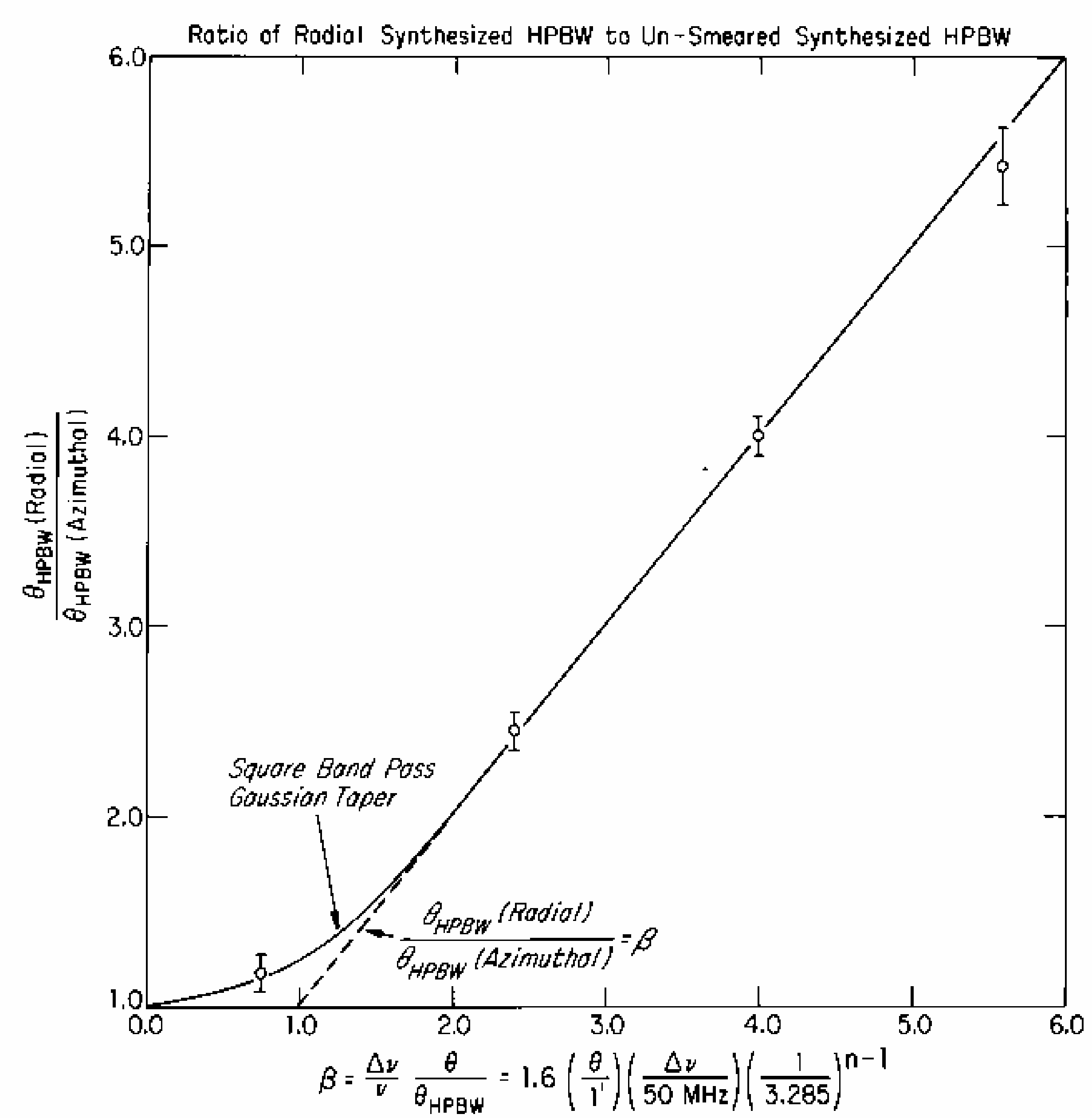

Figure 2 - 19. Ratio of radial to azimuthal beam width, due to finite BW, plotted as a function of $\beta = \beta(\theta,\ \Delta v,\ \text{configuration})$.

3 The VLA Electronics System

Abstract

The VLA electronics system is discussed both in general and at the level of detail appropriate to an astronomer who wishes to understand the major components that affect the radio signals obtained during observations.

The user who wishes to obtain more technical information about the VLA electronics system should read VLA Technical Report Number 29, "An Introduction to the VLA Electronics System", or other technical reports describing individual modules of the VLA electronics system.

3.1 Introduction

The VLA electronics system was conceptually designed by S. Weinreb in 1972-1973 and was further developed by members of the NRAO/VLA Electronics division. The objective was to provide a continuum and spectral line system operating on 27 antennas in four frequency ranges: 1.34 to 1.73 GHz, 4.5 to 5.0 GHz, 14.4 to 15.4 GHz, and 22 to 24 GHz. These frequency ranges or bands are designated by either the approximate central wavelength for each band; 20, 6, 2, and 1.3 cm, respectively, or by the letters L, C, U (for K_u), and K.

Three principal functions are performed in the VLA electronics system: (1) production and delivery of correlator visibility data every 312 ms for the four polarizations and four frequency bands from all N(N-1)/2 pairs of N antennas while operating in continuum mode, with a variable number of frequency channels within a band when operating in one of the spectral line modes; (2) control of antenna and electronics parameters; and (3) monitoring of information about the health and status of N antennas, their electronics, and the control building electronics.

A simplified schematic diagram of the VLA electronics system and its relationship to other systems is shown in Figure 3-1. At the antenna, the rotatable subreflector focuses radiation reflected from the antenna surface onto one of four feeds located on the feed ring at the Cassegrain focus. Control information sent from computers in the control building determines which of the four positions of the rotatable, asymmetric subreflector will be used to obtain the desired feed and frequency band. Radio frequency (RF) signals from each feed are sent via waveguide to the antenna vertex room where they are fed into low noise front ends. The parameters of these front ends, other parameters of the four bands, are given in Table 3-1.

The RF signals from the front ends are converted to intermediate frequencies (IF) 1325, 1425, 1575, and 1675 MHz in the antenna IF system. The four IF frequencies are derived from duplicate dual orthogonal polarizations designated A and B for the one polarization and C and D for the other polarization.

The antenna monitor and control system, commanded by instructions from the control building, both controls the antenna and its electronics and monitors its health and status. Antenna control and feed selection are achieved by commands sent to the antenna control unit (ACU) in the pedestal room of each antenna. The antenna monitor and control system controls and monitors three major electronic systems at the antenna: (1) the duplicated front ends and associated support equipment; (2) the antenna IF system; and (3) the slave local oscillator (LO) system that provides timing and frequency signals needed at many places in the front ends and in the IF system. The slave LO system at each antenna operates under closed loop control based on timing (LO) signals received from and sent to the master local oscillator system in the control building.

Control data sent from the control building to each antenna and data sent from each antenna by the IF, slave LO, and monitor and control systems to the control building are carried by a single 60 mm circular waveguide line along each arm of the array. Data are communicated through the

Table 3 - 1
Parameters of the Four VLA Frequency Bands

VLA Bands	Wavelength	Radio Astronomy Band	System Temperature (T_{sys})[1]	Antenna Efficiency (e_a)
1.34-1.73 GHz	17.0-22 cm	1.400-1.427 GHz	60 K	50 %
4.5-5.0	6.0-6.7	4.99-5.00	50	65
14.4-15.4	1.95-2.08	15.35-15.40	300	54
22.0-24.0	1.25-1.36	23.6-24.0	360	46

waveguide transmission system with a basic 52 ms cycle. During this 52 ms cycle there is 1 ms when control and timing data are being sent from the control building to the antennas and 51 ms when monitor data, LO information, and data from the A, B, C, and D IF output signals are being sent from each antenna to the control building. The input and output data for all the antennas on one arm propagate in the waveguide in the so-called TE_{01} mode. The 1 to 2 GHz band from each

[1] Average values for the antennas

of the arm's antennas modulates a waveguide frequency, $\upsilon_{\text{carrier}}$ that is different for each antenna, ranging from 26.410 GHz to 50.410 GHz. The carrier frequencies are the same in each arm.

In the VLA control building there are three rooms containing the major parts of the control building systems: the central electronics room, the shielded room, and the computer room, as shown in Figure 3-1. The control room where the array operators control and monitor the entire VLA system is not shown because such control and monitoring is achieved solely through CRT terminal interaction with the on-line computer in the shielded room and the computer room. All control commands for antennas or electronics are sent from the on-line computer system through a monitor and control interface to the control building monitor and control system. This system deals with all control information for antennas, antenna electronics, and control building electronics. It also receives all monitor data about the health and status of antennas, antenna electronics, and control building electronics and passes it on in digital form to the on-line computer system. The monitor and control interface in Figure 3-1 is called the serial line controller and the entire monitor and control system is also called the digital communications system (DCS).

The IF signals from each of the four channels, A, B, C, and D, (duplicate dual polarizations) for each of the N antennas, are demultiplexed from the waveguide system and sent to the control building IF system while the timing (LO) information from each antenna is sent on to the master local oscillator system. The local oscillator at each antenna is phase locked to 5 MHz (coarse lock) and 600 MHz (fine lock) signals from the master local oscillator in the control building. Timing signals from each locked LO are returned to the control building and compared with the master oscillator. This round trip phase difference is measured and used to make a correction to the phase for each antenna-IF.

After passing through the control building IF system, the four channels of data from each antenna are sent on to the shielded room. Four channels of data from each of N antennas are sampled and digitized before undergoing variable amounts of delay putting the data from each antenna onto a common time system. Consequently, all signals due to a source at the reference position in the sky arrive at all multipliers at exactly the same time. After delay compensation, 4N digital signals are cross-correlated and self-multiplied to obtain 4N(N-1) cross-correlated outputs (AA, CC, AC, CA, BB, DD, BD, DB for each of N(N-1)/2 pairs) and 4N self-correlator outputs. These are sent to the on-line computer system where each cross-multiplier output is divided by the geometric mean of the outputs of the appropriate self-multipliers (e.g. $\mathrm{A_{jk}}/\sqrt{\mathrm{A_j^2 A_k^2}}$) producing normalized visibilities. For a 10 second period (196 waveguide cycles) data are vector averaged to form the complex visibility sent to the MODCOMP named CORA. The system thus produces duplicate measurements of visibilities for four correlator polarization for N(N-1)/2 antenna pairs in the on-line computer system. Some corrections and calibrations are applied on-line before the data pass on to the off-line computer system for additional editing, correction, and calibration.

Figures 3-2 through 3-4 show three of the major locations of VLA electronics hardware. Figure 3-2 shows the inside of the antenna vertex room as seen from the entrance door. The A rack (right side of picture and the B rack (left side of picture) are shown suspended from the ceiling of the vertex room attached to the underside of the shaped, parabolic antenna surface. At the top of the picture are waveguides carrying signals from the Cassegrain feeds to the cooled front ends in Rack A. Rack A also contains most of the antenna IF system. Rack B contains the antenna slave oscillator system, the IF combiner/divider, monitor and control system modules, and the modem interface to the waveguide communications system.

Figure 3-3 shows sections of the central electronics room in the control building. The racks in the bottom picture contain the master local oscillator system, the monitor and control interface (serial line controller), and the phased array output racks for VLBI observations. In the center of the room, shown in the top picture, are three rows of D Racks. Each D Rack receives/sends signals for a particular antenna from/to the waveguide communications system; it contains an IF combiner/divider, monitor and control modules, the electronics room IF system, modems, and LO modules that communicate with the master LO system. The IF signals from the D Racks for all N antennas are sent to the shielded room where the racks and computer (SPECTRE) shown in Figure 3-4 carry out sampling, delay, and multiplication before the correlator outputs for N(N-1)/2 pairs are sent every 10 s to the correlator data handling computers in the computer room.

Now that we have gone through a greatly simplified description of the VLA electronics system, let us go through the system again at a greater level of conceptual detail.

3.2 A Dataflow Description of the VLA Electronics System

The VLA electronics system is very complex. In this section we will attempt to discuss the aspects of the system that perform critical tasks by discussing the flow of data or signals in and out of various components. It will be a dominantly conceptual discussion in which components may or may not correspond to actual hardware modules.

Figure 3-5, the multi-page foldout, is a block diagram of the VLA electronics system, with conceptual components ordered and connected in terms of the flow of various signals. The diagram is dominantly concerned with the processing of the signals received from an observed source as the signals proceed from the antenna feeds through the system until the raw visibility measurements, V''_{jkp}, where j and k are antenna numbers and p indicates correlator polarization, (AA or BB = RR or XX, CC or DD = LL or YY, AC or BD = RL or XY, and CA or DB = LR or YX), reside in the on-line computer system in the form of complex numbers for a 10 second integration time. Monitor data output is included where necessary for important corrections and calibration. Timing or LO data are indicated as input to critical components, but the hardware modules that do this are not shown.

Let us now follow the details of Figure 3-5 by starting at the left edge of the diagram with the radiation from the asymmetric subreflector arriving at one of the four feeds. All feeds are dual orthogonally polarized feeds. The 20 cm feed providing signals for the 1.34-1.73 GHz frequency range is a dielectric lens surrounded by waveguide elements illuminating a horn. The lens retards wavefronts while the waveguide elements accelerate wavefronts so arrival at the horn is uniform. The 6 cm feed for the 4.5-5.0 GHz range is a corrugated horn. Both the 2 cm feeds for the 14.4-15.4 GHz range and the 1.3 cm feeds for the 22-24 GHz range are multi-mode horns. After each feed, the RF signal passes through a polarization transducer (polarizer) which separates orthogonal polarizations; either circularly polarized signals (R and L) or linearly polarized signals (X and Y) depending upon which type of polarization transducer is mounted at the time. The polarization transducers are changed from one type to another by physically replacing one type with another. The standard mode of operation is with the polarization transducers that give orthogonal circularly polarized signals. The R- or X- polarization is sent via waveguide to the AB front end while the L- or Y- polarization is sent to the CD front end. Before reaching the front ends a calibration signal from a stable noise source is added to each RF signal. This CAL signal is switched at a 9.6 Hz rate. When synchronously detected much further down the line in the signal path, this CAL signal provides a means of gain calibration for a major part of the system since the CAL signal is amplified in the same proportion as the input RF sign needing calibration. The injected CAL signal has a known strength which normally contributes roughly 6% to the RF noise in the signal at the point of injection.

The combined RF and CAL signals then proceed to one of the duplicate front ends inside a cryogenically cooled Dewar maintained at a nominal temperature of 18° K. The R- or X- polarized signals go to the so-called front end and the L- or X- polarized signals go to the so-called CD front end. The AB and CD systems are nominal duplicates of each other. The VLA front ends are based upon a parametric amplifier followed by a GaAs field effect transistor (FET) amplifier designed for 4.5-5.0 GHz RF signals. With the appropriate position of the coaxial switch, the signals from the 6 cm feeds are fed directly into this paramp/FET amplifier. A final stage of RF amplification is provided by a second FET amplifier outside the Dewar.

The RF signals originating from the 20 cm, 2 cm, or 1.3 cm feeds undergo a frequency conversion before being fed into the 4.5-5.0 GHz paramp. Signals in the 1.34-1.73 GHz range pass through a parametric upconverter that multiplies a 3.2 GHz LO signal with the input RF signal to produce a 4.54-5.93 GHz signal which is fed into the 6 cm paramp with the appropriate position of the coaxial switch. Signals in the 14.4-15.4 GHz band undergo lower sideband mixing with a tunable 17-20 GHz LO signal and the resulting signal at 4.5-5.0 GHz is fed into the 6 cm paramp with the appropriate position of the coaxial switch. The 22-24 GHz RF signals in the 1.3 cm band undergo upper sideband mixing with the tunable 17-20 GHz LO signal and the resulting signal at 4.5-5.0 GHz is fed into the 6 cm paramp when the coaxial switch is in the correct position. Because of its function, the coaxial switch in each AB and CD front end is also called the "band-select" switch.

After the signals leave the 6 cm GaAs FET amplifier, subsequent frequency conversions and amplifications are independent of the original RF observing frequency. The RF outputs from the nominally identical AB and CD systems shown in Figure 3-5 are (1) attenuated during solar observations, (2) amplified by the second FET mentioned above, (3) passed through an RF attenuator, and (4) fed into a transfer switch. Depending upon the setting of the transfer switch, the AB and CD signal can be diverted to either A and B channels or C and D channels of the antenna IF system. The transfer switch is helpful for the diagnosis of equipment problems in which it is useful to know if the problem is before or after the transfer switch. Normally, signals from the AB front end go into the A and B IF channels while signals from the CD front end go into the C and D IF channels.

After the transfer switch, a splitter divides each RF signal into nominally identical channels denoted A and B for R- or X-polarization and C and D for L- or Y- polarization.

After the splitters, the A, B, C, and D RF signals are then mixed with a phase shifted LO signal in the 2-4 GHz range to obtain 1025 MHz IF signals. The phase shift applied to the LO signal before mixing applies the equivalent of fine delay adjustment, as discussed in Chapter 2, together with any other real time phase corrections that are desirable at this point. The phase shifter gets a signal in the 2-4 GHz range from the slave LO system, a fringe generator provides the phase shift necessary to keep the signal on a positive maximum of the raw fringe pattern as discussed in Chapter 2, and control information from the on-line computer system provides information about any additional phase shift ($\phi_{\mathrm{j}}^{\mathrm{corr}}$ for the j-th antenna) as discussed in the same section of Chapter 2.

All RF channels are converted to the same IF frequency of 1025 MHz, and passed through filters that limit the IF to bandwidths of 50, 25, or 12.5 MHz. A 300, 400, 550, or 650 MHz LO signal is fed into the frequency offset module which then changes the filtered IF signal at 1025 MHz to IF frequencies of 1325/BW, 1425/BW, 1575/BW, and 1675/BW MHz for channels A, B, C, and D, respectively, before being fed into an automatic level control (ALC) loop. The n/BW notation is used here and later to denote central frequency and bandwidth of an IF signal. The ALC loop maintains a constant IF level on the signal sent to the combiner. The loop is gated so that it does not respond to the noise source periodically turned on at the receiver input. An inset plot in the lower central part of Figure 3-5 shows the wide band CAL signal being measured by the square-law and synchronous detectors. The square law detector measures the gated total power (GTP) level corresponding to the IF total power. The synchronous detector measures the total power amplitude of the CAL signal that was injected at the receiver input with a 26 ms periodicity (9.6 Hz rate).

This detector output provides a measure of the gain and noise temperature up to this point in the system. The gain of the system between the point of noise injection between the front end and the point of measurement in the ALC loop is given by

$$\text{Gain} \;=\; \text{constant} \;\times\; \text{GTP/CAL} \qquad (3-1)$$

where the constant in Equation 3-1 reflects the strength of the injected noise signal and any gain normalization factor one might choose for each frequency band. The GTP and CAL values measured for the A, B C, and D channels are sent as part of the monitor data to the on-line computer system where they are used for gain calibration, as a function of time, using Equation 3-1.

After the ALC loop, the IF signals at a relatively constant power level are fed into a combiner/divider. This component functions as a signal combiner for data sent from the antenna. The combiner puts together, into the 1-2 GHz range, all IF, monitor, and timing (LO) information for transmission down the waveguide to the control building. The same component functions as an IF divider, taking control and timing (LO) information sent from the control building and dividing it into two parts; one portion contains the control commands which are then sent on to the antenna monitor and control system, and the other portion contains the timing (LO) information sent by the master LO system to the antenna slave LO system responsible for generating all of the previously mentioned LO signals. The combiner/divider sends/receives data to/from a modem which sends/receives data to/from the waveguide transmission system. Data are sent through the waveguide to the control building for 51 ms out of every 52 ms. Control and timing data are sent to the antennas for the other 1 ms in the 52 ms cycle. Insets in the middle Figure 3-5 show the frequency spectrum of the data in the send (upper center of Figure 3-5) and receive (lower center of Figure 3-5) cycles. Each antenna of each arm has a waveguide channel with a carrier frequency ($\upsilon_{\text{carrier}}$) listed in the lower central portion of Figure 3-5. The send/receive spectrum covers frequencies from (1.0 GHz + $\upsilon_{\text{carrier}}$) to (2.0 GHz + $\upsilon_{\text{carrier}}$).

As shown in the lower central inset in Figure 3-5, control data are sent to antennas in the form of sidebands at the frequency (1.8 GHz + $\upsilon_{\text{carrier}}$). Timing (LO) information is sent in the form of a (1.2 GHz + $\upsilon_{\text{carrier}}$) signal, a (1.8 GHz + $\upsilon_{\text{carrier}}$) signal, and 5 MHz sidebands of the (1.2 + $\upsilon_{\text{carrier}}$) signal. Basic 600 MHz (1800-1200 MHz) and 5 MHz signals are derived from these signals to control the slave LO system. The upper central inset in Figure 3-5,showing the spectrum of data sent down the waveguide from the antennas to the control building, is somewhat more complicated. During the send cycle for each antenna, the timing information used at the antennas is sent back to the control building in the form of (1.2 GHz + $\upsilon_{\text{carrier}}$), (1.8 GHz + $\upsilon_{\text{carrier}}$), and 5 MHz sidebands on the (1.2 GHz + $\upsilon_{\text{carrier}}$) signal. When these signals reach the master LO system in the central electronics room, the 600 MHz phase is compared with the one sent to the antennas, and a round trip phase ($\phi_{\rm RT}$) correction is derived and added to the monitor data for use in phase corrections in the on-line and off-line computer systems. The monitor data from each antenna are sent as sidebands on the (1.8 GHz + $\upsilon_{\rm carrier}$) signal. Finally, the IF data for the A, B, C, and D channels are sent in 50 MHz passbands centered at (1325 MHz + $\upsilon_{\rm carrier}$), (1425 MHz + $\upsilon_{\rm carrier}$), (1575 MHz + $\upsilon_{\rm carrier}$), and (1675 MHz + $\upsilon_{\rm carrier}$), respectively.

A modem in the central electronics room of the control building takes/sends signals from/to the waveguide and, after splitting/combining signals for the different antennas, sends/takes signals to/from another divider/combiner component. As a combiner during the antenna receive cycle, the control data from the on-line computer and timing (LO) data from the master LO system are combined into the basic spectrum of 1200 MHz and 1800 MHz with sidebands. As a divider during the antenna send cycle, the monitor data are split off and sent to the on-line computer named MONTY, the timing (LO) data are split off and sent to the 600 MHz phase comparator. The data for IF's A, B, C, and D are split off into channels with IF frequencies of 1325/BW, 1425/BW, 1575/BW, and 1675/BW, respectively, where BW is the IF bandwidth selected in the antenna IF system. The AB and CD IF signals are then mixed with 1200 and 1800 MHz, respectively, LO frequencies and the results are mixed with tunable 100-150 MHz (A and B) or 200-250 MHz (C and D) LO signals (fluke synthesizers). The resulting lower IF frequencies are between 0.2 and 50 MHz (called baseband). These baseband signals are then passed through final filtering parameters as listed in Table 3-2.

The 0.2-50 MHz IF signals for each channel are fed through a voltage controlled amplifier that adjusts the IF power to ideal levels for the samplers through an ALC loop coupled to the sampler for that IF signal. These are 3-level 2-bit samplers that incidentally, as a part of their clocking mechanism, insert fine delay adjustments in the signal paths in increments of 625 ps. The outputs from the samplers are converted to digital form before being sent into the modules that apply the bulk of the delay compensation needed for each antenna. The amounts of fine delay adjustment in the samplers and gross delay compensation (in 10 ns increments) applied to the IF's for each antenna are determined from commands from the on-line computer system (BOSS). The large coarse delays, plus the fine delays applied inside the samplers, constitute the total antenna delay compensation discussed in Chapter 2. This and the phase shifting done in the IF system constitute the major phase and time compensations discussed in the same section. A second (narrow band) CAL measurement is made between the V.C. amplifier and the 2-bit sampler as part of the gain calibration system.

3.3 Local Oscillator System

The local oscillator system is a complex network which produces phase stable signals at many points in the electronics system, for frequency conversion to IF and final IF (baseband) frequencies.

At the antenna the LO signals are phase locked to a master oscillator in the control building. The LO system is also used to reduce the fringes to zero frequency. This is accomplished by adjusting the phase of the (2-4 GHz) LO signal sent to the mixer accomplishing (4.5-5 GHz) to 1025 MHz frequency conversion.

Figure 3-6 is a diagram showing the major LO mixings which the user is most likely to encounter. The LO components are connected to the master oscillator by other modules which are not shown. Each LO block contains a technical term (F2, F3, L6, or Fluke synthesizer) for the component, and the indicated LO frequencies (First LO, 2-4 GHz LO (synthesizer frequency), and fluke synthesizer frequency) are used to determine the location of the observing band. Within this band, other parameters can be used to limit the final baseband IF to a particular frequency, primarily for spectral line observations. Values of these frequencies, for a particular sky frequency, can be determined by running the DEC-10 programs LOSER and DOPSET. Further information on these programs can be found in Chapter 12.

3.4 Correlation System

The correlation system is a complex network capable of operating in many modes. In this description we will restrict our discussion to the continuum mode and one spectral line mode. The continuum mode is the most straightforward mode so it will be discussed first. From each antenna sine and cosine signals are formed for each of the baseband channels (A, B, C, D). These eight signals are passed through the delays and on to the multipliers. Sixteen products are formed between all possible pairs of four A and C signals from one antenna and from A and C signals from a second antenna. A similar sixteen products are formed among the B and D channels. Thus in total we have at one instant (92.16 ms)

4	*	4	*	2	*	N(N-1)/2	=	16N(N-1)
Sine & cosine components for A and C		polarizations (A and C products)		Duplicate BD products		Antenna pairs		

cross-correlator products. For 27 antennas there are 11232 products or real numbers describing 5616 complex gains.

An integrator system following the multipliers collects the 92.16 ms samples and integrates them for periods from 52.083 ms to 10 seconds in steps of 52.083 ms. Further operations can be performed by synchronous Modcomp computers (SPECTRE and CORA/B) and an array processor. The array processor normalizes each cross-correlation product by the geometric mean of the corresponding self-correlation products, and passes the data at the level of ten second integration times to both magnetic tape and the off-line computer system. Data accumulated for 12 hours adds up to 24.3×10^6 complex visibility measurements which can be reduced to 3×10^6 complex numbers before computing a map in a single Stokes parameter.

Table 3 - 2
IF Bandwidths and Spectral-Line Channel Bandwidths for
Various Observing Modes

Nominal IF Bandwidth	IF passband[3]	Sampling Frequency	No. of Channels[2] 1[4]	2[4]	4[4]	Channel Bandwidth
50 MHz	0.19-50 MHz	100 Mhz	16	8	4	3.125 MHz
25 MHz	0.19-25 MHz	50 Mhz	32	16	8	781 kHz
12.5 MHz	0.19-12.5 MHz	25 Mhz	64	32	16	195 kHz
6.25 MHz	0.19-6.25 MHz	12.5 Mhz	128	64	32	48.8 kHz
3.125 MHz	0.19-3.125 MHz	6.25 Mhz	256	128	64	12.2 kHz
1.563 MHz	0.19-1.563 MHz	3.125 Mhz	256	128	64	6.1 kHz
781 kHz	190-781 kHz	3.125 Mhz	256	128	64	3.05 kHz
391 kHz	190-781 kHz	3.125 Mhz	256	128	64	1.53 kHz
195 kHz	195-391 kHz	1.563 Mhz	256	128	64	763 Hz
97 kHz	195-391 kHz	781 kHz	256	128	64	381 Hz

The continuum mode operates for bandwidths ranging from 50 MHz to 6.25 MHz. For narrower bandwidths the continuum mode should not be used because the quadrature networks which produce the sine and cosine components do not operate properly.

We will next discuss one of the line modes of the correlator system. In line mode the correlator system is re-configured to provide products for many lags between signals from the two antennas. With the fixed number of multipliers, the number of IF signals correlated must decrease as the number of line frequency channels increases. Table 3-2 tabulates the number of frequency channels

[2] The numbers given indicate the number of channels processed within the nominal bandwidth. The number of usable channels is slightly less because of band edge effects.
[3] The filters are low-pass and the low-Frequency limit is determined by the amplifiers except for the 195-391 kHz band which uses a bandpass filter.
[4] Number of IF's

versus IF bandwidths for the four modes; 1) one IF band, 2) two IF bands, 3) four IF bands, and 4) polarization mode.

The number of frequency channels increases with decreasing IF bandwidth by using the process called recirculation. A narrower bandwidth permits one to sample at a lower sampling rate and, with the multipliers always operating at their maximum rate of 100 MHz, additional time slots become available. In this extra time a constant delay is added onto the sequence of stepped lags and the data is again read out of storage into the multipliers. Thus, with no additional multipliers, the number of channels can be increased up to 512, with an IF bandwidth of 97 kHz.

The allocation of the correlators for the line mode with one IF band is as follows. Suppose that 16 delay steps are used in one baseline. These delay steps will be added first into one IF path and then into the other for a total of 32 leads with lags. If 27 antennas are used with one polarization per channel we have:

32	*	1	*	351	=	11232
delay steps		IF		baselines		correlations

The maximum number of correlators is always 11,232. For other modes of operation the correlators will be allocated differently, but the total will still be 11,232.

In the spectral line mode the Fourier transform of the visibility is taken with respect to the lead and lag time. The transformation and visibility normalization are performed by the synchronous computer, SPECTRE, and an array processor located in the shielded room. Upon completion of these operations the visibilities, as a function of frequency, are passed onto the computer CORA which relays them to the off-line system.

3.5 Technical Descriptions of VLA Electronics

The VLA Technical Reports provide more detailed descriptions of the VLA electronics system and its component modules. Technical Report Number 29, "An Introduction to the VLA Electronics System", provides a more hardware- oriented description of the entire VLA electronics system. Technical Report Number 39, "Correlator System Observer's Manual", discusses details of the correlator system. This report is a basic reference for possible modes of spectral line observing. Other technical reports document individual modules of the system. The reader who wishes to obtain more information about the VLA Electronics System is referred to this series of Technical Reports.

4 Array Control and Data Acquisition

Abstract

Operational aspects of the VLA system for array control and data acquisition are discussed. Since the VLA is controlled by an on-line computer system, using information in a number of array control files stored on disk, we discuss the contents of these files in detail. Most of the time the VLA observer will be concerned only with preparing and modifying the source list file, a procedure which is discussed in detail in Chapter 5; however, one should aware of the contents of the other files, since some observing programs will require modification of information in these files.

4.1 Introduction

The control of the array and the data acquisition process are intimately related because each depends on the other, and because they are coordinated tasks of the on-line computer system. Let us briefly mention the major components of the on-line computer system so we can survey the overall problem of array control and data acquisition.

The on-line computer system has six major parts: the first part is a single MODCOMP minicomputer called BOSS, which generally manages the observing, based on information in a set of system control files, and controls the operation of the other on-line computers; the second part is another MODCOMP minicomputer called MONTY, which handles the monitor data coming back from the antennas and electronics and sends out the control data or commands (from BOSS) which control the antennas and electronics; the third part is a MODCOMP called EUNICE which handles all the unit recording devices (i.e. terminals and line printer) and all message routing between devices and computers; the fourth part is a MODCOMP called SPECTRE, which manages the correlator system; the fifth part is a Floating Point Systems array processor (controlled by SPECTRE), which calculates visibilities, and for line data converts from cross-correlation function to cross-spectral function; and the sixth part consists of two MODCOMP minicomputers called CORA and CORBIN, which handle the correlator data sent from the correlator system every 10 seconds. The off-line computer system plays a secondary role in the operation of the array by providing array operators and observers with supplementary information about the data produced by the array.

The direct control of the array is accomplished by the on-line computer system. The programs that exercise this control mostly derive their parameters from system control files resident on the

MODCOMP disks. The nature and contents of these control files are discussed in Section 2. The portions of these control files of greatest concern to the observer are the source list files specifying each source to be observed with its reference position, frequency, bandwidth, pointing parameters, and various timing and astrometric parameters.

The array operators work in the control room, shown in Figure 4-1, located between the central electronics room and the computer room. They are surrounded by computer terminals and line printers that are the means of communication with the on-line and off-line computer systems. Photographs of the on-line computer system are shown in Figure 4-2. Using the on-line terminals connected to the MODCOMP computers, the operator can request a range of data displays describing the status of any part of the antenna and electronics systems, or correlator, pointing, etc. data. The design of the system is based on the principle that the vast majority of the components of the antennas and electronics will operate in a satisfactory manner under computer control, so the operators need investigate only occasional problems, usually brought to their attention by terminal and line printer output from a data checker program, CHK, that has been instructed about the ranges of correct operation of equipment parameters. The monitor data, which are measurements of about 300 parameters of a single antenna system with its electronics, are the basis for these judgments. The same data allow an on-line program to assign flags which are judgments of data quality for each piece of correlator data.

Figure 4-3 is a schematic diagram illustrating the major features of the array control and data acquisition system. In the upper right portion of Figure 4-3, the terminals and line printer used by the operator to monitor and control the array are shown. Also shown are schematic connections to the on-line and off-line computer systems. Operator commands are shown as sent from terminal to BOSS while data displays can come from almost all computers. MONTY is shown in the critical role of receiving data from all systems and sending all control commands. Control commands are sent to the monitor and control interface, also called the serial line controller, which distributes commands to all antennas, the master LO system, and other electronics. BOSS sends delay control commands to MONTY, which passes them on to the sampler and delay systems preceding the correlators in the shielded room. The left side of Figure 4-3 shows the major data paths to and from the waveguide transmission system together with the appropriate data paths between systems in the central electronics room and the shielded room. We see that the monitor data returns from all antennas to MONTY via the monitor and control interface. LO signals are exchanged between the master LO system and the D racks for each antenna system, which distribute and receive timing information during the send and receive cycles of the waveguide transmission system. We also see that, after the IF data obtained from each antenna is processed a D rack, its antenna-IF (total power) data are sent to the shielded room where the samplers and delay multiplier system produce cross- and self-correlator output for each antenna-IF pair once every six waveguide transmission cycles, which is every 312.5 ms. This large volume of correlator data is sent first to the array processor (AP) and then to the correlator handling computers (every 10 seconds), normalizing the cross-correlator outputs by the self-correlator outputs in the process of producing vector averaged real and imaginary parts of the correlator visibilities. Every ten seconds these correlator data are set to magnetic tape and the off-line computer system by the on-line computers. Monitor data are accumulated on MODCOMP disks by a monitor data logging program that selects monitor data points, for varying time intervals, for periodic logging and later transfer to a monitor data tape.

Because correlator data can be stored in the off-line computer system in nearly real time, observers can monitor the output of the array with a variable time lag. An operator's computer terminal can monitor the real-time 10-second data for any antenna pair. When the system is operating well the observer can, if it is desirable, calibrate and make maps in the off- line computer system within hours after the data are taken. Most observers wait until all data on a source are available before mapping, although they sometimes monitor on-line displays of visibility amplitude and phase for calibrators and program sources. Flagging or calibration are usually not done, however, until all data are written into the data base in the off-line computer system.

The control of source observations is philosophically oriented toward specifying the phase reference position and equipment parameters for continuous segments of Local Sidereal Time (LST). We will use the word "scan" to describe each of these contiguous blocks of observing time and the associated data. The array operates on a scan by scan basis controlled by scan parameter specifications supplied by the observers in a source list control file. The resultant data in the off-line system are then organized according to sequential scans and this is what the user deals with in off-line data processing.

4.2 System Control Files

4.2.1 An Overview of Array Control Files

A series of files containing control information are stored on disk in the on-line computer system. The creation and modification of these files by operators or observers is the most direct and common method of controlling the functioning of the array. However, commands can be sent to any antenna by the operator, temporarily succeeding control file commands. The operator can also control the sequencing of observation specified in a source list file, skipping to an object late in the list, extending the time on the current source, or skipping back to a an object earlier in the list.

Because of their importance let us discuss the major on-line control files. The following is a list of these files, with a brief description of their contents:

a. ARRAY control file - This file contains information applicable to the whole array (mainly time parameters).
b. SUBn control files - These files (for n = 1, 2, or 3 subarrays) contain names of source list files for each subarray, parameters of LO and receiver settings that determine frequencies of operation, and names of the (IF and ROT) files with parameters for IFs and subreflectors.
c. ANTENNAS control file - This file contains information about the subarray number, station location, and other miscellaneous parameters for each antenna.
d. BASELINE control file - this file contains that positions of the antenna stations, delay constants, and the axis intersection defect parameter for each antenna.
e. POINTING control file - this file contains the parameters used to make azimuth and elevation dependent pointing corrections.
f. IF control files - These files contain (one for each observing band) gain calibration and antenna efficiency parameters for each antenna.
g. ROT or SUBR control files - These files contain (one for each observing band) subreflector rotation and front end parameters.
h. Source list files - These files contain sequential lists of source request cards with:
    1. Source Name
    2. Source Qualifier
    3. LST stop time or duration of scan
    4. Right ascension and declination
    5. Epoch of position
    6. Observing band for scan
    7. Observing mode
    8. Calibrator code if a calibrator
    9. Gain code
    10. Bandwidth selection
    11. Feature velocity (for spectral line observations)

plus optional cards for each scan for comments, LO parameters, antenna wrap control, moving source parameters, etc.

Most of these control files are modified only by the array operator or other VLA staff members; the main files created and modified by the observer are the source list files.

For those observers interested in producing their own versions of the systems files in the on-line computer system, we include a column-by-column description of each “card” in the following sections of this chapter. The simplest procedure for producing special system files is to copy the system file, alter it, and catalog the altered file under a new name. The SEDIT text editor on the MODCOMPS is used to do this. CAUTION: Never catalog a file without the telescope operator's permission.

4.2.2 Source List Files

The observer has predominant control over the major parameters of the observing process by preparing the source list files. The determination of which source list files control observing in the n-th subarray is accomplished when array operators put the source file name in the first card image of the SUBn file. This is done when the array operator learns from the observer the name of the appropriate source list files.

The source list file describes what sources are to be observed at what time, with specified positions, frequency bands, observing mode, calibrator type, gain code, bandwidth code, and feature velocity for spectral line observations. Special programs called OBSERV, which will be described in Chapter 5, are the ordinary means by which the observer prepares source list files. However, for completeness, let us now describe the different types of card images in source list files and their formats. Most users will not need to know the details described in the rest of this chapter.

The first card in any source list file must contain observer identification information. Columns 1-2 contain /. indicating an identification card. Columns 3-8 contain the observer's last name truncated to the first six characters, ending in Column 8. Columns 9-13 contain the user's DEC-10 user number, ending in Column 13.

Following the identification card there are any number of source cards. The source card specifies the parameters of observation during specified time interval. This time interval can be specified either in terms of Local Sidereal Time (LST) durations or stop times (LST). There is a one-to-one correspondence between the "scan" discussed elsewhere and the data gathered while the subarray is on source for a particular source card.

On each source card the observer must specify a source name in Columns 1-8, ending in Column 8. Sources are further described by a numerical source qualifier, which is an integer number in Columns 9-13 ending in Column 13. The significance of this number is entirely up to the observer. Leaving this blank results in the source having a numerical qualifier of zero. A blank in column 14 means time is specified in terms of LST stop time, and a dollar sign ($) means time is specified in terms of a duration. Durations begin at the completion of the previous operation. No allowance is made for antenna slewing or setup times. Columns 15-22 contain the LST stop time or duration, with HOURS, MINUTES, and SECONDS specified in I2 format in Columns 15-16, 18-19, and 21-

22, respectively. Columns 24-36 contain the right ascension of the reference position to be tracked, with HOURS, MINUTES, and SECONDS specified in formats I2, I2, and F8.4 in Columns 24-25, 27-28, and 29-36 respectively. Column 38 contains a plus (+) or a blank for positive declinations and a minus (-) for negative declinations. Columns 39-50 contain the numerical specification of declination, with DEGREES, ARCMINUTES, and ARCSECONDS specified in formats I2, I2, and F7.3 in Columns 39-40, 42-43, and 45-50, respectively. A blank in Column 51 means the position is for a standard equinox of 1950.0, a D means it is an apparent position of date, a C means the position is for a standard equinox of 2000.0, and a Y means the position is for an equinox of the year specified in columns 52-55, which otherwise are left blank. Columns 56-57 specify the frequency band for the observations for the AB and CD channel paramps, with LL for 18-22 cm, CC for 6 cm, UU for 2cm, and KK for 1.3 cm under standard conditions of operation. Three other frequency bands are coded into the system: (1) HH is an L-band frequency which was chosen to minimize interference with 12 and 25 MHz bandwidths, and 21 and 18 are the two letter codes for frequencies in the hydrogen and OH bands. If alias cards are used in the SUBn file, then the band designation specified there should be used. Columns 59-60 contain an observing mode parameter, with blanks meaning normal interferometer continuum mode, Px meaning single dish pointing mode for IF x = A, B, C or D, Ix meaning interferometer pointing mode for IF x = A, B, C, or D, TF meaning a mode for the testing of the front ends, D for delay center determination mode, VA for phased-array mode, and VX for a phased-array mode (weak source) where phase updates are applied from a previous (strong source) observation in VA mode. Column 61 is blank if the source is not a calibrator, but with an A or B it is a high quality, unresolved flux and position calibrator; with a C it is reasonably good, unresolved phase calibrator; and with a T it is a point source with poorly determined flux and position. Column 63 contains a gain code which has values between 0 and 8. Gain codes are chosen depending on the strength of the source such that, calling GC the gain code the flux of the source is between $K*2^{GC}$ and $K*2^{CG+1}$ Jy. The value of K varies with observing band, as will be discussed in Chapter 5, however GC ranges from a minimum of 3 to a maximum of 8. Columns 65-68 contain the bandwidth codes, wwww, for the A, B, C, and D IFs, so that the bandwidth = $50/2^{w}$ MHz. Below 6.25 MHz the continuum mode should not be used because the quadrature networks do not operate at narrower bandwidths, and one must use the line mode. Columns 69-80 contain the feature velocity for spectral line observations.

When there is a series of source cards, with specified durations or different LST stop times, the on-line computers initiate a change to the parameters of the next source card every time a duration is exhausted or an LST stop time is reached. The time it takes for the antennas to move to the next source position, and the subreflector rotation time, use up from tens of seconds to roughly a minute of time during the first part of each scan.

Each source card can be followed by optional cards, which are of six different types: (1) a comment card; (2) a repeat source list card; (3) an antenna wrap option card; (4) a proper motion option card, used for the Sun, planets, comets, etc.; (5) a local oscillator option card; and (6) a spectral line LO card used for spectral line observations.

The optional comment card can be used to associate observer's comments with specific source cards. Columns 1-3 must contain //* to identify the comment card. Column 4 must be left blank. Observer's comments can then be typed in any of Columns 5-80.

The optional repeat source list card (REW) allows the observer to instruct the system to repeat observing with the current source list until further notice, or to repeat a list involving LST stop times covering a full 24-hour period. The repeat source list card has /REW in Columns 1-4 and follows all other source cards.

More detailed control of repetitive observations is possible with the BAC card. On this card /BAC is placed in columns 1-4 and columns 7-13 contain a (right adjusted) integer which specifies the number of source cards to "back up". The default is n = 1 corresponding to a jump to the previous source card. One can specify n < 0, in which case observing control will skip forward -n "cards" in the source list file.

The optional antenna control card (AN) allows the observer to force motion to a new elevation and azimuth, mainly to control cable wrap problems. Columns 1-4 must contain //AN identifying an antenna control card. Columns 5-60 contain elevation, and azimuth specifications for individual antennas. Each antenna is allocated two columns (one for elevation "plunge" and one for azimuth "wrap"). Odd column numbers after //AN contain a U, D, or blank for elevation specification. U means use elevations greater than 90° are possible), an L for counterclockwise wrap, or a blank for don't care.

The above procedure is used when it is desirable to control the wrap on individual antennas, which is usually not the case. To control entire arms of the entire array at once, additional columns on the antenna wrap card are used. To control an array arm, or the entire array, place an identification parameter in Column 71. Use a W, E, or N for specific arms or an A for the entire array. In Column 72 place a U, D, or blank for elevation specification, and in Column 73 put an L, R, or blank for the azimuth control.

The optional proper motion card (PM) is used for observations where the source position changes significantly during a scan. Columns 1-4 must contain //PM to identify the type of card image. Columns 11-20 contain the rate of change of source right ascension in seconds of time per day in a format of F10.0. Columns 21-30 contain the rate of change of source declination in seconds of arc per day in a format of F10.0. Columns 32-39 contain the IAT time corresponding to the position specified on the source card, with HOURS, MINUTES, and SECONDS in I2 format in Columns 32-

33, 35-36, and 38-39, respectively. The date is assumed to be the IAT date of observation. Finally, Columns 41-50 contain the equatorial horizontal parallax in seconds of arc in F10.3 format. The observer should be cautioned that the epoch of the position parameters is still active. In the published ephemeris (where these data can be found), the positions of the Sun and major planets are in coordinates of date while, for asteroids, positions are in 1950 coordinates.

The optional local oscillator card (LO) allows source by source control of LO frequencies and synthesizer settings. Columns 1-4 must contain //LO for identification purposes. Columns 5-6 contain the bias digits for upconverters and mixers for AB and CD channels, using the same code as the LO and receiver setting specification card images in the SUBn files. The SUBn files are discussed later in this chapter. Columns 5-80 contain the same information in the same format as the LO and receiver setting specification cards in the SUBn files. Indeed, one can think of this optional card image as allowing the observer to change from a "standard" set of LO frequencies and synthesizer settings, defined by the system or by the user, to a new set each scan. If no LO card image follows a particular source card image, the default parameters are used.

Finally, the optional spectral line card (LI) allows source-by-source control of spectral line parameters for spectral line observations. Columns 1-4 must contain //LI. The remaining parameters on the card are identical to those on the external LO frequency card used in the SUBn files, and, indeed, modify these parameters on a source- by-source basis.

The following is a sample section of a source list file. The cards are for observations of the Sun so examples of the observation request card, the LO control card, and the moving source card are given:

```
./HJELLM  11
3C84      1$ 0 08 00  3 16 29.566   41 19 51.92      CC    4 0000
3C84      1$ 0 08 00  3 16 29.566   41 19 51.92      CC    4 0000
//LO                                                     SUNCIF    OFFCROT
SUN       0$ 0 15 00  7 39 49.6824  21 27 31.720D    CC    7 2222
//PM       226.678  -561.152  0  0        8.6600
//LO                                                     SUNCIF    OFFCROT
3C84      1$ 0 08 00  3 16 29.566   41 19 51.92      CC    4 0000
//LO                                                     SUNCIF    OFFCROT
```

In this example of a source list file, the first scan (where the source qualifier is 1) is a calibrator observation, with the normal situation of solar attenuators turned off. The subsequent card images are for observations with the solar attenuators switched on by appropriate entries in the non-standard IF and ROT files named SUNCIF and OFFCROT. One then alternates a calibrator observation with a solar observation. Since the Sun undergoes large proper motions, it is necessary to use the moving source (PM) card.

It should be emphasized that, most of the time, only the source request card is used in the source list file, and LO, LI, and PM cards are not present.

4.2.3 Remaining System Control Files

In this section we give the details for the seldom used process of producing card images for each system file that an observer may want to create. You should discuss such changes with a staff scientist and/or array operators before attempting to produce these files.

4.2.3.1 The ARRAY File

The array file contains three lines of information, which can be thought of as 80 column card images, corresponding to three major classes of control information.

The first card image contains time information: dUT1/dIAT is placed in Columns 1-15 in units of seconds per day; Columns 16-30 contain the modified Julian date at which dUT1/dIAT projects to UT1 = UTC; and Columns 31-45 contain the value of IAT - UTC.

The second card image in the ARRAY control file contains the coordinates of the pole: in Columns 1-15 and 16-30 the values of X and Y in seconds of arc, respectively, relative to the conventional international origin are supplied; in Columns 31-45 and 46-60 the rates of change dX/dt and dY/dt, respectively, are (optionally) given in units of seconds of arc per day; and in Columns 61-75 the modified Julian day epoch for X and Y are (optionally) supplied. The information on the first two card images is taken directly from the U. S. Naval Observatory Time Service Announcements Series 7. All parameters use an F format.

The third card image in the ARRAY file contains miscellaneous control function information which will be used to indicate who can control various one-of-a-kind devices. Columns 1-4 specify the controlling subarray for the four quadrants of the correlator system- only this subarray can change its mode; Columns 6-9 specify the controlling subarray for each of the final synthesizers for the four (ABCD) IFs; Column 11 is blank when the de-icers are off and has a T when they are turned on; and Column 12 is blank if refraction corrections are to be based on measurements of the weather station, but contains a T if estimated values of refraction, based on a seasonal and diurnal model, are to be used.

4.2.3.2 Subarray Files SUBn = SUB1, SUB2, SUB3

Since the VLA can function in up to three subarrays, there must be a subarray file for each subarray in operation. The antennas that are to function in each subarray are specified in the ANTENNAS control file.

The first card image in a SUBn file gives the names of the source list files that will control the observing in that subarray. This looks something like FILE1bFILE2bFILE3bFILE4 (where b indicates a required space), which prescribes that the observing in this subarray should first be controlled by the source list in FILE1. When this source list is completed, control changes to FILE2, then to FILE3, and FILE4 in sequence. When a source list file has been completed, each letter in its name is replaced by a "\", e.g., FILE1 is replaced with \\\\\.

The remaining card images in a SUBn file are optional combinations of three types:

1. Alias card - optional means of specifying nonstandard band designations.
2. LO and receiver setting card (LO) - optional specification of LO frequencies, synthesizer settings, and the names of fields with alternative IF parameters, front end parameters, and subreflector rotation parameters.
3. External LO frequencies card (LI) - optional card associated with the spectral line system for specification of special parameters for this mode of operation.

Alias cards cannot precede the first card with source list file names. On an alias card, Columns 1-2 specify the desired nonstandard band notation, replacing the standard LL, CC, UU, KK, UC, or CU. Columns 3-4 contain the letters AL (for alias), and Columns 5-6 contain the standard band codes being replaced and for which an LO card will be supplied. Examples of alias card images are: 18ALLL 21ALLL which might be used when the observer wishes to use both 18 and 21 cm wavelengths; the cards inform the computer that both are at L band.

The LO and receiver setting card is always present for the standard band and frequency setting, and additional ones are used for every new band designation made on an alias card. In SUBn files columns 1-2 contain the AB and CD band designations according to standard on-line usage (L, C, U, K), or as changed by an alias card; however, in source list files columns 1-2 of the LO card contain //, and the band designation is determined by the previous source list card. Columns 3-4 always contain the letters LO. Columns 5-6 contain bias digit codes for upconverters and mixers for AB and CD sides, according to a code whereby 0 means center frequency of entire band, 1 means center frequency of bottom third of band, 2 means center frequency of middle third of band, and 3 means center frequency of top third of band. Columns 7-13 and 14-20 contain the AB and CD, respectively, first LO (front end) frequencies in GHz and F7.1 format. Columns 21-25, 26-30, 31-35, and 36-40 contain the A, B, C, and D, respectively, (2-4 GHz LO) synthesizer frequencies. The B synthesizer frequency is 300 MHz higher than the A synthesizer frequency and the D synthesizer frequency is 550 MHz higher than the C synthesizer. These LO frequencies are determined by the expression

$$\mathrm{f}(2-4\ \mathrm{GHz\ LO}) = 2400 + 50\mathrm{n} \pm 10,$$

where n is an integer such that f lies within the range 2710 to 4010 MHz. The synthesizers being set are the L6 modules shown in Figure 3.6.

Continuing with the LO and receiver setting card, Columns 41-50 and 51-60 are the fluke synthesizer settings in F10.1 format, with ranges of 100-150 MHz and 200-250 MHz, for the AB and CD channels, respectively. Columns 61-70 contain the left-adjusted name of the file containing IF gain calibration parameters, the so-called IF files. Columns 71-80 contain the left-adjusted name of the file containing front end and subreflector parameters, the so-called ROT files with subreflector rotation parameters.

The SUBn files should always contain LO and frequency card images for the standard band combinations. The following is a minimum SUBn file, without alias cards, followed by explanations of each LO card entry:

FILE1 FILE2 FILE3 FILE4

CCLO			3560	3860	3310	3860	100.0	200.0	SYSCIF	SYSCROT
LLLO00	-3.2	-3.2	3340	3640	3090	3640	100.0	200.0	SYSLIF	SYSLROT
UULO	19.6	19.6	3290	3590	3040	3590	100.0	200.0	SYSUIF	SYSUROT
KKLO	17.6	17.6	3560	3860	3310	3860	100.0	200.0	SYSKIF	SYSKROT
Band	AB First LO	CD First LO	A	B	C	D	AB Fluke Synth.	CD Fluke Synth.	"IF" File	"ROT" File
			2-4 GHz LO synthesizer settings							

Bias Digits

As seen in the above example, standard system IF files are named SYSCIF, SYSLIF, SYSUIF, and SYSKIF for the C, L, U, and K bands, respectively, and the standard system ROT files are named SYSCROT, SYSLROT, SYSUROT, and SYSKROT. Observers who use nonstandard IF and ROT files must supply different designations. Any modification of files beginning with the letters SYS, or of the ANTENNAS, ARRAY, or SUBn files, should be done only with the advice and consent of the array operator.

An additional LO frequency card (LI), to be used in the spectral line system to further specify frequencies within the band determined by the LO card, is optionally supplied, with one card for each band. Formats are as follows. In SUBn files columns 1-2 contain the AB and CD band designations; however, in source list files the LI cards have // in columns 1-2, and the band is determined by the previous source list card. Columns 3-4 must contain the characters LI, indicating it is a spectral line card. Columns 6-9 contain the default IF bandwidth codes, if not specified on the source cards (0-9 for each of four IFs). Column 11 contains an L if it is a line observation card and a C if it is a continuum card. Column 12 indicates which velocity system is to be used, with T for topocentric, H for heliocentric, L for the local standard of rest, and a blank if an LO setting from an LO card is to be used. Column 13 gives the units of the velocity of the feature to be centered in the band, with V or blank for km/sec and F for kHz. Column 14 contains a Y if the fluke synthesizers are to be up-dated, and a blank if they are not. Columns 15-17 contain the correlator mode code. Columns 18-19 specify the averaging time, where a blank, 0, or 1 means 10 seconds, and a larger integer (n) means 10n seconds. Columns 21-23 contain the beginning channel number. Columns 24-26 contain the LOG (base2) of the number of channels. Certain standard line frequencies can be specified by putting a line transition code into columns 27-30 (i.e. H, H_2O, H_2CO, 1612, 1665, 1667, 1720), in which case columns 31-46 must remain blank; alternatively, columns 27-30 may be left blank and one can specify a spectral line rest frequency (in MHz) in columns 31-46. Finally, columns 47-63 and 64-80 contain the AB and CD external LO frequencies (in MHz).

DEC-10 programs called DOPSET and LOSER can be used to calculate the frequencies for the LO and LI cards, as discussed in Chapter 12.

4.2.3.3 ANTENNAS File

The ANTENNAS file supplies miscellaneous information about each antenna. Columns 1-5 contain the physical ID number of an antenna in I5 format, ending in Column 5. Columns 6-10 contain the DCS (digital communication system) address, in octal, ending in Column 10. Columns 11-15 contain the station ID in (A2,I1) format ending in Column 15 as, for example, CW5. Columns 16-20 contain delay line number in I5 format. Column 40 contains a T if elevations greater than 90 degrees are forbidden, and is blank if they are allowed. Column 44 contains a minus sign (-) if the antenna is to be ignored because it is nonoperational. Column 45 has the number of the subarray to which the antenna is assigned. In column 51, a T means the round trip phase correction is to be turned off. A T in column 55 means that phase switching for this antenna is to be switched off at both the antenna and in the delay/muliplier hardware. A T in column 56 means that data should not be collected from this antenna (spectral line only). This file is modified only by VLA staff. The following is an example of a card image in the ANTENNAS file, corresponding to antenna #1 located on station W8:

```
 1   1 AW1          T   1    T   T
```

4.2.3.4 BASELINE file

The BASELINE file contains the antenna station positions, a delay constant, and the axis intersection defect parameter. On each card image, Columns 1-2 contain the antenna's physical ID number ending in Column 2. Columns 3-15, 16-30, and 31-45 contain, respectively, L_x, L_y, and L_z for the station positions in nanoseconds with an F15.4 format. Columns 46-60 contain a delay constant in nanoseconds with an F15.4 format. Columns 61-70 contain the axis intersection defect parameter ("K" term) in units of nanoseconds with F10.4 format. This file is modified only by VLA staff.

The following is an example of a card image in the BASELINE file:

```
 1  509.530   -1338.480       -745.203       -1545.0
```

4.2.3.5 POINTING file

The pointing file contains the pointing parameters for the Azimuth (AZ) and Elevation (h) dependent pointing formula for each antenna. This card image is in free format with the following information in order: the antenna physical ID number; the arm reference angle in degrees; the azimuth tilt E-W component, A1; the azimuth tilt N-S component, A2; the coefficient of a COS(AZ) term, A3; the coefficient of a SIN(AZ) term, A4; the axis perpindicularity error, A5; the collimation error, A6; the azimuth encoder offset, A7; the elevation tilt E-W component, E1; the elevation tilt N-S component, E2; the coefficient of a cos(h) term, E3; the coefficient of a sin(h) term, E4; and, the second to the last number, the elevation encoder offset, E5. Thus there are seven azimuth pointing parameters (A1, A2, A3, A4, A5, A6, and A7) and five elevation pointing parameters (E1, E2, E3, E4, and E5). The last parameter on the card is the approximate reading (in turns) of the 600 MHz round trip phase detector; this parameter is used to resolve ambiguities about which lobe of the 600 MHz cycle is correct. The following is an example of a POINTING file card image:

$1,\ -60+0.14,\ -1.00, 0.,\ 0.,\ 0.,\ -0.91,\ +42.02,\ +0.14,\ -1.00,\ 0.0,\ 0.0,\ -0.30,\ 0.25$

4.2.3.6 The ROT or SUBR files with Front End

The front end or subreflector files contain various subreflector and front end parameters. These are usually referred to as ROT files because they contain subreflector rotation parameters. The standard system ROT files are called SYSCLROT, SYSCROT, SYSUROT, and SYSKROT for the four observing bands. The choice of which ROT files are operative for a particular subarray is made by putting the ROT file name in Columns 71-80, left-adjusted, in the SUBn file for each subarray.

There is one ROT file for each frequency band, and within a ROT file there is one card image for each antenna. Columns 1-5 contain the (physical) antenna ID number ending in Column 5. Columns 6-40 contain subreflector rotation and focus parameters. In Columns 6-10 there is the azimuth collimation error, in arcminutes, in format F5.2. In Columns 11-15 there is the elevation collmation error, in arcminutes, in format F5.2. Columns 16-30 contain the computer command for the subreflector rotation setting in format F15.1. Columns 31-35 contain the FO focus parameter, a computer command, in F5.1 format starting in Column 31; and Columns 36-40 contain the F1 focus parameter, a computer command, in F5.1 format starting in Column 36. The focus curve is computed from

$$\text{focus} = \text{F0} + \text{F1} \sin(\text{h})$$

where h is the elevation.

Various front end parameters are specified in columns 44-70. If column 44 contains a T, the AB paramp output is switched into the CD IF system and the CD paramp output is switched into the AB IF system; however, if this column is blank, the normal situation of AB into A and B IFs and CD into C and D IFs will occur. A T in column 45 means to use this antenna for a reference for interferometer pointing. The paramps for AB and CD channels can be turned off by placing the letter T in columns 47 and 48, respectively. The 5 GHz attenuator (usually 8 dB) following the AB and CD paramps can be inserted in the signal path by putting the letter T in columns 49 and 50, respectively. The choice of high or low DC gain in the frequency converter detectors for all four IFs is chosen by placing a T or a blank in columns 52-55. The solar calibration noise tube is turned on (for antennas 17 and 18) by placing a T in column 57. For solar observations, a 20 db attenuator, located between the second stage paramp and the FET amplifier, is turned on if a T is in column 58. A T placed in column 63 means the on-line system temperature correction will be applied to the data; a blank means it will not. The standard noise tube can be turned on by a T in column 64 and turned off by a blank. A T in column 65 means the noise tube will switch on and off at a 9.6 Hz rate; a blank means it will not switch. Columns 67-70 should have T's if the frequency converter alternate input switches are to be turned on for ABCD IFs, and should be blank if they are to be turned off. Finally, columns 71-74 contain the front end filter codes for ABCD IFs. A blank or zero for an IF selects the unfiltered, full bandwidth; however, a 1 selects 25

MHz bandwidth at an IF frequency of 1025 MHz while a 2 selects 12.5 MHz bandwidth at an IF frequency of 1027 MHz. The latter specifications are useful only for P band.

4.2.3.7 IF Files with Gain Calibration Parameters

The IF files contain gain calibration parameters for each antenna. The IF files used to control the observing in the n-th subarray are specified by putting the IF file name in Columns 61-70 of the IF and receiver setting card image in the SUBn file. The standard system parameters are in IF files named SYSCIF, SYSLIF, SYSUIF, and SYSKIF, so when the user changes IF parameter files other names must be used. There will always be a different IF file for each frequency band. There is a single card image in each IF file for each antenna and IF combination. Columns 1-4 contain the physical antenna ID number in format I4, ending in Column 4. Column 5 contains the IF identification character: A, B, C or D. Columns 6-15 contain the IF peculiar delay in nanoseconds in F10.4 format. Columns 16-20 contain the IF peculiar phase (positive for decreasing phase) in degrees in F5.1 format. Columns 21-25 contain the zenith efficiency parameter E0. Columns 26-30 and 31-35 contain the E1 and E2 parameters for surface accuracy deterioration with elevation. Columns 36-40 contain the E3 parameter for atmospheric absorption. The latter four parameters are in format F5.4. The net efficiency is calculated from E = E0 (sin(h)-1)E1 + (cos(h))E2 - (csc(h)-1)E3. Columns 41-45 contain the noise tube temperature (in degrees) in format F5.3. A T in Column 50 means that this IF is out of operation and should be ignored, whereas a blank means the IF is in operation. Finally, a T in column 51 means a constant delay of 0.32 μsec should be added to the delay for this IF.

5 Preparation for Observing

Abstract

We discuss what the observer does to prepare for observing with the VLA. This includes the things that must be done before arriving at the VLA site, the things that are to be done to prepare the observing program, and discussion of many details that might affect observing programs. The most important responsibility of the observer is the planning and preparation of the text file(s) that control the observing process in the on-line computer system.

Because of their role in preparing an observing program, we discuss various means of supplying source names and positions and the OBSERV program for preparing observing control files in the DEC-10. Also discussed are the details involved in using non-standard frequencies, and the known sources of interference.

5.1 Introduction

Considering the complexity of the VLA, the instrument is usually relatively easy to use. Observing procedures are automated to the extent that that once the appropriate control files are generated there is nothing for the observer to do except carry out data reduction. If one uses the VLA in a standard operating configuration, there are few system parameters that the user needs to be concerned with. The most significant parameters are time of observation, observing duration per scan, band (sky frequency), and bandwidth. Solar system objects, especially the sun, require further complications such as moving coordinates. The philosophy of the observing session requires careful thought. Considerations such as u-v plane coverage, signal-to-noise ratio, the total amount of observing time per object, and the location of sun and moon should be evaluated before an observing proposal is submitted. In this chapter we will discuss various items to consider when organizing an observing program, and how to prepare the observing source list.

5.2 Preliminary Planning for VLA Observing

5.2.1 VLA Staff Aid

Each scheduled observing program is assigned a VLA staff member who should be the first person consulted concerning problems before, during, and after observing. For observers inexperienced with the VLA this staff member should be consulted at least a few weeks before the observing run begins. Current characteristics of the array and the status of software should be discussed so the user can optimize use of the instrument. In addition to the user obtaining current status information, it is important that the staff member be familiar with the planned program so that advice can be optimized.

5.2.2 Materials to Bring Along

The user should plan to bring along all information critical to carrying out the observing program. Although some library facilities are available at the VLA site, the user should not count on obtaining critical information at the site. At the very least, the observer should prepare and bring along the following: (1) a list of all sources, with source positions, that might be observed; (2) an assessment of the minimum amount of observing time and u-v coverage needed to attain the goals of the program; (3) an estimate of maximum flux densities of sources, good to at least a factor of two; and (4) a calibration plan matched to the characteristics of program sources. Positions for any epoch may be used; however, epoch 1950.0 positions are treated as "standard". Although it is important to plan in advance, it is best to delay generation of the final observing program until arrival at the VLA site.

5.2.3 Arrival at the Site

Observers should come to the VLA site at least one or two days before the observing begins. Since you cannot count on your staff contact being available on weekends, unless special arrangements have been made, and because other staff that you might need to consult with are not around on weekends, this advance time should occur during the week. Observers should also plan to spend about a week after the observing run for editing, calibration, mapping and initial image processing. Experience has shown that, even if the user is planning further data reduction elsewhere after leaving the site, intolerable and impossible demands on VLA staff and facilities can occur when observers attempt to get everything done in only a few days.

5.2.4 First Things to Do

Upon arrival at the site, the first priority is to get settled in a room in the Visiting Scientist Quarters and to be sure that the logistics of eating are well in hand. This is to avoid finding yourself after 4:30 pm with room or meal problems and no one to help you straighten them out.

Inexperienced observers should next talk with the VLA staff member assigned to help them out. At this point a re-discussion of the goals of the program should occur, with specific evaluation of the current status of everything needed to accomplish the program. Discussions with recent observers and other VLA staff may also be valuable. Although your VLA staff contact should be your main source of information, outside of documentation, other input is often very helpful.

5.3 Detailed Planning of Observations

5.3.1 Need for Planning

Many small details need to be considered in the planning of a VLA observing program. The flexibility of the VLA gives the user many options (and defaults) that may effect scientific results.

Observers should finalize, on paper, their observing and calibration plans for at least the first several hours of observing. If possible, it is a good idea to have an observing plan, with alternatives, prepared for the entire observing run. However, if this covers more than 24 hours, it may be wise to delay the most detailed planning of all but the first 24 hours because actual experience while observing tends to lead to modifications of programs. In the detailed plan the sequence of calibration should be established and the times of observation of all sources, whether in LST durations or stop times, should be roughly specified. In many cases this means establishing a specific cycle of observations of an hour or two that is repeated a number of times. Once the cycles or detailed times of observation are planned, the observer should check such things as elevation limits, excessive move times, azimuth limits, and adequacy of integration time and hour angle coverage. The OBSERV program that we will discuss shortly is an aid in both preparing and checking the observing program.

5.3.2 Calibration Strategy

It is wise to err on the side of overcalibration, particularly if the quality of the weather is uncertain. At least 10%, and sometimes as much as a third of the observing time, should be spent on calibrators. For 6 and 20 cm observations, about five minutes out of each half hour should be devoted to phase calibrators. For 2 and 1.3 cm observations, five minutes out of each fifteen or twenty minutes may suffice. Phase calibrators are chosen from either the observer's own knowledge that they are point sources (at the appropriate wavelength) with good positions, or from the observer's perusal of the Calibrator Manual at the VLA. In addition, the flux densities of phase calibrators, all of which tend to be time variable and for which flux density histories are never completely adequate, will need to be determined by boot-strapping from observations of good flux density calibrators. Tables of information about these are also available in the Calibrator Manual. All VLA flux densities are based on 3C286. It is best to include this source at least once for each frequency and bandwidth to be used, if at all possible. If not, secondary flux calibrators are available, including a number of circumpolar sources that can be observed at any time.

If more than one frequency is being used, it is recommended that all observations involve the basic sequence CALIBRATOR – SOURCE – CALIBRATOR for 1.3 and 2 cm and SOURCE – CALIBRATOR or CALIBRATOR –SOURCE for 6 and 20 cm. For high frequency observations it is important to choose a phase calibrator as close to the source as possible to reduce differential atmospheric effects. During bad weather, observations at 2 and 1.3 cm may not be possible.

For astrometric programs demanding extremely good phase stability, for accurate flux density measurements, and for large dynamic range mapping, more stringent calibration procedures may be necessary.

5.3.3 Lists of Phase and Amplitude Calibrators

One can obtain information about phase and amplitude calibrators from the Calibrator Manual. This manual has four sections. You may obtain a printed copy of any section by following the instructions at the beginning of the Calibrator Manual. Calibrators are sometimes not good for all bands, configurations, and purposes. Study the limitations of the calibrators near your sources and carefully choose which you think are optimum. One need not supply positions for sources in the Calibrator Manual because they will read in by the OBSERV program (from a calibrator information file) when the calibrator name is given.

5.3.4 Planning u-v Coverage

The number of antennas available at a particular frequency may vary from day to day. Because of malfunctions one or two antennas may be down during any particular observation. The maximum possible u-v plane coverage for a 27-element array is shown in Figure 5-1. Several synthesized beam shapes are shown in Figure 5-2. With the "CLEAN" and self calibration programs one may not need extensive u-v coverage to obtain quality maps. One of the most important considerations in choosing the amount of observing time is signal-to-noise ratio (SNR). Once the SNR is greater than 10 or so on a map feature of interest, the CLEAN algorithm can remove the sidelobes of the beam produced by limited u-v coverage. To successfully apply self calibration, which can remove some phase errors, one must have a good SNR, on cell-to-cell basis in the u-v plane, and not just a good SNR on a feature in the final map. The definition of a good SNR in the u-v data for self calibration is complicated. Very extended features can cause problems both for CLEAN and self calibration. An inexperienced observer should contact a VLA staff scientist for advice.

The maximum and minimum sidelobe levels of a synthesized beam are major indicators of image quality. These levels for the 27-element observing situations corresponding to Figure 5-1 are listed Table 5-1. In addition, Table 5-2 shows sidelobe levels for various tracking ranges for a source with 30° declination.

Table 5 - 1
Maximum and Minimum Beam Sidelobe Levels

Declination (degrees)	Maximum (fraction)	Minimum (fraction)
80	0.07	-0.14
60	0.08	-0.17
40	0.11	-0.25
20	0.16	-0.40
0	0.2	-0.42
20	0.2	-0.4
40	0.2	-0.44

Table 5 - 2
Sidelobe Levels for $\delta = 30°$ Buildup Map

H_{start}	H_{stop}	H_{range}	Inner 1/4 Maximum Sidelobe Level	Outer 3/4 Maximum Sidelobe Level
-6^h	-5^h45^m	15^m	27%	12%
-6^h	-5^h30^m	30^m	16	4
-6^h	-5^h	1^h	9	4
-6^h	-4^h	2^h	8	3
-6^h	-3^h	3^h	7	2
-6^h	-2^h	4^h	5	2
-6^h	0^h	6^h	3	2
-6^h	$+6^h$	12^h	3%	<1%

5.3.5 Sensitivity, Resolution, and Confusion

In addition to the question of the u-v coverage obtained for VLA observing, it is necessary to be aware of the sensitivity, resolution, and confusion limitations of the observations. Table 5-3 summarizes the approximate parameters of these limitations for the standard 27-antenna observing situation. As seen from Table 5-3, one of the principal advantages of the VLA is the sensitivity of its 130 m collecting area. A bandwidth of 50 MHz was assumed for the sensitivity calculations in Table 5-3, so scaling with the square root of the bandwidth should be applied for other cases.

5.3.6 Subarray Operation

The VLA can operate antennas in up to three subarrays, with each sub- array operating independently and simultaneously. Depending upon the goals of the observing program, it may be desirable to use more than one subarray. For example, if simultaneous frequency coverage is important while sensitivity and u-v coverage is no problem, it may be desirable to schedule different frequencies in different subarrays. However, for practical reasons involving the VLA calibration programs, you should never use fewer than three antennas in a subarray and it is strongly recommended that there be at least four, to allow for one possible antenna-IF failure. One achieves subarray operation by having a different source list file for each subarray and having the array operator modify the subarray files (SUBn) to indicate which antennas and which source list files are to be used in each subarray. The user should be warned that, because the number of antenna pairs in a subarray is N(N-1)/2, where N is the number of antennas, one rapidly loses both sensitivity and u-v coverage by reducing N. Under most circumstances, the user will be much better off using only one subarray, but alternating observations of different types.

Table 5 - 3
Sensitivity, Resolution, and Confusion Limits with 27 Antennas

Frequency	1.34-1.73	4.5-5.0	14.4-15.4	22.0-24.0 GHz
Wavelength	22.4-17.3	6.67-6.00	2.08-1.95	1.36-1.25 cm
Band Designation	20 cm	6 cm	2 cm	1.3 cm
	L	C	U	K
System Temperature	60	60	120	400 °K
RMS Sensitivity in 10 minutes (50 MHz bandwidth)	0.13	0.10	0.2	1.0 mJy
RMS Sensitivity in 12 hours (50 MHz bandwidth)	0.015	0.012	0.03	0.12 mJy
Untapered Brightness[1] Temperature (A configuration)	6.9	5.5	34	54 °K
Dynamic Range Without Self Calibration[2]	100	50	25	10?
Antenna Beam Size (HPBW)	30′	9′	3.7′	2′
Brightest Source Expected in Antenna Beam	100	2.3	<0.1	<0.01 mJy

5.3.7 Final Details of Source Scheduling

Once the basic questions of calibration procedures, subarrays, and integration times for sources

[1] RMS sensitivity in brightness temperature for an untapered map is given approximately by

$$\Delta \mathrm{T} \simeq \left(\frac{1.46\lambda^2}{\theta_1\theta_2}\right)\Delta \mathrm{S}$$

Where θ_1 and θ_2 are the half-power synthesized beamwidths in arcseconds, λ is the wavelength in cm, and ΔS is the rms sensitivity per beam area in mJy.

[2] Dynamic range is extremely dependent on declination, time of day, season, and frequency of calibration.

and calibrators are settled, more detailed source scheduling can proceed. It is recommended that a written plan of sources and observation times be prepared, either for the entire program or for basic cycles repeated often in the basic program. At the very least, you need to figure out the sidereal times (LST) for the first and last time the array will be on each source. Also, check that the source is above elevation limits using Figures 5-3 or 5-4.

Figure 5-3 is a plot showing the correspondence between Altitude- Azimuth and Hour Angle-Declination. Figure 5-4 shows the hour angle limits as a function of declination for 8°, 10°, and 20° elevation limits. The 10° limit is useful for scheduling if you want maximum hour angle coverage without danger of encountering the 8° instrumental limit. The 20° limit is useful when you want to avoid large air masses.

5.3.7.1 Bandwidth Selection

Selection of the observing bandwidth depends upon a number of considerations. Maximum sensitivity is obtained with 50 MHz bandwidth, although the field of view will be limited, as seen from Table 5-3. However, with observations of small sources this is no problem, and is, in fact, desirable to limit problems with confusion. In almost all cases, detection experiments should be carried out with 50 MHz bandwidth, as should mapping of faint, small extended sources. For larger sources and the larger array configurations, a narrower bandwidth should be used to widen the field of view. Independent of any other consideration, 50 MHz bandwidth is most desirable for 2 and 1.3 cm operation; this provides needed sensitivity and it does not limit the field of view. For observations at 20 cm, where interference may appear in the 50 MHz bandwidth but not in the 25 or 12 MHz bandwidths, it may be desirable to choose a narrower band which is interference free (cf. Section 6 in this Chapter).

5.3.7.2 Move Times

The time required for slewing the antenna from one source to another must be considered when choosing a duration time. You do not *not* get your duration time in addition to the slew time. If you specify a 10 minute duration, and the slew time is 4 minutes, the antennas will be on the source roughly 6 minutes. The OBSERV program can predict move times.

The antenna slew rates are: 20°/minute in elevation and 40°/minute in azimuth. Be sure to include slew times when choosing the observing time for each source. In addition, it takes 30-50 seconds for the system to completely "set-up" after the antennas slew. On-source calibration times can frequently be as short as 2 minutes, so slew and set-up times are important to consider when choosing short durations.

Tracking a source near the zenith can cause difficulties because of the large rate of change in azimuth. Since it is not possible to observe a source within 0.3 degrees of the zenith, sources between declinations 33° 40′ and 34° 30′ should not be scheduled near transit (cf. Fig. 5-3).

The next consideration is the slewing direction. The antennas will always follow the shortest path when moving to the next source. However, if azimuth cable limits will be encountered before reaching the source, or during the tracking duration you have specified, the computer will instruct those antennas to slew in the opposite direction. You have three choices in coping with the antenna cable wrap problem:

1. Do nothing. You can ignore the situation and let the computer decide. This technique is the least effort but may lead to missing a calibrator scan entirely, or part or all of a scan on a program source.
2. Schedule carefully. If you find out where the antennas are pointing at the end of the previous program, you may be able to schedule your sources so as to minimize cable unwrapping at an inconvenient time.

   The cable wrap limits are listed in Table 5-4 lists information about these antenna wraps and azimuths, where Z is the true azimuth and AZ = Z - 180° is the "antenna azimuth".

Table 5 - 4
Antenna Wrap and Azimuth Information

Range in Z	Antenna Azimuth (AZ)		
	CCW limit	Center	CW limit
180° ± 265°	95°	360°	625°

3. Insert cable wrap cards. You can force the antennas to wind in a particular direction any time you choose. The procedure for adding a cable wrap (AN) card is explained later in this chapter in the section on OBSERV. In addition to controlling the direction of rotation in azimuth, you can allow or disallow the "over-the-top" mode in which the antennas are capable of tipping 35° beyond the zenith. This capability may be enabled unless you inhibit it with a cable wrap (AN) card in the OBSERV program. Allowing over-the-top observing can cause confusion in determining what paths the antennas will take on their next slew, because they will remain over-the-top until a limit is anticipated when slewing, or until you prohibit it with an AN card. The CHKOBS features in a DEC-10 program called OBSERV, will give position information that is very helpful in keeping track of antenna movement. If you anticipate difficulty in using over-the-top geometry, we suggest arranging your schedule to avoid it or to prohibit it with

an AN card. If you choose the latter, an AN card must accompany each source card in which you think the computer may choose to move the antennas over the top.

5.3.7.3 Primary Beam Considerations

In some instances the desired field of view may be so wide that the antenna beam attenuates the signal at the edge of the field. One can approach this problem in two ways. Either allow the attenuation and try to correct for it later, or observe the field with multiple antenna positions. If maximum flux accuracy is desired, the second approach is superior. If having all the sources in one map, or minimizing observing time, is important the first approach may be satisfactory. However, one should be aware of the reduction in signal-to-noise ratio. In the extreme case of sources near the first null in the beam, all signal will be lost.

It is sometimes possible to take advantage of the first null in the antenna pattern. If a strong source is in the vicinity of the source of interest, the beam null ($\approx 3.4' \lambda_{\rm cm}$ from the field center) may be placed on the strong source. Except for an unusual case, the peak of the beam need not point exactly at the source of interest.

Figure 5-5 shows the antenna pattern for the four main observing bands. Beyond the plotted curve the beam pattern is too poorly known to allow reasonable measurements of surface brightness.

5.3.7.4 Polarization Calibration

Polarization data are always gathered with the VLA. Normally IF channel A (or B) receives right-hand circular polarization and channel C (or D) receives left-hand circular polarization. Polarization data are calibrated with the DEC-10 program POLCAL after the regular calibration procedures are completed.

POLCAL will solve for the system polarization parameters and the calibrator polarization parameters simultaneously. Thus any calibrator suitable for one's program can also be used for the system polarization calibration. The calibrator should be observed at several hour angles corresponding to a wide range of parallactic angles. (See Figure 5-6 for a plot of parallactic angle vs. hour angle.) Good parallactic angle coverage is the most important requirement for good polarization calibration. If this is not possible, one may be able to borrow calibration parameters. The antenna polarization does not change quickly, so using previously determined parameters may be adequate. The determination of absolute position angle requires at least one observation of a strongly polarized calibrator (like 3C286 or other sources in the Calibrator Manual) with known position angle.

5.3.7.5 Standard vs Non-Standard Frequencies

Selection of standard frequencies for each observing band is recommended unless other considerations are important. The default frequencies are listed in Table 5-5.

Table 5 - 5
Standard Continuum Observing Frequencies

	BAND				
Bandwidth [MHz]	21 cm HH [MHz]	20 cm LL [MHz]	6 cm CC [MHz]	2 cm UU [GHz]	1.3 cm KK [GHz]
50.0		1464.90	4885.10	14.9649	22.4851
25.0	1413.00	1452.40	4872.60	14.9774	22.4726
12.5	1406.75	1446.15	4866.35	14.9837	22.4664
6.25		1443.03	4863.23	14.9869	22.4632
3.125		1441.46	4861.66	14.9883	22.4617
1.5625		1440.68	4860.88	14.9891	22.4609
0.78125		1440.29	4860.49	14.9895	22.4605

As this is written, a few VLA antennas have been equipped with an experimental system operating at 300-350 MHz. This system, called P band, is being tested for possible use as a standard VLA low frequency system.

5.3.7.6 Bandwidth Effect on Intensity and Beam

A wide bandwidth, which is usually chosen to improve the sensitivity, can decrease the field-of-view and broaden the synthesized beam. Beam broadening and central intensity loss should be considered when choosing a bandwidth. If a wide field of view is necessary, you must decide what loss can be tolerated at the edge of the field, and choose the appropriate bandwidth. However, as the bandwidth is narrowed, the observation time for a source must be increased to maintain the same sensitivity. In addition to causing a loss of intensity, the bandwidth also widens the radial dimension of the synthesized beam as the distance from the phase center increases. These bandwidth effects are discussed in more detail in Chapter 2 where figures show the quantitative effects of bandwidth on point source intensity and beam shape. Table 5-6 lists a few values of the intensity loss due to finite bandwidth, for all four VLA configurations, as a function of $\beta = (\Delta v/v)(\theta/\theta_{\rm HPBW}) = 1.6(\theta/1')(\Delta v/50 \text{ MHz})(1/3.285)^{n-1}$ (n = 1, 2, 3, and 4 for the A, B, C, and D configurations), where θ is the angular displacement from the phase reference position.

Table 5 - 6
Loss of Peak Intensity Due to Finite Bandwidth[3]

$\beta = (\Delta v/v)(\theta/\theta_{\rm HPBW})$	$I_{\rm beam}$ / I_o	θ(BW=50MHz)			
		A	B	C	D
0	1.0	0	0	0	0
0.52	0.95	$13''$	$40''$	$2'$	$8'$
0.74	0.90	$20''$	$60''$	$3'$	$11'$
1.0	0.80	$25''$	$80''$	$4'$	$15'$
2.0	0.50	$50''$	$3'$	$9'$	$30'$

5.3.7.7 Integration Time and Its Effect on Intensity

Increasing the integration time interval of the correlated signals to too large a value can cause a loss of intensity for map features far away from the phase center. The loss increases as the distance from the phase center increases. In Table 5-7 we list one measure of the effects of averaging time: the averaging times for which intensity loss equals that due to finite bandwidth. The normal integration time is 10 seconds in the on-line computer system and on the MODCOMP archive tapes. However, under special circumstances one can request a minimum integration time of 3 1/3 seconds. Unlike bandwidth losses, intensity losses due to too large an averaging time (greater than 10 or 3 1/3 seconds) can be removed by re-filling data bases with shorter averaging times.

Table 5 - 7
Averaging Time for Which Integration Time Losses Equal Bandwidth Losses for δ = 90°

v[MHz]	Averaging Time (seconds)				
	Δv = 50 MHz	25 MHz	12.5 MHz	6.25 MHz	2.125 MHz
1460	415	210	105	55	25
4885	140	70	35	18	9
15000	45	22	10	5	3
23000	30	15	7	3	2

If one is greatly concerned with losing intensity by integration, a conservative approach should be adhered to. However, since the worst case only occurs during part of the tracking on a particular source, and since increasing integration time reduces disk storage space and reduces off-line computer program execution time, it is well worth choosing the maximum possible integration time.

5.3.7.8 Correlator Saturation and Bandwidth Codes

At various stages in the VLA data processing system the real and imaginary parts of the visibility function are stored as 16 bit integers, with an associated "gain code" that indicates the scaling factor between these integers and the true visibilities. As part of the preparation for observing the user must estimate the flux level and associated gain code for each source to be observed. If a gain code is to high for a weak source, the visibility may not be represented with sufficient accuracy. On the other hand, too low a gain code for a strong source will result in "saturation" where the stored real or imaginary parts of the visibility should exceed 32767, but are truncated in the high order bits, resulting in an unpredictably bad number.

The weakest sources should have a gain code of 3 while the strongest sources should have a gain code of 8. As a rough rule of thumb, if S is the flux density of a source (above 8 Jy at 20 and 6 cm, above 80 Jy at 2 and 1.3 cm), the gain code should be such that $K * 2^{GC} \Leftarrow S \Leftarrow K*^{GV+1}$, where $K \approx 1$ for 20cm and 6 cm, and $K \approx 10$ for 2 cm and 1.3 cm.

A more correct treatment of the problem is required when sources are so strong that they contribute significantly to the system temperature. It may be possible to arrange for test observations to determine the gain code for which saturation occurs for particular strong sources.

5.4 Activities During Observing

5.4.1 Responsibilities of the Array Operators

The operation of the array, involving antennas, electronics, and on- line computers, is the responsibility of the array operator on duty. The user provides the operator with the names of source list files, together with other information such as which antennas are to operate in which sub- arrays; however, everything else related to operation of the array is the responsibility of the array operator. In any situation where the array operator may deem it necessary to override the wishes of observers, they have the authority to do so. This will occur only under circumstances where their knowledge of what is necessary for safe and proper operation makes them, in fact, more knowledgeable than the observer.

Because of the complexity of their job, VLA array operators are fairly knowledgeable about the VLA antennas, electronics, and on-line computer hardware and software. They are also knowledgeable about use of the off- line computer system, particularly the use of programs dealing with visibility data. Because of this, as long as it does not conflict with their prime responsibilities for array operation, the array operator can provide some help in these areas.

The array operators can also point the way to individuals who may be sources of information about areas where questions arise. They are always the best single source of information about the status of the antennas and electronics.

Because the operators carry out their responsibilities in an open control room, several things are recommended. First of all, cultivate a polite relationship with them. Except for emergencies, do not interrupt them if they are in the midst of important activities. Do not carry out loud conversations in the control room. Keep them informed about your whereabouts in case they need to consult with you about problems and recommended changes. Provide them with information about source list files and usage of antennas in subarrays well in advance. Always give them an exact copy of the listing of source list files. Finally, listen well to their advice. While it is likely that you know more about the scientific results you want to get out of your data, no one, except perhaps a few other VLA staff members, knows more about how to run the VLA for your benefit than the array operators.

5.4.2 Repair of Malfunctioning Equipment

The speed of repair of malfunctioning equipment will depend upon circumstances. Problems causing the entire array to be down will result in call-out of whatever personnel are necessary. Problems that remove an antenna from the array, that can be solved by module substitutions, will be taken care of by the technician on duty; however, since there is no duty technician during the

Midnight to 8 shift, a problem occurring during that time will be deferred. Serious problems that cannot be fixed without extensive work are deferred until normal working hours (Mon-Fri., 8:30 to 4:30, except NRAO Holidays) when staff are available. In addition, at any one time there are about three antennas designated as available for minor repair work. Any of these antennas can be taken out of the array when the technicians wish to carry out their work.

5.4.3 On-Line Programs and Displays

There are several terminals and a printer in the control room devoted entirely to communication with the on-line computers, and through them, with the antennas and electronics. Some of these continually display messages generated by the on-line data checker program, CHK. Other terminals are used for specific status or data displays, but can be used to send specific commands to antennas and electronics, over-riding previous instructions. One can also generate special status listings on the printer. One of the terminals is mostly used for display of antenna status parameters and the sending of commands. Another tends to be used for modification of control files and skipping around in source lists to change the observing situation. The program listing visibility data on an on-line terminal or printer is called D10.

If you are dubious about the quality of data to expect due to, say, atmospheric problems, it is advisable to use D10 look at the calibrator phases, which should be constant on short time scales, for a long baseline. If phases are are particularly bad, you may want to request the array operator to switch to an alternate observing file which is better suited to current circumstances.

In addition to the basic CHK and D10 programs, there are a number of other on-line programs or services of interest to the observer.

The operator can, on request, manipulate source list files from a console terminal. One can extend the observing time on a given source, skip ahead to other source request cards, or skip back to other source request cards. Typing /SLIst produces a display of the source request card before the current one, the current one, and the next three source request cards. The operator can also change observing modes. Thus, for example, one can switch to pointing mode to check pointing if a problem is suspected.

A program always used during start-up, and available for use at any time when certain problems are suspected, is called STUpid. This program checks delay centers, phase centers, and pointing offsets. It requires about twenty minutes per observing band to carry out these checks.

Another program that can be run in place of the D10 display is a program that takes data from calibrators and displays normalized antenna-IF gains. This provides one of the quickest ways to detect abnormal behavior of specific antenna-IF systems.

5.4.4 Monitoring Calibrators

The monitoring of antenna or correlator gains and phase centers for point source calibrators is the most straightforward way of assessing system performance.

Much of the time the array operator will be able to diagnose faulty equipment through judicious hunting amongst antenna-IF status displays that rely on the monitor data. At other times the user can both contribute to the diagnosis of the problem and prepare for off-line editing of data by more detailed examination of calibrator data in the off-line computer data base produced by FILLER. The LISTER and VISPLT programs provide the primary means for this type of evaluation. As an example, plots of calibrator phases should be stable. Problems with phases are sometimes revealed only when the observer systematically plots calibrator phases for a reference antenna against all other antennas. One can find periods of phase instability due to unlocked LOs, phase jumps, or systematic phase variations from such plots. In addition to sometimes helping understand equipment problems that can be fixed, these are all things the user will need to cope with in the process of off-line editing and data correction.

5.4.5 Monitoring Source Results

The evaluation of calibrator behavior will usually inform the user about the fraction of data that is probably good. Often the observer can spend a great deal of time during the observing process evaluating program sources. Examination of calibrators will provide information about system gains and phase centers, and this information can then be used to make first order evaluations of program sources. Scan average amplitudes will reveal source strength and structure information. For point sources, particularly in detection experiments, phase plots will reveal information about the presence and location of sources.

The user who has attained normal proficiency with the off-line data reduction programs will find that, by judicious preparation of batch jobs to carry out editing, correction, and calibration, one can calibrate and map sources while the observing is still going on. This is the best way to evaluate what you are getting from the array, and often the use of the array can be optimized when you know your results to first order while you still have scheduled observing time that you can replan. Because all the data are not available until the observing run is completed, you generally repeat the whole process of editing, correction, calibration, and mapping at a more leisurely pace after the observing run is finished. Some observers choose to wait until this stage before doing any editing, correction, calibration, or mapping. Indeed, for some observing programs this is the only reasonable course. However, the best use of the array will generally be made by those who actively begin, and go as far as they can with, the process of editing, correction, calibration, and mapping while the observing is still going on.

There is a special class of problems that cause spurious signals to be inserted in data, most of the time at such low levels as to be unnoticed in calibrator data. The most obvious of these is interference generated both outside and inside the VLA. Spurious signals are also obtained when one antenna observes part of another antenna causing "shadowing" when very close antennas are pointed in particular directions. These signals are caused by leakage from vertex room equipment. Even nastier, because of unpredictability, are problems with correlator and sampler hardware which result in the addition of spurious signals. These are recognized by source data that makes no sense. Examples are a few correlators showing higher amplitudes than others, with strong tendencies for phases like 90, -90, 135, -45 degrees, etc. Problems have been found where all AA correlators showed 20 mJy more in amplitudes than all CC correlators, and it was certain that circularly polarized sources were not being observed. Problems of the latter type will not usually be found in calibrator data or antenna-IF status information. For this reason, it is important for the observer to look for things like this himself. In experiments involving detection of weak sources, this is usually found either from evaluation of source amplitudes or from finding inexplicable "noise" behavior in maps.

5.4.6 Useful Practices

During and after the observing the observer will find it useful to have copies of important control files that affect the parameters of the observing. At a minimum, the observer should carefully keep copies of the ANTENNAS file and any source list files that control the observing. The ANTENNAS file will be a convenient record of which antennas are on which stations, together with the assumed station positions. The source list files become useful when questions about what you intended to observe, and in what way, arise. In addition, human errors about source positions happen with sufficient frequency that a record of what positions were supplied to the on-line computers is often useful. For observers using subarrays or nonstandard IF and ROT files, it will be useful to archive copies of the files actually used.

5.4.7 Radio Interference

5.4.7.1 L Band (1340 - 1730 MHz)

Interference is most likely to be encountered in the 18-22 cm band. Table 5-8 shows a listing of the frequency allocations within the VLA tuning range. Note that there are only four bands, much narrower than the possible VLA observing bands, allocated to radio astronomy on an exclusive basis and there is one band, 1660-1670 MHZ, which is shared. The numbers of unclassified government assignments in the area, including White Sands Missile Range, provide some idea of frequency usage. However, they do not include classified assignments and, except at 1350-1400 MHz, there are also non-government assignments. Much of the equipment at White Sands is used only sporadically. Usage can be heavy during special training missions which typically occur for one or two weeks of each year. Only the 1400-1427 MHz band can be depended upon to be free from man-made signals.

5.4.7.2 C Band (4500-5000 MHz)

As Table 5-6 shows, only 10 MHz of this band is allocated to radio astronomy on an exclusive basis. Internationally, the WARC of 1979 extended the radio astronomy allocation down to 4800 MHz on a secondary basis, but this is unlikely to be implemented within the U.S. Experience shows that very little interference is encountered in the top 150 MHz of the band where most VLA observations have been made. Frequency monitoring by G. Bonebrake in 1976 revealed only a weak sporadic signal at 4700 MHz.

5.4.7.3 U Band (14.4-15.4 GHz)

The band 15.35-15.4 GHz is allocated exclusively to radio astronomy and passive services, and at the 1979 WARC radio astronomy was given an international allocation in the band 14.47-14.5 GHz to protect the Formaldehyde line. Very few cases of interference have been experienced at the VLA site in the 14.4-15.4 GHz band.

5.4.7.4 K Band (22-24 GHz)

Within K band 22.21-22.5 GHz is allocated to radio astronomy on a primary basis shared with fixed and mobile communications services, and the band 23.6-24 GHz is allocated exclusively to radio astronomy and passive services. There is very little evidence of any interference in the 22-24 GHz band.

Table 5 - 8
Simplified Listing of U.S. Frequency Allocations
Within VLA Bands

VLA Band	Allocation Band	Allocated Services[4]	No. of Unclass. Gov. assignments[5]
1340-1720 MHz	1300-1350 MHz	AERONAUTICAL RADIO NAVIGATION	9
”	1350-1400 MHz	RADIO LOCATION, fixed, mobile	4
”	1400-1427 MHz	RADIO ASTRONOMY	
”	1427-1535 MHz	FIXED, MOBILE	104
”	1535-1660 MHz	MOBILE SATELLITE, AERO. RADIO NAV.	3
”	1660-1670 MHz	RADIO ASTRONOMY, MET. AIDS	1
”	1670-1710 MHz	METEOROLOGICAL AIDS, MET. SAT.	5
”	1710-1850 MHz	FIXED, MOBILE	55
4500-5000 MHz	4400-4990 MHz	FIXED, MOBILE	42
”	4990-5000 MHz	RADIO ASTRONOMY	
14.4-15.4 GHz	14.3-14.5 GHz	RADIO NAV. SAT., FIXED SAT., FIXED, MOBILE	3
”	14.5-15.35 GHz	FIXED, MOBILE	5
”	15.35-15.4 GHz	RADIO ASTRONOMY	
22.0-24.0 GHz	22.0-23.6 GHz	FIXED, MOBILE	1
”	23.6-24.0 GHz	RADIO ASTRONOMY	

5.4.8 Local Oscillator and Map Frequencies

Standard operating frequencies are programmed into the VLA so that observers with no frequency preference, other than for a particular band, can set up their observing program without consideration of the various local oscillator frequencies in the system. These default frequencies are listed in Table 5-5. These frequencies may change from time to time, so if a frequency range is critical the observer should talk to a VLA operator about the default frequencies. The formulation for calculating the sky frequency from the local oscillator frequencies is given below.

The HH band is a special frequency range of L band which was chosen for minimum interference at 25 and 12.5 MHz bandwidth. Do not use the HH band with any other bandwidths because of interference problems.

[4] Upper case letters indicate a primary allocation, lowercase a secondary allocation.

[5] Assignments are taken from a listing which includes all unclassified government allocations within the area between longitudes 106°W and 109°W and between latitudes 32°30′ N and 35°30′N. for transmitter power exceeding 100W with area is extended to that between 105° and 110°W and 32° and 36°N.

Bandwidths of 3.13 MHz and smaller should not be used in the continuum mode because the quadrature networks in the correlator system do not work properly. However, the narrow bandwidths can be used for line observing.

The choice of center observing frequency is restricted by the passbands of the receivers and the local oscillator frequencies available. The suggested usable ranges of the receivers are given in Table 5-3.

Within a particular band the local oscillator (LO) frequencies determine the observing frequency. The observing frequency formula is

$$f_0 = f_1 \pm (f_{L6} - f_A + f_D + f_S + f_{BB}). \qquad (5-1)$$

Each term is determined as follows.

a. f_1 is the frequency of the oscillator which mixes with the incoming signal. The resultant passes into the C band receiver. f_1 values for the four bands are:

Band	Frequency	Comment
L	-3.2 GHz	fixed
C	0 GHz	fixed
U	19.6 GHz	standard
K	17.6 GHz	standard

The F3 module (for U and K bands) may be set to any frequency between 17.0 GHz and 20.0 GHz satisfying the following condition:

$$f_1 = 17.1 + N \times 0.3 \pm 0.1 \text{ GHz}$$

b. The sideband of the first mixer for each of the four bands is:

Band	Sign	Comment
L	+	fixed
C	+	fixed
U	−	fixed
K	+	fixed

This determines the sign following the f_1 term.

c. The L6 module may be set to any frequency between 2710 MHz and 4010 MHz which satisfies the following condition:

$$f_{L6} = 2400 + N \times 50 \pm 10.1 \text{ MHz}.$$

d. f_A values for the four IF channels are:

IF	Frequency	Comment
A	300 MHz	fixed
B	400 MHz	fixed
C	550 MHz	fixed
D	650 MHz	fixed

e. f_D values for the four IF channels are:

IF	Frequency	Comment
A	1200 MHz	fixed
B	1200 MHz	fixed
C	1800 MHz	fixed
D	1800 MHz	fixed

f. f_s ranges for the four IF channels are:

IF	Frequency	Comment
A	100 to 150 MHz	tunable
B	200 to 250 MHz	tunable
C	-250 to -200 MHz	tunable
D	-150 to -100 MHz	tunable

These frequencies are actually generated from four 100 to 150 MHz synthesizers. In order to produce f_S, the synthesizers are set to:

IF	Synthesizer Setting
A	f_S
B	$f_S/2$
C	$-f_S/2$
D	$-f_S$

For example, if f_S in the C IF were -260 MHz, the C synthesizer would be set to 130 MHz. (This is done for you). It will be noticed that, since the synthesizers are tunable in 1 Hz steps, IF channels A and D are tunable in steps of 1 Hz, but B and C in steps of 2 Hz.

For polarization measurements, it is essential that the local oscillators of channels A and C (and B and D) be locked. This is done in the synthesizer phase lock (L17) module, which forces the following relationships:

$$f_S(A) - f_S(C) = f_S(B) - f_S(D) = 350 \text{ MHz}.$$

Thus, if f_S were chosen to be 110 MHz, for the A IF, f_S for the C IF must be -240 MHz. When these values are put into Equation (5-1), calculations for the A and C IFs will give the same observing frequency.

It is possible to override these constraints by setting the L17 module in independent mode.

g. The values of f_{BB} are:

Bandwidth	f_{BB} [MHz]	OBSERV Program	Comment
50 MHz	25	0	fixed
25 MHz	12.5	1	fixed
12.5 MHz	6.25	2	fixed
6.25 MHz	3.13	3	fixed
3.13 MHz	1.56	4	fixed
1.56 MHz	0.78	5	fixed
0.78 MHz	0.39	6	fixed

These bandwidths are not the hardware filter bandwidths, but 1/2 the sampling rate of the correlator system. The 3 dB filter bandwidths will be about 8% narrower. However, these bandwidths are the basis for frequency calculations. The user specifies the bandwidth code n ($0 < n < 7$) such that the sampled bandwidth is $50/2^n$ MHz.

6 Useful Plots and Tables

Name of Figure	Original Chapter Figure Number
Inner and outer VLA wye plans	1-6
u-v coverage for 27-antenna VLA at various declinations	2-12
Azimuth-elevation diagram for given (HA, DEC)	5-3
Hour angle limits plotted as a function of declination	5-4
Central intensity loss due to finite bandwidth	2-17
Beam shape due to finite bandwidth	2-18
Ratio of radial to azimuthal BW due to finite BW	2-19

Name of Table	Original Chapter Table Number
VLA antenna parameters	1-1
VLA observing bands and associated spectral lines	1-2
Parameters of the four VLA observing bands	3-1
IF Bandwidth's and Spectral-line channel Bandwidth's	3-2
Default sky frequencies for various bands and BW's	5-5
Sidelobe levels for full traking with 27 antennas	5-1
Sidelobe levels for 30° source with Varying Integ. Time	5-2
Sensitivity, resolution, and confusion limits (27 ant.)	5-3

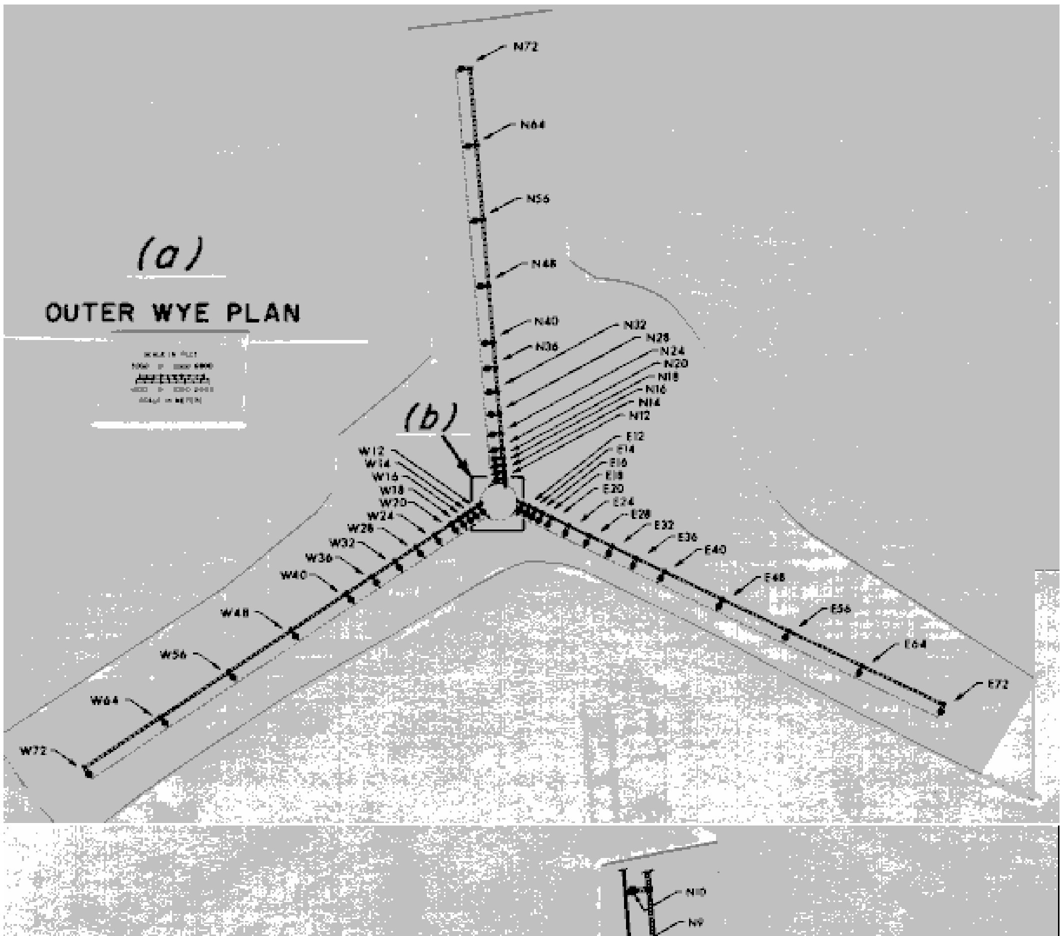

Figure 1 - 6. The outer (a) and inner (b) parts of the VLA.

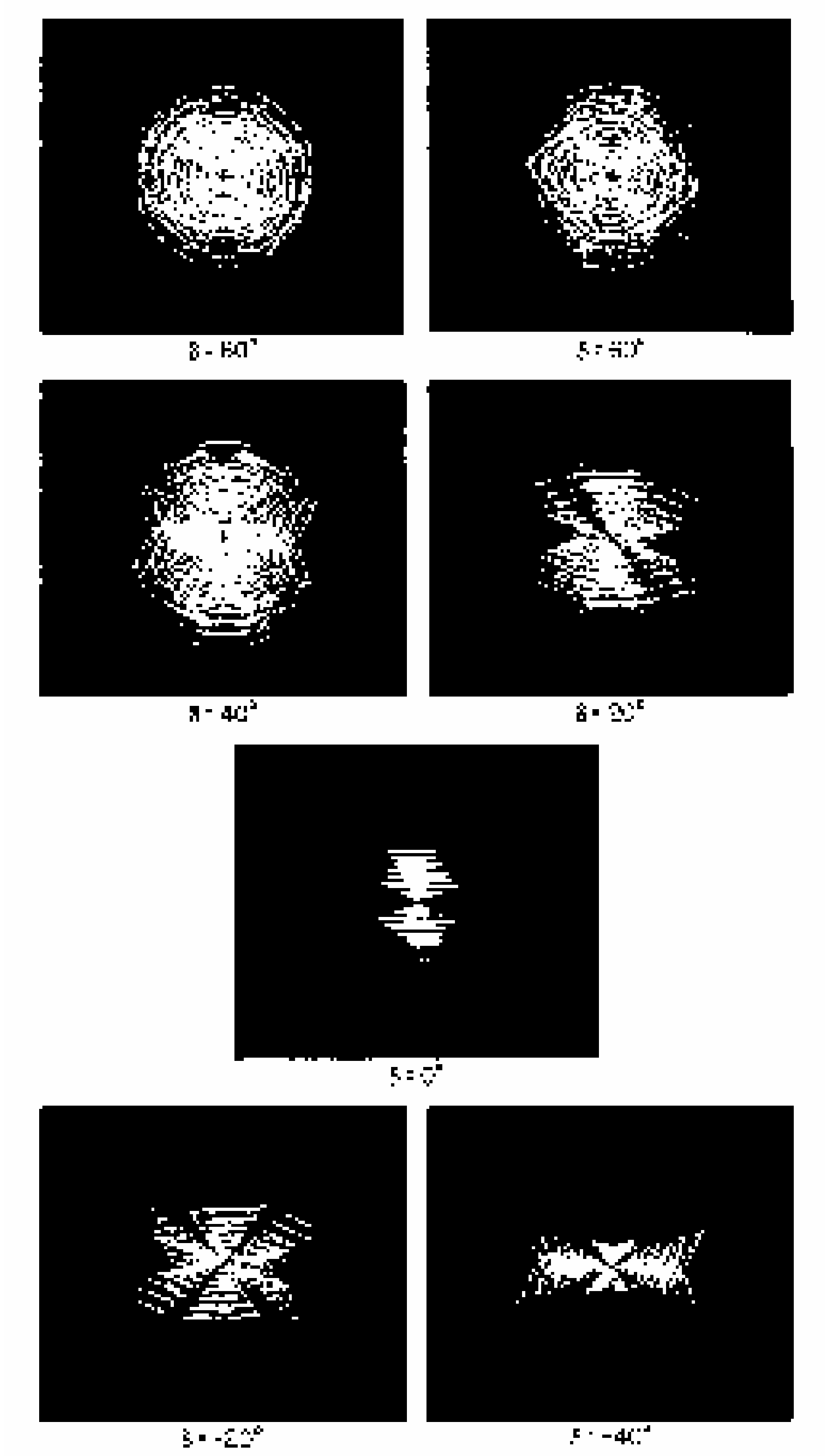

Figure 2 - 12. The possible u-v plane coverage for the 27-antenna VLA for declinations of 80°, 60°, 40°, 0°, −20°, −40°.

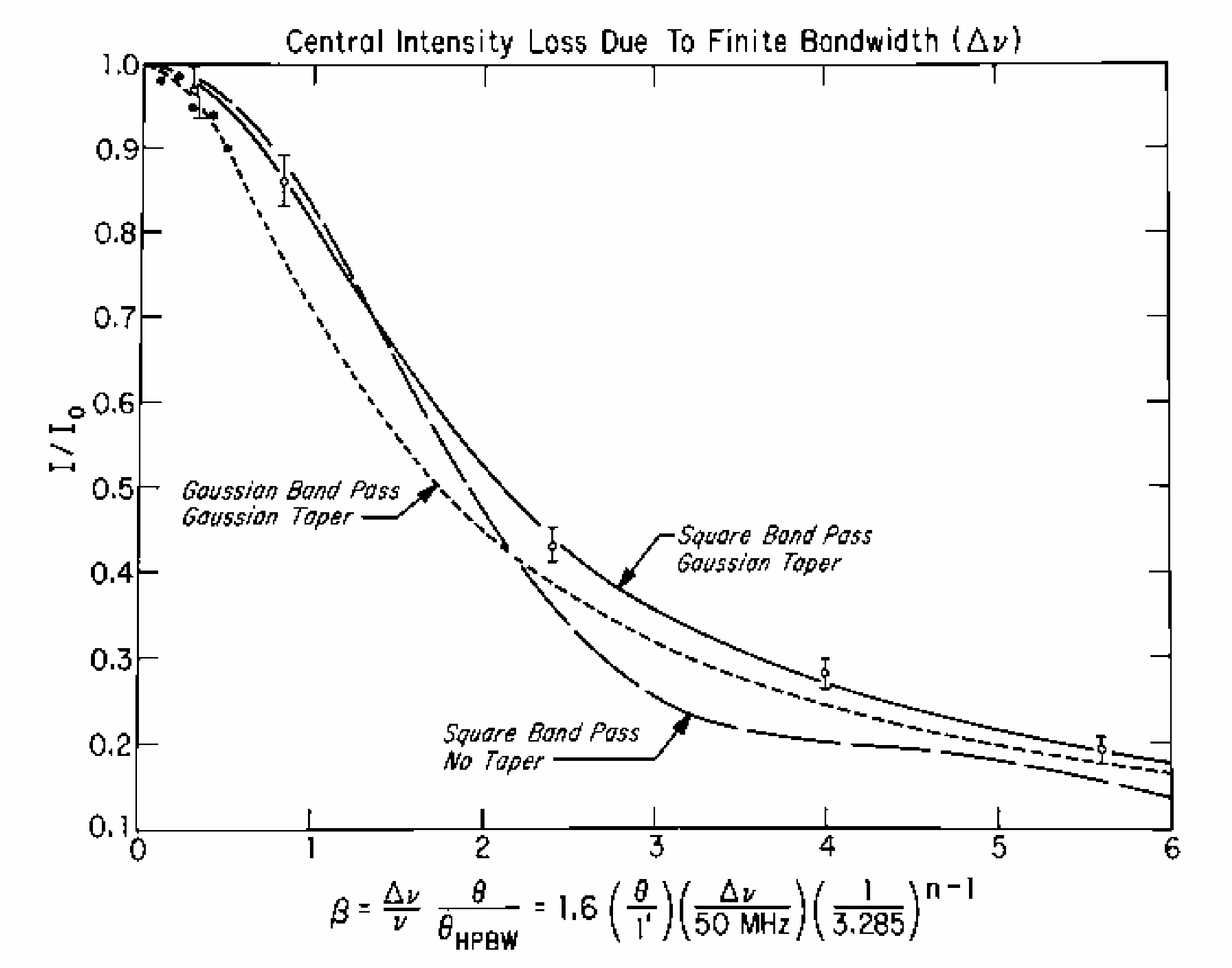

Figure 2 - 17. Central intensity loss (due to finite bandwidth $\Delta\upsilon$) plotted as a function of $\beta = beta(\theta,\ \Delta\upsilon,\ \text{n})$, where θ is angular displacement from the phase center and n = 1, 2, 3, and 4 for the A, B, C, and D configurations.

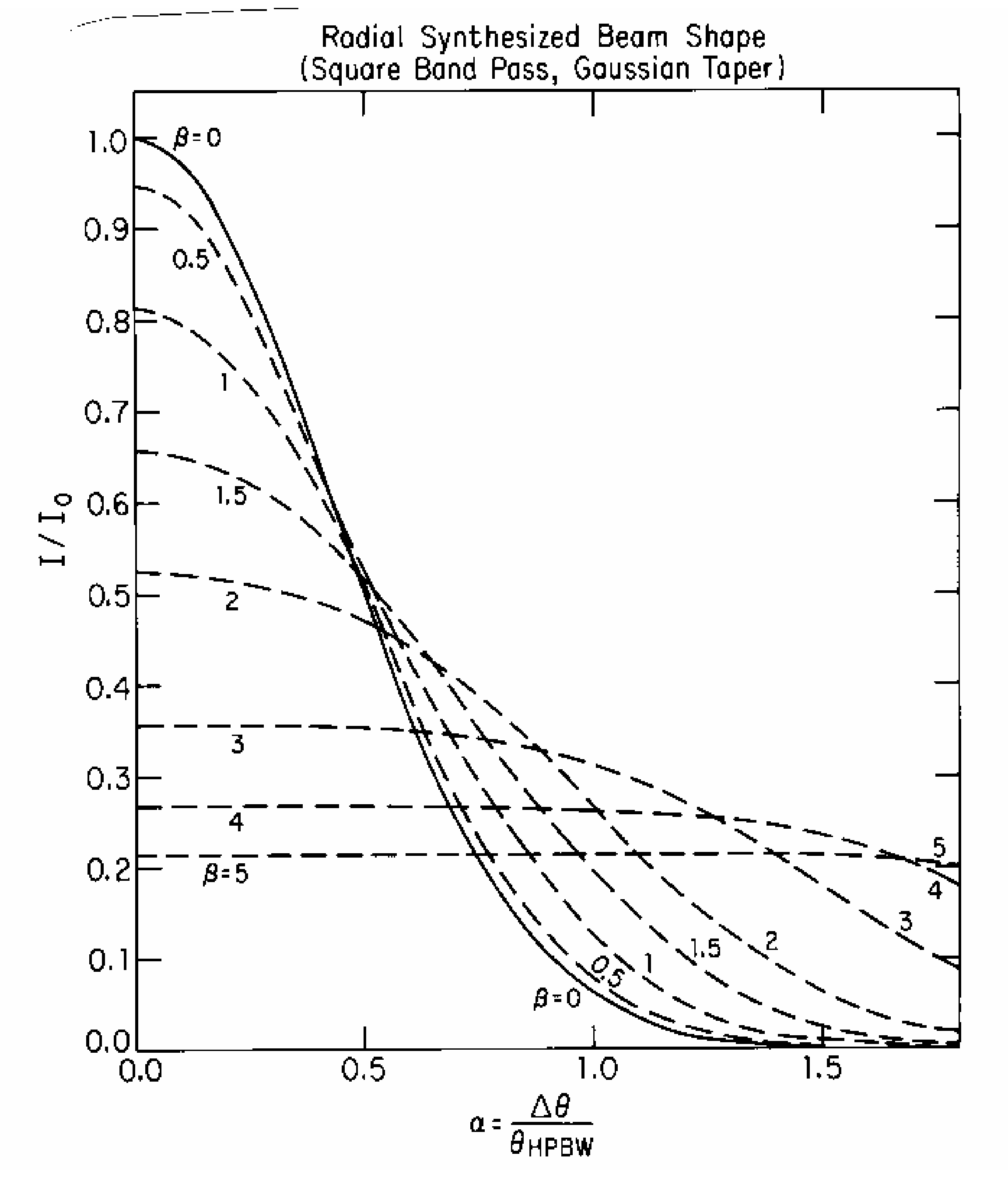

Figure 2 - 18. Beam shape due to finite bandwidth for a number of values of $\beta = \beta(\theta,\ \Delta v,\ \text{configuration})$.

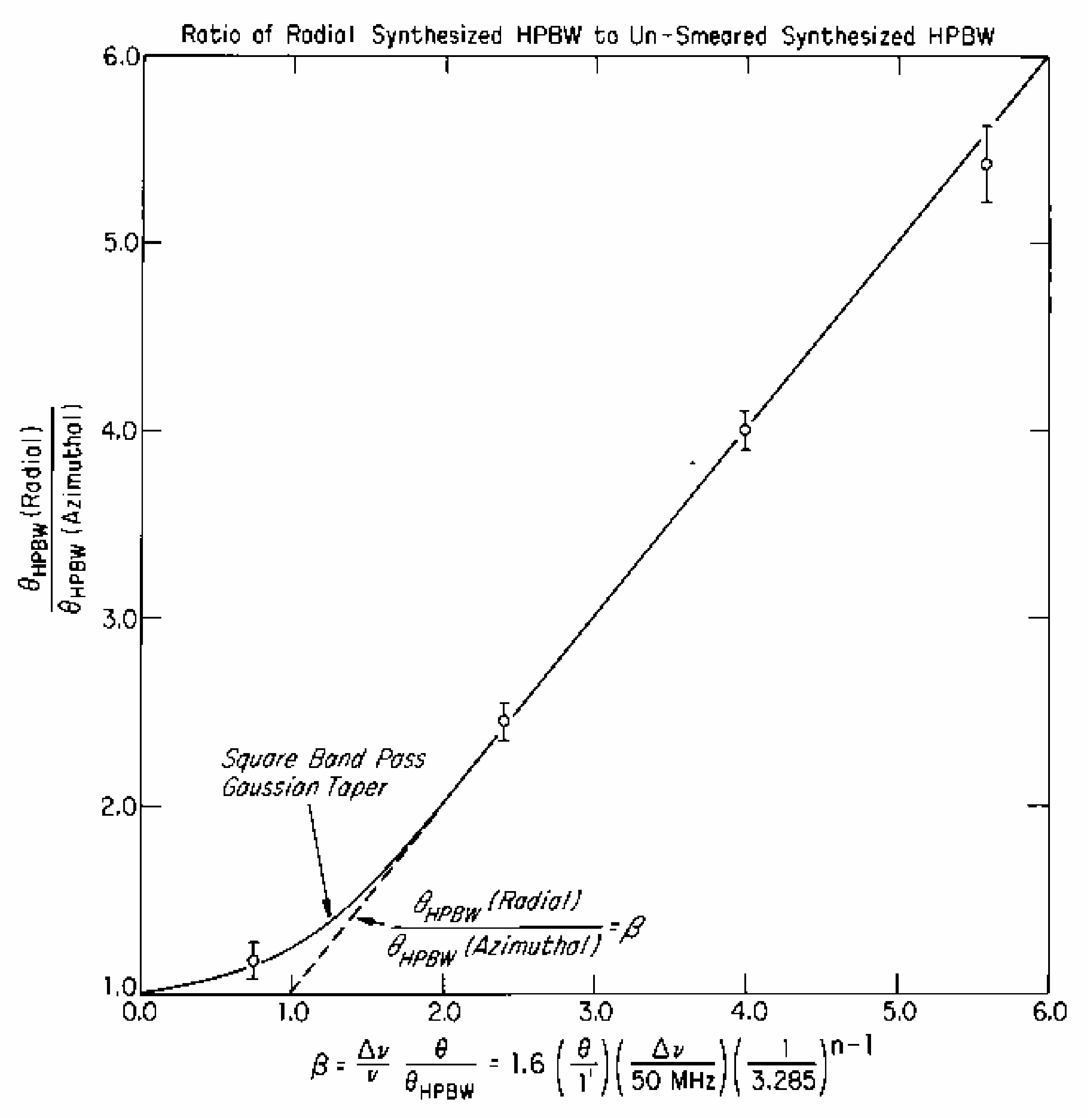

Figure 2 - 19. Ratio of radial to azimuthal beam width, due to finite Bandwidth, plotted as a function of $\beta = \beta(\theta,\ \Delta v,\ \text{configuration})$.

Table 1 - 1
VLA Antenna Parameters

main reflector diameter		25 m (82 feet)
antenna half-power beamwidth		1.5 λ (λ in cm)
total geometric aperture		491 square meters
focal length of main reflector		9 m
maximum asymmetric subreflector width		1.83 m
rms surface accuracy for panels		$<$ 0.38 mm
rms surface accuracy for panel setting		$<$ 0.46 mm
rms surface accuracy for gravity, wind, thermal		$<$ 0.36 mm
nonrepeatable pointing errors for wind $<$ 15 mph and $<$ 5 degrees temperature differences of structure		$<$ 15 arcsec
slew rate, azimuth		40 degrees per minute
slew rate, elevation		20 degrees per minute
drive, servo controlled 5 hp motors		2 per axis
minimum elevation		8 degrees
maximum elevation		125 degrees
minimum zenith angle for tracking		0.5 degrees
azimuth limits relative to track azimuth		$\pm$ 270 degrees
total weight of antenna		419,000 pounds
resonant freqency, torsional		2.2 Hz
resonant freqency, rocking		2.3 Hz
wind speed limit:	precision operation	$<$ 15 mph
	normal operation	$<$ 45 mph
	survival at stow (snow / ice load 20 lbs / sq. ft)	$<$ 110 mph

Table 1 - 2
VLA Observing Bands and Associated Lines

VLA Band: Frequency	VLA Band: Wavelength	Protected Band	Atomic and Molecular Lines
1340-1730 MHz	18-21 cm	1400-1427 MHz	Neutral H (Hydrogen) 1420.4 MHz
			H, He, etc. recombination lines
			$HCONH_2$ (Formamide) 1538-1542 MHz
			OH 1612, 1665, 1667, 1721 MHz
			HCOOH (Formic Acid) 1639 MHz
4500-5000 MHz	6 cm	4990-5000 MHz	$HCONH_2$ 4617-4620 MHz
14.4-15.4 GHz	2 cm	15.35-15.4 GHz	H_2CO 14.489 GHz
22.0-24.0 GHz	1.3 cm	23.6-24.0 GHz	H_2O 22.35 GHz
			NH_3 (Ammonia) 22.834-23.870 GHz

Table 3 - 1
Parameters of the Four VLA Freqency Bands

VLA Bands	Wavelength	Radio Astronomy Band	System Temperature (T_{sys})[1]	Antenna Efficiency (e_a)
1.34-1.73 GHz	17.0-22 cm	1.400-1.427 GHz	60 K	50 %
4.5-5.0	6.0-6.7	4.99-5.00	50	65
14.4-15.4	1.95-2.08	15.35-15.40	300	54
22.0-24.0	1.25-1.36	23.6-24.0	360	46

[1] Average values for the antennas

Table 3 - 2
IF Bandwidths and Spectral-Line Channel Bandwidths for
Various Observing Modes

Nominal IF Bandwidth	IF passband[3]	Sampling Frequency	No. of Channels[2] 1[4]	2[4]	4[4]	Channel Bandwidth
50 MHz	0.19-50 MHz	100 Mhz	16	8	4	3.125 MHz
25 MHz	0.19-25 MHz	50 Mhz	32	16	8	781 kHz
12.5 MHz	0.19-12.5 MHz	25 Mhz	64	32	16	195 kHz
6.25 MHz	0.19-6.25 MHz	12.5 Mhz	128	64	32	48.8 kHz
3.125 MHz	0.19-3.125 MHz	6.25 Mhz	256	128	64	12.2 kHz
1.563 MHz	0.19-1.563 MHz	3.125 Mhz	256	128	64	6.1 kHz
781 kHz	190-781 kHz	3.125 Mhz	256	128	64	3.05 kHz
391 kHz	190-781 kHz	3.125 Mhz	256	128	64	1.53 kHz
195 kHz	195-391 kHz	1.563 Mhz	256	128	64	763 Hz
97 kHz	195-391 kHz	781 kHz	256	128	64	381 Hz

Table 5 - 5
Standard Continuum Observing Freqencies

	BAND				
Bandwidth [MHz]	21 cm HH [MHz]	20 cm LL [MHz]	6 cm CC [MHz]	2 cm UU [GHz]	1.3 cm KK [GHz]
50.0		1464.90	4885.10	14.9649	22.4851
25.0	1413.00	1452.40	4872.60	14.9774	22.4726
12.5	1406.75	1446.15	4866.35	14.9837	22.4664
6.25		1443.03	4863.23	14.9869	22.4632
3.125		1441.46	4861.66	14.9883	22.4617
1.5625		1440.68	4860.88	14.9891	22.4609
0.78125		1440.29	4860.49	14.9895	22.4605

[2] The numbers give indicate the number of channels processed within the nominal bandwidth. The number of usable channels is slightly less because of band edge effects.
[3] The filters are low-pass and the low-frequency limit is determined by the amplifiers except for the 195-391 kHz band which uses a bandpass filter.
[4] Number of IF's

Table 5 - 1
Maximum and Minimum Beam Sidelobe Levels

Declination (degrees)	Maximum (fraction)	Minimum (fraction)
80	0.07	-0.14
60	0.08	-0.17
40	0.11	-0.25
20	0.16	-0.40
0	0.2	-0.42
20	0.2	-0.4
40	0.2	-0.44

Table 5 - 2
Sidelobe Levels for $\delta = 30°$ Buildup Map

H_{start}	H_{stop}	H_{range}	Inner 1/4 Maximum Sidelobe Level	Outer 3/4 Maximum Sidelobe Level
-6^h	-5^h45^m	15^m	27%	12%
-6^h	-5^h30^m	30^m	16	4
-6^h	-5^h	1^h	9	4
-6^h	-4^h	2^h	8	3
-6^h	-3^h	3^h	7	2
-6^h	-2^h	4^h	5	2
-6^h	0^h	6^h	3	2
-6^h	$+6^h$	12^h	3%	<1%

Table 5 - 3
Sensitivity, Resolution, and Confusion Limits with 27 Antennas

Frequency	1.34-1.73	4.5-5.0	14.4-15.4	22.0-24.0 GHz
Wavelength	22.4-17.3	6.67-6.00	2.08-1.95	1.36-1.25 cm
Band Designation	20 cm	6 cm	2 cm	1.3 cm
	L	C	U	K
System Temperature	60	60	120	400 °K
RMS Sensitivity in 10 minutes (50 MHz bandwidth)	0.13	0.10	0.2	1.0 mJy
RMS Sensitivity in 12 hours (50 MHz bandwidth)	0.015	0.012	0.03	0.12 mJy
Untapered Brightness[5] Temperature (A configuration)	6.9	5.5	34	54 °K
Dynamic Range Without Self Calibration[6]	100	50	25	10?
Antenna Beam Size (HPBW)	30′	9′	3.7′	2′
Brightest Source Expected in Antenna Beam	100	2.3	<0.1	<0.01 mJy

[5] RMS sensitivity in brightness temperature for an untapered map is given approximately by

$$\Delta \mathrm{T} \simeq \left(\frac{1.46\lambda^2}{\theta_1\theta_2}\right)\Delta \mathrm{S}$$

Where θ_1 and θ_2 are the half-power synthesized beamwidths in arcseconds, λ is the wavelength in cm, and ΔS is the rms sensitivity ber beam area im mJy.

[6] Dynamic range is extremely dependent on declination, time of day, season, and freqency of calibration.

Table of Contents

Short Contents